Structural Characterization and Reactivity of a Room Temperature-Stable, Antiaromatic Cyclopentadienyl Cation Salt

Yannick Schulte,[a] Christoph Wölper,[a] Susanne M. Rupf,[b] Moritz Malischewski,[b] Gebhard Haberhauer,[c]* and Stephan Schulz[a;d]*

[a] Institute of Inorganic Chemistry, University of Duisburg-Essen, Universitätsstraße 5-7, D-45141 Essen

E-mail: stephan.schulz@uni-due.de; https://www.uni-due.de/ak_schulz/index_en.php

[b] Institute of Inorganic Chemistry, Freie Universität Berlin, Fabeckstraße 34-36, D-14195 Berlin

[c] Institute of Organic Chemistry, University of Duisburg-Essen, Universitätsstraße 5-7, D-45141 Essen

E-mail: gebhard.haberhauer@uni-due.de; https://www.uni-due.de/akhaberhauer/

[d] Institute of Inorganic Chemistry and Center for Nanointegration Duisburg-Essen (CENIDE), University of Duisburg-Essen, Carl-Benz-Straße 199, D-47057 Duisburg.

E-mail corresponding authors: stephan.schulz@uni-due.de; gebhard.haberhauer@uni-due.de

Graphic TOC

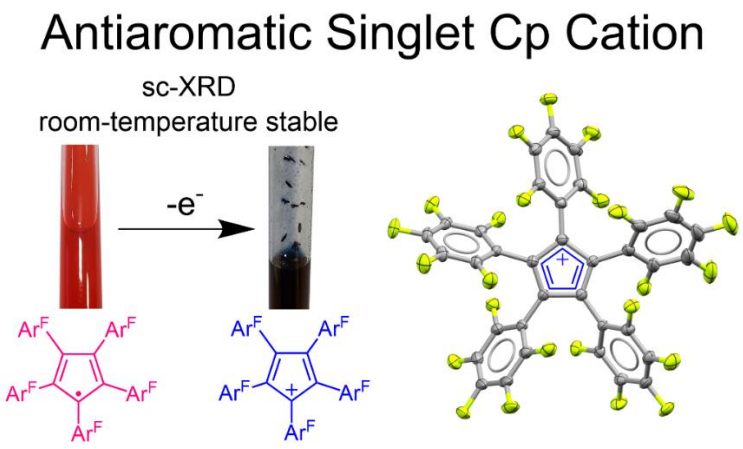

Abstract. **The singlet states of cyclopentadienyl (Cp) cations are considered as true prototypes of an antiaromatic system. Due to their high reactivity, their isolation in the solid state as a salt has so far failed. We present here the synthesis of the first room temperature-stable Cp cation salt $Cp(C_6F_5)_5Sb_3F_{16}$ ($1{\cdot}Sb_3F_{16}$) by single electron oxidation of the corresponding Cp radical $Cp(C_6F_5)_5$· (2) with either an excess of XeF_2 and $SbF_5{\cdot}SO_2$ or by hydroxide abstraction from $Cp(C_6F_5)_5OH$ (D) with $SbF_5{\cdot}SO_2$ in hexafluorobenzene. $1{\cdot}Sb_3F_{16}$ was characterized by sc-XRD, SQUID, UV-vis, and EPR spectroscopy. Although the aromatic triplet state of the $Cp(C_6F_5)_5$ cation 1 is energetically favored in the gas phase according to quantum chemical calculations, the coordination of the cation by either $Sb_3F_{16}^-$ ($1a{\cdot}Sb_3F_{16}$) or C_6F_6 ($1b{\cdot}Sb_3F_{16}$) in the crystal lattice stabilizes the antiaromatic singlet state, which is present in the solid state. The calculated hydride and fluoride ion affinities of 1 are higher than those of the tritylium cation $C(C_6F_5)_3^+$. In addition, results from reactions of $1{\cdot}Sb_3F_{16}$ with CO, which most likely yields the corresponding carbonyl complex, and 2 with selected model substrates (Cp_2Fe, $(Ph_3C{\cdot})_2$, and Cp*Al) are presented.**

Faraday's discovery of benzene was quickly recognized as "the most important chemical result of 1825".[1,2] At that time, the understanding of chemical structure was still in its infancy and more than 30 years passed before Kekulé's famous daydream in front of the fireplace in his dark apartment shed light on the bonding situation in this unique compound.[3,4,5] Nevertheless, the relative inertness and low enthalpy of the hydrogenation of benzene were difficult to explain in the 19th century. This became even more puzzling in 1911, when Willstätter prepared 1,3,5,7-cyclooctatetraene and showed that it reacted like an alkene, rendering the hypothesis that all cyclic conjugated polyenes would behave like aromatics implausible.[6] It was soon recognized that the exact number of π-electrons was important for the chemical behavior of these cyclic molecules,[7] but an explanation for this phenomenon was lacking until the seminal work of Hückel, who applied the rather new theory of quantum mechanics to the π electrons of cyclic alkenes.[8] He formulated what came to be known as “Hückel's rule” and explained why those systems with (4n+2) π electrons (n being a natural number) were particularly stable. At that time, only representatives with n = 1 like benzene and the cyclopentadienyl anion were known. The experimental evidence for cyclic π systems was greatly expanded in 1958 and 1960 by Breslow's cyclopropenyl cation[9,10] (n = 0) and Katz's cyclooctatetraene dianion[11] (n = 2), which were found to be stabilized by aromaticity, supporting Hückel's predictions. It is now textbook knowledge that planar, conjugated cycles with (4n + 2) π electrons are aromatic systems that exhibit high thermodynamic stability, tend to equalize bond lengths, and maintain their cyclic delocalization of electrons during a chemical reaction.

However, much more difficult to define and quantify is the concept of antiaromaticity, introduced by Breslow in the 1960s to describe the destabilization of planar, conjugated cycles with 4n π electrons.[12] In antiaromatic molecules, cyclic π conjugation has a destabilizing effect on the system. Accordingly, the system tries to avoid this destabilization by distortion and, therefore, antiaromatic systems often represent only transition states. Local minima on the potential hypersurface, *i.e*., molecules that may, in principle, be isolated, (only) partially retain their antiaromaticity and are unstable and highly reactive, making isolation an enormous challenge. Another obstacle in isolating antiaromatic systems with 4n π electrons is the fact that the triplet states of these systems are aromatic. Thus, in some cases, the (aromatic) triplet state is energetically lower than the (antiaromatic) singlet state, making isolation of the antiaromatic state almost impossible. Textbook examples of 4n π electron systems with antiaromatic character used to be the cyclopropenyl anion, the cyclobutadiene molecule, and the cyclopentadienyl cation. However, it has now been shown that the cyclopropenyl anion is a non-aromatic system[13] and the cyclobutadiene molecule should be considered as a maverick (and thus not antiaromatic).[14] This leaves only the cyclopentadienyl cation as a possible prototype of an antiaromatic system.

Unfortunately, the cyclopentadienyl cation ($C_5H_5^+$) is an unstable compound,[15] that has a triplet ground state as demonstrated by low temperature EPR[16] as is also true for substituted Cp cations such as $C_5Cl_5^+$.[17,18] According to Baird’s rule, “the lowest triplet state for 4n rings is aromatic since the bonding energy is significantly greater than for the diradical reference structure”.[19,20] Therefore, the ground states of $C_5H_5^+$ and $C_5Cl_5^+$ must be considered as aromatic and not antiaromatic. In contrast, the singlet ground state seems to be more favored for pentaaryl-substituted Cp cations although the singlet-triplet energy gap is very small.[21-24] They persist as long-lived species in solution due to the substantial delocalization of the positive charge (electronic effect) and steric shielding (kinetic effect).

To the best of our knowledge, Cp cations have not yet been structurally characterized by single-crystal X-ray diffraction (sc-XRD), as they are typically highly labile species,[12] *i.e*. according to the thermodynamic criteria for $C_5H_5^+$.[25-27] Only Cp cations with strongly electron-donating substituents are stable species,[28] but to the best of our knowledge, all attempts to isolate a crystalline salt of a Cp cation have so far failed due

to the occurrence of a number of side reactions (Scheme S42, electronic supplementary material), which led to the decomposition of the target molecules.[29-36] For example, heating a solution of the $C_5Me_5^+$ cation to room temperature yielded tetramethylpentafulvene by deprotonation,[36] whereas the $C_5Ph_5^+$ cation decomposed by C–H cleavage and formation of additional C–C bonds,[34] and the $C_5Cl_5^+$ and $C_5Br_5^+$ cations were found to dimerize.[35] In 2002, the structure of a stable $B(C_6F_5)_4$ salt of the pentamethylcyclopendadienyl cation ($C_5Me_5^+$) was reported,[29] however this was later shown to be the pentamethylcyclopentenyl cation.[30-33] More recently, the reaction of triplet tetrachlorocyclopentadienylidene with BF_3 in low-temperature noble gas matrices has been reported, yielding a zwitterion consisting of a positively charged antiaromatic singlet cyclopentadienyl cation and a negatively charged BF_3 unit (Scheme 1).[37]

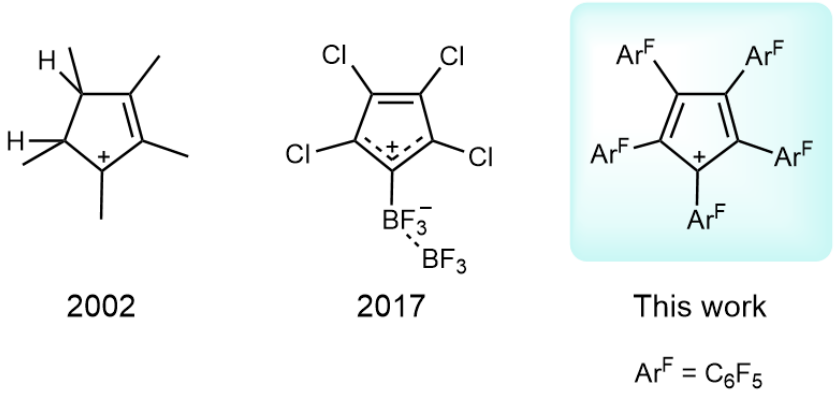

Scheme 1: The pentamethylcyclopentenyl cation that was first misidentified as the Cp* cation,[29-33] the cyclopentadienyl zwitterion obtained by Sander *et al.* in rare gas matrices,[37] and this work featuring a room temperature-stable and crystalline Cp cation.

In order to be able to isolate a stable cyclopentadienyl cation, a number of requirements for the substitution pattern of the Cp ring must be met: C-H bonds are potential weak points of possible decomposition reactions and should therefore be avoided. Furthermore, the substituents should be sterically demanding in order to suppress dimerization reactions. In 2014 Dutton *et al*. suggested in a computational study that electron-withdrawing substituents (*e.g*. CF_3 or C_6F_5) could be advantageous for the isolation of stable cyclopentadienyl cations since the cation would then be similar to the isoelectronic neutral borole.[38] As perfluoropentaphenylborole $BC_4(C_6F_5)_5$ is a stable (although highly reactive) compound,[39] $Cp(C_6F_5)_5^+$ seemed to be a worthwhile target even if the high electron deficiency would make the synthesis of this compound realistic only under strongly oxidizing or highly Lewis acidic conditions.

We report here the isolation of a room temperature-stable cyclopentadienyl cation containing five chemically very robust and bulky pentafluorophenyl substituents (C_6F_5) and its structural characterization by sc-XRD. Detailed quantum chemical studies revealed that these Cp cations adopt singlet ground states.

Results and Discussion

Synthesis and Characterization of 1·Sb_3F_{16} and 2. 1·Sb_3F_{16} was synthesized in a 4-step reaction starting from commercially available bromopentafluorobenzene **A** *via* the formation of the known perfluorotolane **B**[40-41] and tetrakis(pentafluorophenyl)tetracyclone **C** (Scheme 2).[42] Temperature-controlled reaction of **C** with C_6F_5MgBr gave pentakis(pentafluorophenyl)cyclopentadienole **D** in good yield (58 %).

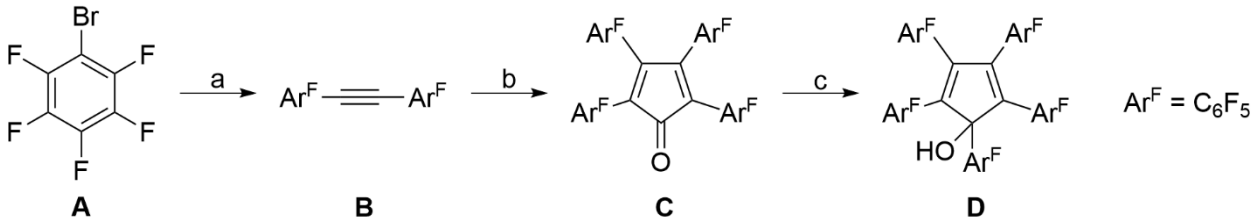

Scheme 2: Synthesis of pentakis(pentafluorophenyl)cyclopentadienole **D**. a) EtMgBr in thf/Et_2O (*i*), diglyme, CuBr (*ii*), tribromoethylene, diglyme, 120 °C (*iii*); b) $Co_2(CO)_8$, decaline, 25 °C, then 190 °C (*i*), I_2 (ii); c) C_6F_5MgBr, thf, - 78 °C to 25 °C.

Our attempts to functionalize **D** were hindered by its remarkably low reactivity. We attribute this both to the appearance of the energetically unfavorable Cp cation intermediate **1** in nucleophilic substitution reactions and to the steric protection by the bulky C_6F_5 substituents. For example, **D** is stable to triflic anhydride in the presence/absence of strong bases (pyridine, 4-dimethylaminopyridine), to HBr in acetic acid and to PCl_5 at temperatures up to 110 °C in toluene, respectively. In marked contrast, **D** reacts under superacidic conditions with $SbF_5{\cdot}SO_2$ to form **1·Sb$_3$F$_{16}$** containing the desired Cp cation **1**, whereas the corresponding cyclopentadienyl radical **2** is formed in the reaction with the Friedel-Crafts-type superacid system $AlBr_3$/EtBr/benzene (Scheme 3). The high oxidation potential of **1·Sb$_3$F$_{16}$** requires the use of solvents resistant to these constraining conditions (SO_2, hexafluorobenzene). Oxidation of radical **2** with an excess of XeF_2 and $SbF_5{\cdot}SO_2$ in C_6F_6 also yielded **1·Sb$_3$F$_{16}$**, while reactions of **1·Sb$_3$F$_{16}$** with very weak reducing agents, *i.e*. alkanes, dichloromethane (DCM), difluorobenzene and even polypropylene syringes, yielded radical **2**.

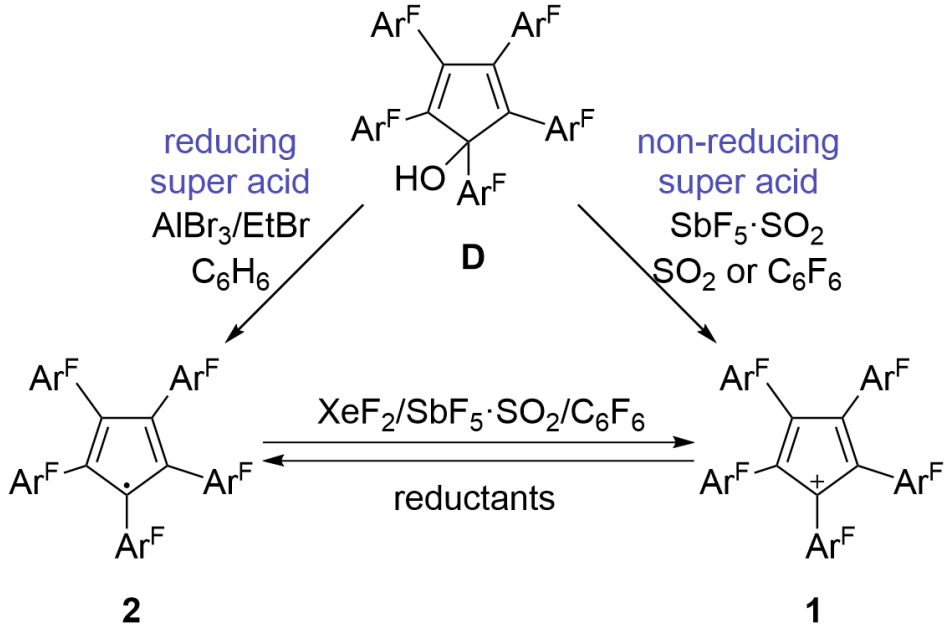

Scheme 3: Preparation of **1·Sb$_3$F$_{16}$** and radical **2** by reaction of alcohol **D** with reducing or non-reducing Lewis acids and their interconversion by oxidation or reduction.

The reaction of **D** with $SbF_5{\cdot}SO_2$ in SO_2 was monitored by *in situ* NMR spectroscopy, which showed the complete conversion of **D** (Figure S8). Alcohol **D**, **1·Sb$_3$F$_{16}$**, and radical **2** were also distinguished by UV-vis spectroscopy. While the pale yellow alcohol **D** shows no strong absorption in the visible region, **1·Sb$_3$F$_{16}$**

and **2** have absorption maxima at 977 nm and 546 nm, respectively (Figure S7). Solutions of **1·Sb₃F₁₆** and **2** in SO_2 and toluene, respectively, were also investigated by EPR spectroscopy. **2** gives a signal that is typical for a Cp radical with a g value of 2.0033 and a line width of 0.75 mT (Figure S11), while no EPR signal was detected for **1·Sb₃F₁₆**. A SQUID measurement on solid $Cp(C_6F_5)_5Sb_3F_{16}\cdot 1.5\ C_6F_5$ also showed no evidence of paramagnetism. Cyclic voltammetry (SO_2, NBu_4SbF_6) showed that the interconversion of **2** and **1** occurs at an anodic peak potential of E_{pa} = +2.30 V vs. ferrocene (Figure S9). This value is significantly higher than the anodic peak potential of the perfluorotritylium cation $C(C_6F_5)_3^+$ (+1.11 V vs. Cp_2Fe in o-difluorobenzene).[43]

Solid State Structures of 1·Sb₃F₁₆. Crystallization of **1·Sb₃F₁₆** from a solution in hexafluorobenzene at 6 °C yielded two distinct solvates, $Cp(C_6F_5)_5Sb_3F_{16}\cdot 1.5C_6F_6$ (**1a·Sb₃F₁₆**) and $Cp(C_6F_5)_5Sb_3F_{16}\cdot 2C_6F_6$ (**1b·Sb₃F₁₆**, Figure 1).

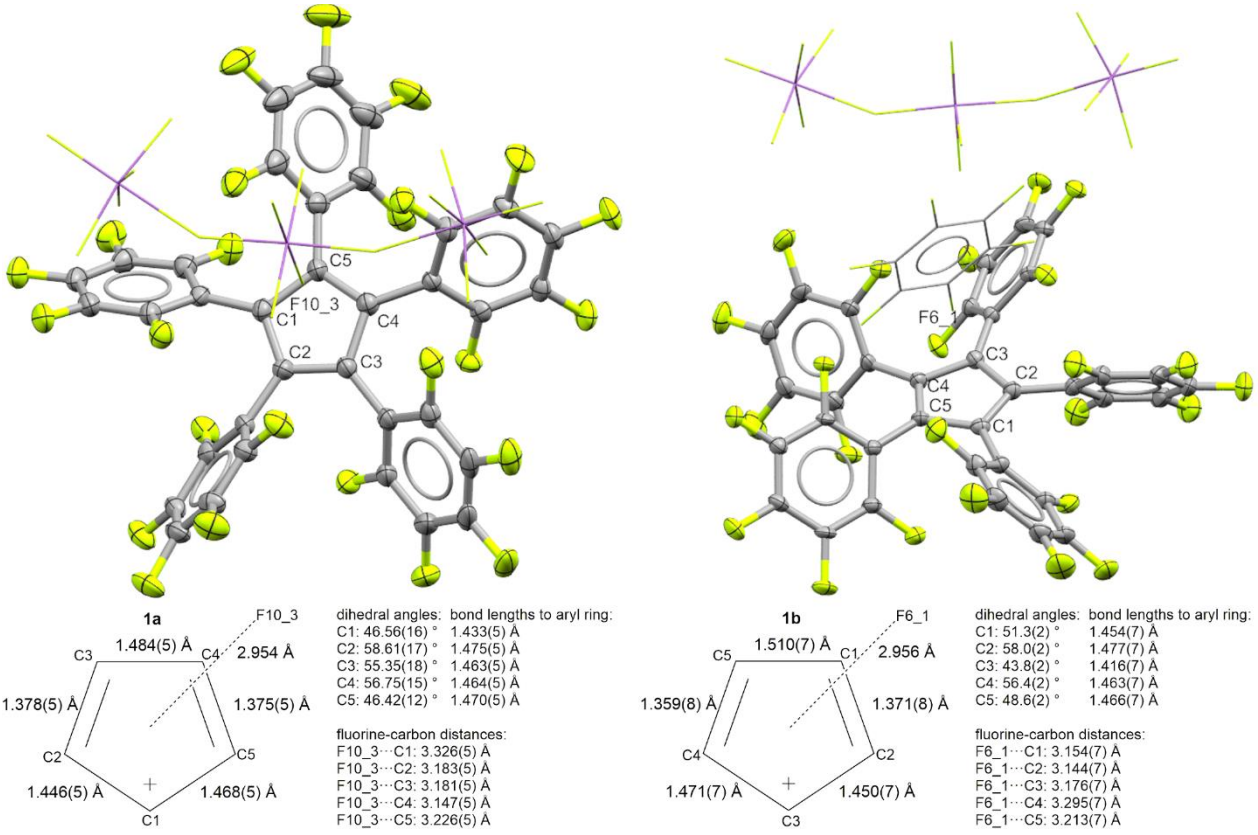

Figure 1. Molecular structures of **1a·Sb₃F₁₆** (left) and **1b·Sb₃F₁₆** (with counter anion, right), including selected bond lengths and dihedral angles between the Cp plane and the aryl groups (defined as best fit planes of the five Cp carbon atoms and six aryl carbon atoms). Anions and solvent molecules are depicted as wireframe models. Ellipsoids are drawn at a probability level of 50%. Non-participating solvent molecules are omitted for clarity.

Despite the intentionally low nucleophilicity of both the solvent (C_6F_6) and the counteranion ($Sb_3F_{16}^-$), the Cp cations in both structures show a weak interaction with a negatively polarized fluorine atom of the counter anion ($Cp(C_6F_5)_5Sb_3F_{16}$ **1a·Sb₃F₁₆** in $Cp(C_6F_5)_5Sb_3F_{16}\cdot 1.5\ C_6F_6$) or the solvent ($Cp(C_6F_5)_5C_6F_6$ **1b·Sb₃F₁₆** in $Cp(C_6F_5)_5Sb_3F_{16}\cdot 2\ C_6F_6$). The distances between the carbon atoms of the Cp ring and these fluorine atoms are in the same range as the sum of the van-der-Waals radii of carbon and fluorine (3.17 Å)[44]. The different solvates were distinguished by their crystal habit (**1a·Sb₃F₁₆** platelets, **1b·Sb₃F₁₆** needles), but

unfortunately, crystals of **1b·Sb_3F_{16}** suitable for a sc-XRD study were only obtained in a single experiment and the large size of the crystal resulted in uneven irradiation by the X-ray beam. The bond lengths and angles of **1a·Sb_3F_{16}** should therefore be considered more reliable than those of **1b·Sb_3F_{16}**. Both structures show a planar (rms deviation 0.018 Å) Cp cation. The C−C bond lengths of the central Cp rings show the characteristic bond length alternation that is expected for an antiaromatic singlet Cp cation (*vide infra*). The angles between the planes of the aryl groups bonded to a carbon atom with a higher calculated charge (C1, C3, C5; see 1a_singlett, Fig. S44) and the plane of the Cp ring are smaller and show a shorter aryl-Cp bond due to a better π-conjugation.

Quantum Chemical Calculations. For a better understanding of the electronic structures, we have calculated the key structures and energies of the singlet and triplet states of the cyclopentadienyl cation **1** using density functional theory (DFT) approaches. Geometry optimizations were performed using (U)B3LYP[45-46]-D3BJ[47] and (U)CAM-B3LYP[48]-D3BJ calculations, and the 6-31G(d), 6-311++G(d,p) and TZP basis sets were applied. In addition, the open-shell singlet states were calculated using UB3LYP-D3BJ/6-31G(d), UCAM-B3LYP-D3BJ/6-31G(d) and UB3LYP-D3BJ/6-311++G(d,p) with the "guess = mix" keyword. In all cases these calculations converged to the closed-shell states. Single-point calculations were performed with the double-hybrid method B2PLYP[49]-D3BJ and the TZ2P basis set. The S-T gaps calculated with B3LYP and CAM-B3LYP range from -5 to -6 kcal/mol (Table S3). That is, in agreement with calculations for other cyclopentadienyl cations, the triplet state is expected to be energetically more favored than the singlet state. Single-point calculations using the double-hybrid method B2PLYP-D3BJ also lead to the same result, although the S-T gap here is only -2.3 kcal/mol (Table S3).

Discussion. Comparing the calculated C−C bond lengths in the triplet state cyclopentadienyl cation **1**, almost identical bond lengths are found (1.431−1.434 Å for B3LYP-D3BJ/TZP; see Table S4), emphasizing the aromatic state of the triplet system. In marked contrast, the singlet state of cation **1**, shows a strong C−C bond length alternation (1.366−1.539 Å for B3LYP-D3BJ/TZP; see Table S4), as was also observed in the solid-state structures of the cyclopentadienyl cations **1a** (1.375−1.484 Å) and **1b** (1.359−1.510 Å) as determined by sc-XRD. Thus, the experimental results of the sc-XRD studies indicate that the cyclopentadienyl cations (**1a·Sb_3F_{16}** and **1b·Sb_3F_{16}**) in **1·Sb_3F_{16}** adopt singlet states in the solid state. A similar bond lengths alternation was observed in the isoelectronic perfluoropentaphenylborole (1.356–1.585 Å), which also has a singlet ground state.[39] In addition, EPR studies of **1·Sb_3F_{16}** gave no evidence for the presence of a triplet (radical) species under EPR conditions. In contrast, the singlet state is energetically less favorable than the triplet state according to quantum chemical calculations. A possible reason for these findings is that the counterions strongly influence the structure of the Cp cation in the solid: The negatively charged counterion localizes the positive charge on one carbon atom by spatial approach. The interaction of the anion with the differently positively polarized centers is then greater than the interaction of the anion with five equally positively polarized carbon atoms due to the shorter distance to one carbon atom. The calculated APT (atomic polar tensor) and NBO (natural bond orbitals) charges show that in the singlet cation there is a strong localization of the positive charge at C1, whereas in the triplet cation the charge is delocalized over the five carbon atoms (Figure S44). Accordingly, the approach of a negatively charged counterion can lead to an inversion of the S-T gap.

To verify this, the S-T gap of the **1·SbF_6** ion pair was also calculated using B2PLYP-D3BJ/TZ2P//B3LYP-D3BJ/TZP. Indeed, there is a preference, albeit very small, for the singlet state over the triplet state (ΔG = 0.36 kcal/mol; Table S3). In addition, single point calculations of **1a·Sb_3F_{16}** and **1b·Sb_3F_{16}** were performed using B2PLYP-D3BJ/TZ2P, with geometric data obtained from the X-ray structure analyses of **1a·Sb_3F_{16}** and

1b·Sb_3F_{16}. The obtained S-T gaps are 4.2 kcal/mol for **1a·Sb_3F_{16}** and 8.1 kcal/mol for **1b·Sb_3F_{16}**, showing that the singlet states are unambiguously present in the solid state.

The degree of (anti)aromaticity can also be evaluated using geometric criteria.[50] For example, the harmonic oscillator model of aromaticity (HOMA) index can be applied:[51,53]

$$HOMA = 1 - \frac{\alpha}{n}\sum_{i}^{n}(R_{opt} - R_i)^2$$

In this equation, R_{opt} corresponds to the optimal bond length, which is assumed to be 1.388 Å for a C–C bond. R_i represents an individual bond length; n is the number of bonds included in the sum and α is an empirical constant (257.7 $Å^{-2}$).[52] For aromatic systems the HOMA equals 1 and for non-aromatic systems it is zero. Antiaromatic molecules usually have negative HOMA values. Inserting the calculated (B3LYP-D3BJ/TZP) values for **1**(S) and **1**(T) and the experimentally determined data for **1a** and **1b** into this equation gives the following result: HOMA(**1**(S)) = -0.69, HOMA(**1**(T)) = +0.49, HOMA(**1a**) = +0.01 and HOMA(**1b**) = -0.39. That is, while the triplet state of **1** should be aromatic, the singlet state of **1** and the cyclopentadienyl cation **1b** found in the solid state are anti-aromatic.

These findings are further supported by the application of another criterion of aromaticity, the nucleus independent chemical shift (NICS).[50,53] Negative NICS values indicate diatropic ring currents and aromaticity, positive values indicate paratropic ring currents and antiaromaticity, and values close to zero indicate a non-aromatic molecule. Therefore, the NICS values were calculated using CAM-B3LYP/def2-TZVP//CAM-B3LYP-D3BJ/6-311++G(d,p) along a line perpendicular from the center of the ring plane to 5 Å, with a step size of 0.1 Å for the singlet and triplet state of cyclopentadienyl cation **1** (Figure S43). In agreement with the HOMA values, the triplet state of cyclopentadienyl cation **1** is found to be aromatic, while the singlet state shows anti-aromatic behavior.

In order to quantify the Lewis acidity of $Cp(C_6F_5)_5^+$, its hydride (HIA) and fluoride ion affinities (FIA) were calculated. The resulting very high values of 1021 kJ/mol (HIA) and 771 kJ/mol (FIA) even exceed those of the recently isolated highly reactive perfluorotritylium cation $C(C_6F_5)_3^+$ (HIA: 955 kJ mol^{-1}; FIA: 697 kJ mol^{-1}),[43] rendering cyclopentadienyl cation **1** an extremely superacidic species. The FIA of $Cp(C_6F_5)_5^+$ also exceeds that of SbF5, explaining why SbF_5 (FIA: 496 kJ mol^{-1})[54] must be used in excess for its synthesis.

Reactivity Studies of 1·Sb_3F_{16} and 2. In addition to their structural and spectroscopic characterization, we investigated the reactivity of **1·Sb_3F_{16}** and radical **2** in more detail. **1·Sb_3F_{16}** was found to react readily with the weak Lewis base carbon monoxide in C_6F_6 or SO_2, but unfortunately, we could not isolate a crystalline product. However, we propose the formation of the carbonyl complex **4** in analogy to the previously reported synthesis of an isoelectronic borole carbonyl complex, which was formed in the reaction of CO with the highly Lewis acidic perfluoropentaphenylborole.[55] The formation of **4** was indirectly confirmed by its reaction with water to the corresponding carboxylic acid **5**, which was identified by ^{19}F NMR spectroscopy and sc-XRD. **5** decarboxylates already under the hydrolysis conditions (H_2O, 25 °C) with formation of the novel pentakis(pentafluorophenyl)cyclopentadiene **6** (Scheme 4)

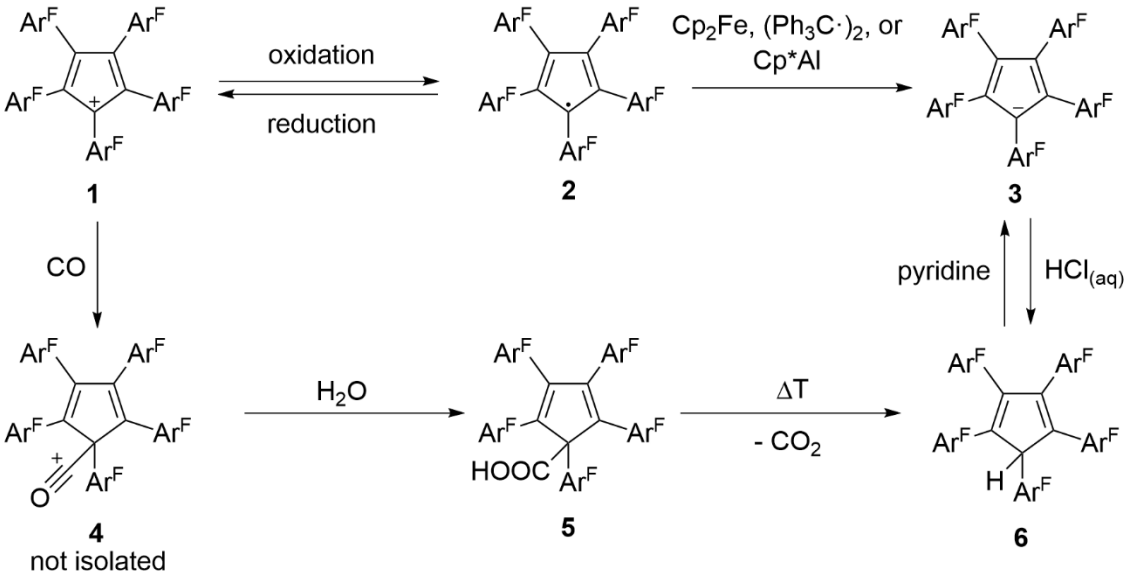

Scheme 4: Reactions of **1·Sb_3F_{16}** and **2**.

Pentakis(pentafluorophenyl)cyclopentadienide **3**, the conjugated base of **6**, was proposed by Reed and Richardson as a "carbon-based weakly coordinating anion", but has not yet been prepared.[56] Compared to the more electron-deficient pentacyanocyclopentadiene[56] and pentakis(trifluoromethyl)-cyclopentadiene,[57,58] compound **6** is expected to be less acidic. However, its larger size and the presence of non-basic C_6F_5 side arms as well as its stability to polymerization and HF formation, make it nonetheless an interesting choice as a strong carbon acid, which forms a weakly coordinating anion (WCA). We have roughly estimated the pK_a value of **6** by chemical means to be between -1 and 4.76,[59] because **3** is protonated by hydrochloric acid, but not by acetic acid, while **6** can be deprotonated with pyridine to give the pyridinium salt pyrH-**3**.

Another promising approach to the formation of salts of anion **3** is the direct reaction of radical **2** with reducing agents. To investigate the scope of this reaction, we performed cyclic voltammetry studies with **2** (o-difluorobenzene, $NBu_4B(Ph\text{-}3,5(CF_3)_2)_4$), which showed a reversible reduction to **3** at a half wave potential of 0.48 V *vs.* ferrocene. Thus, the oxidizing ability of **2** is in a synthetically useful range between NO^+ and Cp_2Fe^+.[60] "Innocent" oxidants, i.e. oxidants that produce no adverse byproducts, have recently gained increased interest because traditional one-electron oxidants such as NO^+ or Ag^+ can induce side reactions due to their Lewis acidity or participation in ligand exchange.[61] Therefore, **2** is a potentially good candidate for such a reagent and has the added advantage of not producing byproducts such as silver metal, NO, or ferrocene, thus avoiding separation difficulties, and reactions of **2** can be monitored visually due to its intense pink color. **2** is purified by sublimation and can be stored for several months even in contact with air and moisture and can be washed with water without significant decomposition (see synthetic details). To investigate its practical usefulness, we have reacted **2** with ferrocene, Gomberg's dimer $(Ph_3C\cdot)_2$, and Cp*Al (Scheme 4), in all cases yielding the respective salts of anion **3** ($FeCp_2$ **3** (**3a**), Ph_3C **3** (**3b**), $(Cp^*)_2Al$ **3** (**3c**)) in single-crystalline and pure form. The molecular structures of **3a-c** have been determined by sc-XRD. They show the expected nearly symmetrical Cp rings with C−C bond lengths ranging from 1.405 Å to 1.415 Å (Table S1). The cations are located near the negatively charged Cp ring with shortest Cp(centroid)-H distances of 2.546 Å, 2.683 Å, and 3.131 Å, respectively (Table S1, Figures S37-39).

Conclusion. The synthesis and structural characterization (sc-XRD) of **1·Sb_3F_{16}** containing the first room-temperature stable cyclopentadienyl cation **1** is reported. sc-XRD, EPR, and SQUID studies prove that **1** adopts the singlet state in the solid state, which is stabilized most likely due to weak intermolecular contacts with solvent or anion molecules. In contrast, the triplet ground state is energetically favored in the gas phase according to quantum chemical calculations. **1·Sb_3F_{16}** shows a high oxidation potential and a very high Lewis acidity. In addition, it reacts readily to the corresponding radical **2**, while the reaction with CO and hydrolytic work-up finally afforded the corresponding pentakis(pentafluorophenyl)cyclopentadiene **6**. The unprecedented access to Cp anions with five C_6F_5 substituents could also enable the preparation of perfluorinated metal complexes in the future and thus provide new impulses in the hitherto poorly explored field of coordination chemistry with fluorinated Cp ligands.[62]

Methods & Protocols

Manipulations were performed under a dry, oxygen-free argon atmosphere, with anhydrous solvents, using cannula and glove-box techniques. **1·Sb_3F_{16}** was synthesized by the reaction of pentakis(pentafluorophenyl)cyclopentadienole **D** with $SbF_5{\cdot}SO_2$ under superacidic conditions, while the reaction of **D** with the Friedel-Crafts-type superacid system $AlBr_3$/EtBr/benzene afforded the corresponding radical **2** in a single step. Oxidation of radical **2** with an excess of XeF_2 and SbF_5 in C_6F_6 also gave the cyclopentadienyl cation **1**, while reactions of **1** with very weak reducing agents gave radical **2**. Hydrolysis of the product obtained from the reaction of **1·Sb_3F_{16}** with carbon monoxide gave the carboxylic acid **5**, which decarboxylates to form pentaphenylcyclopentadiene **6**. The products were characterized by multinuclear NMR (**D**, **3a-d**, **5**, **6**), IR (**D**, **2**, **3a-d**, **5**, **6**), and UV-Vis spectroscopy (**D**, **1**, **2**), and sc-XRD (**B**, **1**, **2**, **3a-c**, **5**, **6**) and details are given in the electronic supplementary material.

Data availability

All data generated or analyzed during this study are included in this published article (and its supplementary information files). The structures of **B**, **1a-b**, **2a-b**, **3a-c**, **5**, and **6** in the solid state were determined by single-crystal X-ray diffraction and the crystallographic data have been deposited with the Cambridge Crystallographic Data Centre as supplementary publication nos. CCDC-2246848 (ys_712a, **1a**), -2246849 (ys_712, **1b**), -2246850 (ys_631a_tw4, **2a**), -2246851 (ys_681, **2b**), -2246852 (ys_679a, **3a**), -2246853 (ys_682am_sq, **3b**), -2246854 (ys_695c, **3c**), -2246857 (ys_719m_sq, **5**), -2246858 (ys_705, **6**), -2246859 (ys_584, **B**), and -2246860 (ys_586 hexakis(pentafluorophenyl)benzene). Copies of the data can be obtained free of charge on application to CCDC, 12 Union Road, Cambridge, CB21EZ (fax: (+44) 1223/336033; e-mail: deposit@ccdc.cam-ak.uk).

Code Availability

DFT and double-hybrid DFT methods, as implemented in the quantum chemistry program packages Gaussian16 Amsterdam Density Functional (ADF), were employed to calculate molecular geometries, orbital energies, charges, NBOs and NICS values. All data generated or analyzed are included in the supplementary information file.

References

1. Faraday M. XX. On new compounds of carbon and hydrogen, and on certain other products obtained during the decomposition of oil by heat. *Phil. Trans. R. Soc.* **115**, 440-466; 10.1098/rstl.1825.0022 (1825).

2. Kaiser, R. “Bicarburet of Hydrogen”. Reappraisal of the Discovery of Benzene in 1825 with the Analytical Methods of 1968. *Angew. Chem. Int. Ed. Engl.* **7**, 345-350; 10.1002/anie.196803451 (1968).
3. Kekulé, A. Ueber die s. g. gepaarten Verbindungen und die Theorie der mehratomigen Radicale. *Justus Liebigs Ann. Chem.* **104**, 129–150; 10.1002/jlac.18571040202 (1857).
4. Kekulé, A. Ueber die Constitution und die Metamorphosen der chemischen Verbindungen und über die chemische Natur des Kohlenstoffs. *Justus Liebigs Ann. Chem.* **106**, 129–159; 10.1002/jlac.18581060202 (1858).
5. Schultz, G. Feier der Deutschen Chemischen Gesellschaft zu Ehren August Kekulé's. *Ber. Dtsch. Chem. Ges.* **23**, 1265–1312; 10.1002/cber.189002301204 (1890).
6. Willstätter, R. & Waser, E. Über Cyclooctatetraen. *Ber. Dtsch. Chem. Ges.* **44**, 3423–3445; 10.1002/cber.191104403216 (1911).
7. Balaban, A. T., Schleyer, P. v. R. & Rzepa, H. S. Crocker, not Armit and Robinson, begat the six aromatic electrons. *Chem. Rev.* **105**, 3436–3447; 10.1021/cr0300946 (2005).
8. Hückel, E. Quantentheoretische Beiträge zum Benzolproblem. *Z. Physik* **70**, 204–286; 10.1007/BF01339530 (1931).
9. Breslow, R. & Yuan, C. The sym-Triphenylcyclopropenyl Cation, a Novel Aromatic System. *J. Am. Chem. Soc.* **80**, 5991–5994; 10.1021/ja01555a026 (1958).
10. Breslow, R., Groves, J. T. & Ryan, G. Cyclopropenyl cation. *J. Am. Chem. Soc.* **89**, 5048; 10.1021/ja00995a042 (1967).
11. Katz, T. J. The Cycloöctatetraenyl Dianion. *J. Am. Chem. Soc.* **82**, 3784–3785; 10.1021/ja01499a077 (1960).
12. Breslow, R. Novel aromatic and antiaromatic systems. *Chem. Rec.* **14**, 1174-1182; 10.1002/tcr.201402070 (2014).
13. Kass, S. R. Cyclopropenyl Anion: An Energetically Nonaromatic Ion. *J. Org. Chem.* **78**, 7370-7372; (10.1021/jo401350m) (2013).
14. Wu, J. I. C., Mo, Y., Evangelista, F. A. & Schleyer, P. v. R. Is cyclobutadiene really highly destabilized by antiaromaticity? *Chem. Commun.* **48**, 8437-8439; (10.1039/C2CC33521B) (2012).
15. Breslow, R. & Hoffman, J. M. Antiaromaticity in the parent cyclopentadienyl cation. Reaction of 5-iodocyclopentadiene with silver ion. *J. Am. Chem. Soc.* **94**, 2110–2111; 10.1021/ja00761a051 (1972).
16. Saunders, M. *et al.* Unsubstituted cyclopentadienyl cation, a ground-state triplet. *J. Am. Chem. Soc.* **95**, 3017–3018; 10.1021/ja00790a049 (1973).
17. Breslow, R., Hill, R. & Wasserman, E. Pentachlorocyclopentadienyl Cation, a Ground-State Triplet. *J. Am. Chem. Soc.* **86**, 5349–5350; 10.1021/ja01077a072 (1964).
18. Vančik, H., Novak, I. & Kidemet, D. IR Matrix Spectroscopy of Pentachlorocyclopentadienyl Cation $C_5Cl_5^+$. Effect of Chlorine as a Substituent. *J. Phys. Chem. A* **101**, 1523–1525; 10.1021/jp961610h (1997).
19. Baird, N. C. Quantum organic photochemistry. II. Resonance and aromaticity in the lowest 3.pi.pi.* state of cyclic hydrocarbons. *J. Am. Chem. Soc.* **94**, 4941–4948; 10.1021/ja00769a025 (1972).
20. Karas, L. J. & Wu, J. I. Baird’s rules at the tipping point. *Nat. Chem.* **14**, 723–725; 10.1038/s41557-022-00988-z (2022).
21. Yager, W. A. A Stable Triplet State of Pentaphenylcyclopentadienyl Cation. *J. Am. Chem. Soc.* **85**, 2033–2034; 10.1021/ja00896a042 (1963).
22. Breslow, R., Chang, H. W., Hill, R. & Wasserman, E. Stable Triplet States of Some Cyclopentadienyl Cations. *J. Am. Chem. Soc.* **89**, 1112–1119; 10.1021/ja00981a015 (1967).

23. Broser, W., Siegle, P. & Kurreck, H. Über substituierte Pentaphenyl-cyclopentadienyl-Verbindungen und Tetracyclone, IV Unsymmetrischp-methyl- und *p*-phenyl-substituierte Pentaphenyl-cyclopentadienyl-Kationen und -Radikale. *Chem. Ber.* **101**, 69-83; 10.1002/cber.19681010111 (1968).
24. Broser, W., Kurreck, H. & Siegle, P. Über substituierte Pentaphenylcyclopentadienyl-Verbindungen und Tetracyclone, III. Symmetrische Cyclopentadienyl-Kationen mit nachweisbaren Triplettzuständen. *Chem. Ber.* **100**, 788-794; 10.1002/cber.19671000312 (1967).
25. Breslow, R. & Mazur, S. Electrochemical determination of pK_R^+ for some antiaromatic cyclopentadienyl cations. *J. Am. Chem. Soc.* **95**, 584–585; 10.1021/ja00783a046 (1973).
26. Breslow, R. Quantitative studies on aromaticity and antiaromaticity. *Pure Appl. Chem.* **28**, 111–130; 10.1351/pac197128020111 (1971).
27. Lossing, F. P. & Traeger, J. C. Stabilization in cyclopentadienyl, cyclopentenyl, and cyclopentyl cations. *J. Am. Chem. Soc.* **97**, 1579–1580; 10.1021/ja00839a053 (1975).
28. Gompper, R. & Glöckner, H. Stable Cyclopentadienylium Salts. *Angew. Chem. Int. Ed. Engl.* **23**, 53–54; 10.1002/anie.198400532 (1984).
29. Lambert, J. B., Lin, L. & Rassolov, V. The Stable Pentamethylcyclopentadienyl Cation. *Angew. Chem. Int. Ed. Engl.* **41**, 1429-1431; 10.1002/1521-3773(20020415)41:8<1429::AID-ANIE1429>3.0.CO;2-J (2002).
30. Otto, M. *et al.* The Stable Pentamethylcyclopentadienyl Cation Remains Unknown. *Angew. Chem. Int. Ed. Engl.* **41**, 2275; 10.1002/1521-3773(20020703)41:13<2275::AID-ANIE2275>3.0.CO;2-1 (2002).
31. Jones, J. N., Cowley, A. H. & Macdonald, C. L. B. The crystal structure of the 'pentamethylcyclopentadienyl cation' is that of the pentamethylcyclopentenyl cation. *Chem. Commun.,* 1520–1521; 10.1039/b205081a (2002).
32. Müller, T. Comment on the X-Ray Structure of Pentamethylcyclopentadienyl Cation. *Angew. Chem. Int. Ed. Engl.* **41**, 2276–2278; 10.1002/1521-3773(20020703)41:13<2276::AID-ANIE2276>3.0.CO;2-W (2002).
33. Lambert, J. B. Statement. *Angew. Chem. Int. Ed. Engl.* **41**, 2278; 10.1002/1521-3773(20020703)41:13<2278::AID-ANIE2278>3.0.CO;2-K (2002).
34. Breslow, R. & Chang, H. W. The Rearrangement of the Pentaphenylcyclopentadienyl Cation. *J. Am. Chem. Soc.* **83**, 3727-3728; 10.1021/ja01478a046 (1961).
35. Rupf, S. M., Pröhm, P. & Malischewski, M. The 2+2 cycloaddition product of perhalogenated cyclopentadienyl cations: structural characterization of salts of the $C_{10}Cl_{10}^{2+}$ and $C_{10}Br_{10}^{2+}$ dications. *Chem. Commun.* **56**, 9834-9837; 10.1039/d0cc04226a (2020).
36. Jutzi, P. & Mix, A. Synthesen mit dem Reagenz Pentamethylcyclopentadienylbromid/Silbertetrafluoroborat: Das Pentamethylcyclopentadienyl-Kation als reaktive Zwischenstufe. *Chem. Ber.* **125**, 951–954; 10.1002/cber.19921250429 (1992).
37. Costa, P., Trosien, I., Mieres-Perez, J. & Sander, W. Isolation of an Antiaromatic Singlet Cyclopentadienyl Zwitterion. *J. Am. Chem. Soc.* **139**, 13024-13030; 10.1021/jacs.7b05807 (2017).
38. Kalon J. Iversen, David J. D. Wilson & Jason L. Dutton. A Computational Study on a Strategy for Isolating a Stable Cyclopentadienyl Cation. *Chem. Eur. J.* **20**, 14132–14138; 10.1002/chem.201403748 (2014).
39. Fan, C., Piers, W. E. & Parvez, M. Perfluoropentaphenylborole. *Angew. Chem. Int. Ed. Engl.* **48**, 2955–2958; 10.1002/anie.200805865 (2009).
40. Webb, A. F. & Gilman, H. Reactions of some perhaloarenes with metals and metal halides. *J. Organomet. Chem.* **20**, 281–283; 10.1016/S0022-328X(00)80121-7 (1969).
41. Cairncross, A., Sheppard, W. A. & Wonchoba, E. Pentafluorophenylcopper tetramer, a reagent for synthesis of fluorinated aromatic compounds. *Org. Synth.* **59**, 122; 10.15227/orgsyn.059.0122 (1979).

42. Birchall, J. M., Bowden, F. L., Haszeldine, R. N. & Lever, A. B. P. Polyfluoroarenes. Part IX. Decafluorotolan: synthesis, properties, and use as an organometallic ligand. *J. Chem. Soc., A,* 747; 10.1039/j19670000747 (1967).
43. Hoffmann, K. F. *et al.* The Tris(pentafluorophenyl)methylium Cation: Isolation and Reactivity. *Angew. Chem. Int. Ed. Engl.* **61**, e202203777; 10.1002/anie.202203777 (2022).
44. Bondi, A. van der Waals Volumes and Radii. *J. Phys. Chem.* **68**, 441–451; 10.1021/j100785a001 (1964).
45. Becke, A. D. Density-functional exchange-energy approximation with correct asymptotic behavior. *Phys. Rev. A* **38**, 3098–3100; 10.1103/physreva.38.3098 (1988).
46. Lee, C., Yang, W. & Parr, R. G. Development of the Colle-Salvetti correlation-energy formula into a functional of the electron density. *Phys. Rev. B* **37**, 785–789; 10.1103/physrevb.37.785 (1988).
47. Grimme, S., Ehrlich, S. & Goerigk, L. Effect of the damping function in dispersion corrected density functional theory. *J. Comp. Chem.* **32**, 1456–1465; 10.1002/jcc.21759 (2011).
48. Yanai, T., Tew, D. P. & Handy, N. C. A new hybrid exchange–correlation functional using the Coulomb-attenuating method (CAM-B3LYP). *Chem. Phys. Lett.* **393**, 51–57; 10.1016/j.cplett.2004.06.011 (2004).
49. Grimme, S. Semiempirical hybrid density functional with perturbative second-order correlation. *J. Chem. Phys.* **124**, 34108; 10.1063/1.2148954 (2006).
50. Gleiter, R. & Haberhauer, G. *Aromaticity and Other Conjugation Effects*. (Wiley-VCH, 2012).
51. Julg, A. & Franois, P. Recherches sur la géomtrie de quelques hydrocarbures non-alternants: son influence sur les énergies de transition, une nouvelle définition de l'aromaticité. *Theoret. Chim. Acta* **8**, 249–259; 10.1007/BF00527311 (1967).
52. Krygowski, T. M. & Cyrański, M. Separation of the energetic and geometric contributions to the aromaticity of π-electron carbocyclics. *Tetrahedron* **52**, 1713–1722; 10.1016/0040-4020(95)01007-6 (1996).
53. Chen, Z., Wannere, C. S., Corminboeuf, C., Puchta, R. & Schleyer, P. v. R. Nucleus-independent chemical shifts (NICS) as an aromaticity criterion. *Chem. Rev.* **105**, 3842–3888; 10.1021/cr030088 (2005).
54. Erdmann, P., Leitner, J., Schwarz, J. & Greb, L. An Extensive Set of Accurate Fluoride Ion Affinities for p-Block Element Lewis Acids and Basic Design Principles for Strong Fluoride Ion Acceptors. *Chemphyschem* **21**, 987–994; 10.1002/cphc.202000244 (2020).
55. Fukazawa, A. *et al.* Reaction of pentaarylboroles with carbon monoxide: an isolable organoboron carbonyl complex. *Chem. Sci.* **3**, 1814; 10.1039/c2sc20336g (2012).
56. Richardson, C. & Reed, C. A. Exploration of the pentacyano-cyclo-pentadienide ion, C(5)(CN)(5)(-), as a weakly coordinating anion and potential superacid conjugate base. Silylation and protonation. *Chem. Commun.* 706-707; 10.1039/b316122f (2004).
57. Sievers, R., Sellin, M., Rupf, S. M., Parche, J. & Malischewski, M. Introducing the Perfluorinated Cp* Ligand into Coordination Chemistry. *Angew. Chem. Int. Ed. Engl.* **61**, e202211147; 10.1002/anie.202211147 (2022).
58. Laganis, E. D. & Lemal, D. M. 5H-(Perfluoropentamethyl)cyclopentadiene, an extraordinary carbon acid. *J. Am. Chem. Soc.* **102**, 6633–6634; 10.1021/ja00541a075 (1980).
59. Goldberg, R. N., Kishore, N. & Lennen, R. M. Thermodynamic Quantities for the Ionization Reactions of Buffers. *J. Phys. Chem. Ref. Data* **31**, 231-370; 10.1063/1.1416902 (2002).
60. Connelly, N. G. & Geiger, W. E. Chemical Redox Agents for Organometallic Chemistry. *Chem. Rev.* **96**, 877–910; 10.1021/cr940053x (1996).
61. Schorpp, M. *et al.* Synthesis and Application of a Perfluorinated Ammoniumyl Radical Cation as a Very Strong Deelectronator. *Angew. Chem. Int. Ed. Engl.* **59**, 9453-9459; 10.1002/anie.202002768 (2020).

62. Sievers, R., Parche, J., Kub, N. G. & Malischewski, M. Synthesis and Coordination Chemistry of Fluorinated Cyclopentadienyl Ligands. *Synlett*; 10.1055/s-0042-1751426 (2023).

Acknowledgements

The University of Duisburg-Essen is acknowledged for generous financial support. We thank B. Geoghegan and G. E. Cutsail III (MPI CEC, Mülheim an der Ruhr, Germany), for EPR and SQUID measurements, M. Weinert for CV studies, and T. Schaller, F. Niemeyer, and B. Römer (University of Duisburg-Essen) for NMR measurements. M.M and S.M.R. thank the Deutsche Forschungsgemeinschaft (DFG, German Research Foundation) for financial support (project ID 387284271, SFB 1349).

Author contributions

Y. Schulte: Conceptualization, Investigation, Validation, Formal Analysis, Writing - Original Draft, Visualization. C. Wölper: Single Crystal X-ray Analysis. S. M. Rupf / M. Malischewski: cyclic voltammetry studies in liquid SO_2. G. Haberhauer: Writing – Original Draft – Review and Editing, Visualization, performing calculations. S. Schulz: Conceptualization, Writing – Original Draft – Review and Editing, Visualization, Supervision, Project administration.

Additional Information

Supplementary information (general experimental procedures, experimental details synthesis and characterization, quantum chemical details) is available in the online version of the paper. Reprints and permissions information is available online at www.nature.com/reprints.

Competing financial interests

The authors declare no competing financial interests.

Supporting Information

Structural Characterization and Reactivity of a Room Temperature-Stable, Antiaromatic Cyclopentadienyl Cation Salt

Yannick Schulte,[a] Christoph Wölper,[a], Susanne M. Rupf,[d] Moritz Malischewski,[d] Gebhard Haberhauer,[b] and Stephan Schulz[a;c]**

[a] Institute of Inorganic Chemistry, University of Duisburg-Essen, Universitätsstraße 5-7, D-45141 Essen, Germany

email: stephan.schulz@uni-due.de; https://www.uni-due.de/ak_schulz/index_en.php

[b] Institute of Organic Chemistry, University of Duisburg-Essen, Universitätsstraße 5-7, D-45141 Essen, Germany

email: gebhard.haberhauer@uni-due.de; https://www.uni-due.de/akhaberhauer/

[c] Institute of Inorganic Chemistry and Center for Nanointegration Duisburg-Essen (CENIDE), University of Duisburg-Essen, Carl-Benz-Straße 199, D-47057 Duisburg, Germany.

[d] Institute of Inorganic Chemistry, Freie Universität Berlin, Fabeckstr. 34-36, D-14195 Berlin, Germany

E-mail: moritz.malischewski@fu-berlin.de

Table of Contents

Experimental Section

General Procedures. All manipulations were performed using standard Schlenk and glovebox techniques under argon, which was dried by passing through preheated reduced BTS catalyst and molecular sieve columns. Toluene and *n*-hexane were dried with a MBraun solvent purification system, while benzene, THF, and deuterated benzene, and THF were distilled from Na/K alloy. Hexafluorobenzene was stirred with oleum for three days, washed with saturated K_2CO_3 solution (after careful phase separation), dried with $MgSO_4$, followed by molecular sieves (4 Å), and finally distilled from $SbF_5{\cdot}SO_2$. Decaline and deuterated DCM were dried over molecular sieves. All solvents except SO_2 were degassed and stored over activated molecular sieves (4 Å). SO_2 was stored over P_2O_5. ^1H, ^{13}C, and ^{19}F NMR spectra were referenced to internal C_6D_5H (^1H: δ = 7.16 ppm; ^{13}C: δ = 128.06 ppm), thf-d_7 (^1H: δ = 1.72 ppm; ^{13}C: δ = 25.31 ppm), acetone-d_6 (^1H: δ = 2.05 ppm; ^{13}C: δ = 53.84 ppm) and $CHDCl_2$ (^1H: δ = 5.32 ppm; ^{13}C: δ = 53.84 ppm) and external $CFCl_3$ (^{19}F: δ = 0 ppm).

IR spectra were recorded in a glovebox using a BRUKER ALPHAT FT-IR spectrometer equipped with a single reflection ATR sampling module.

Microanalysis was not performed, because the analysis of a model compound (bromopentafluorobenzene calc.: C 29.18 %, H 0 %, N 0 %; found: C 1.94 %, H 0.25 %, N 0.157 %) showed that our equipment is not suitable for the analysis of highly fluorinated compounds.

Cyclovoltammetric studies in 1,2-difluorobenzene were performed in a glovebox using a Metrohm Autolab PGSTAT 204 potentiostat with a three-electrode setup consisting of a Pt disk (d = 1 mm) working electrode, Pt wire counter electrode, and an Ag wire pseudo-reference electrode, and ferrocene as internal standard. Positive feedback compensation was utilized to reduce the effects of solvent resistances. Cyclic voltammetry in SO_2 was performed on an Interface 1010 B Potentiostat/Galvanostat/ZRA from Gamry Instruments. The investigations were carried out starting from 0 V going to the oxidation first and then to the reduction. The measurements were performed in anhydrous and oxygen-free SO_2 under argon atmosphere using 0.1 M $TBASbF_6$ as supporting electrolyte and platinum wires as working-, counter-, and quasireference electrodes. SO_2 was distilled from CaH_2 and stored in a stainless-steel cylinder. Voltammograms were internally referenced against $FeCp_2^{0/+}$ using $Li_2B_{12}Cl_{12}$[1] as internal reference. The OriginPro 2017G software was used to plot the data.[2]

For EPR measurements, samples of **1** and **2** in SO_2 and toluene, respectively, were prepared in a glovebox in 50 µL capillaries (Hirschmann), sealed with critoseal. Continuous-wave (CW) X-band EPR spectra at room temperature (~9.43 GHz) were collected using a Bruker MS 5000 spectrometer. The spectra were obtained with 100 kHz field modulation frequency, 0.1 G modulation amplitude, and a scan time of 240 s. An effective time constant of 0.05 sec was applied digitally to the ~60 k point spectrum. The EPR data were processed and analysed in Matlab R2019b and simulated using the EasySpin package (v. 6.0.0-dev.30).[3]

Starting reagents were commercially available or freshly prepared.

Synthetic Details

Caution!: Pentafluorophenyl copper and the complex of pentafluorophenylmagnesium bromide with diethyl ether have not, to the best of our knowledge, been reported to be explosive. However, a variation of the preparation described here, in which the complex of pentafluorophenylmagnesium bromide with diglyme was dried *in vacuo,* resulted in a vigorous

decomposition under pressure build-up which destroyed the apparatus. This happened only once although the preparation was carried out several times. Caution should be exercised because the exact cause of the decomposition is unknown. The following procedure avoids isolation of this complex.

Bis(pentafluorophenyl)ethyne B: 400 mmol (9.72 g) of magnesium turnings were suspended in diethyl ether (133 mL). At 0 °C 400 mmol (43.59 g, 29.9 mL) bromoethane was slowly added to this suspension. The resulting mixture was warmed to room temperature and stirred overnight. The light gray solution was cooled to 0 °C and 400 mmol (98.78 g, 50.65 mL) of bromopentafluorobenzene, 500 mmol (67.1 g, 71.4 mL) of diglyme (diethylene glycol dimethyl ether), and 400 mmol (57 g) of CuBr were slowly added in sequence. The resulting white semi-solid mass was dried *in vacuo* for 1 h and then re-suspended in 400 mL diglyme. 100 mmol (9.76 mL, 26.47 g) of tribromoethylene was added slowly at 0 °C. The suspension slowly turned brown upon stirring at 120 °C for 24 h. It was then diluted on air with 500 mL ethyl acetate, 100 mL saturated $NH_4Cl_{(aq)}$ solution, 40 mL acetic acid, and 200 mL H_2O. The aqueous phase was discarded, and the organic phase was washed five times with H_2O. It was then dried with $MgSO_4$, concentrated on a rotary evaporator, and stripped of any remaining volatiles at 10^{-3} mbar. A by-product (probably decafluorobiphenyl) was removed by sublimation at 60 °C/10^{-3} mbar. The remaining crude product was crystallized from methanol at -30 °C.

Yield 14.4 g, 40.1 mmol, 40 %. **^{19}F NMR** (376 MHz, C_6D_6) δ -135.61 – -135.75 (m, 4F, *ortho*), -150.34 (t, 2F, $^3J_{FF}$ = 22.0 Hz, *para*), -161.29 – -161.47 (m, 4F, *meta*), ppm. Other analytical data are consistent with those reported in the literature.[1]

Comments: The protocol was adapted from a literature procedure.[4] In contrast to Webb and Gilman, we found a higher reaction temperature and the use of diglyme instead of THF more convenient due to the shorter reaction time. The aqueous workup prevents the formation of finely divided Cu_2O, which is otherwise difficult to remove by filtration.

Tetrakis(pentafluorophenyl)cyclopentadienone C: 40.1 mmol (14.4 g) of bis(pentafluorophenyl)ethyne and 42.1 mmol (14.4 g) of $Co_2(CO)_8$ were suspended in decaline (100 mL) and stirred until gas evolution has stopped (4 h). The solution was then stirred at 190 °C for 24 h to form a metal mirror. The flask was cooled to room temperature, the solution was diluted with 100 mL of ethyl acetate and 86.3 mmol (21.9 g) of I_2 was added. The suspension was stirred until dissolution of the metal mirror and complete cessation of gas evolution (15 min). The solution was diluted with ethyl acetate (500 mL) and washed with aqueous $NaHSO_3$ solution (200 mL, 30 %). The aqueous phase was discarded. The organic phase was dried with $MgSO_4$ and filtered over about 50 mL of active Al_2O_3. All volatiles were removed first on a rotary evaporator and then by distillation at up to 160 °C/10^{-3} mbar. The product was then washed with 100 mL of *n*-hexane at -78 °C and recrystallized from $CHCl_3$ at -30 °C.

Yield 12.0 g, 16.1 mmol, 80 %. **^{19}F NMR** (376 MHz, C_6D_6) δ -137.57 – -137.82 (m, 8F, *ortho*), -145.76 (t, 2F, $^3J_{FF}$ = 21.6 Hz, *para*), 147.97 (t, 2F, $^3J_{FF}$ = 21.6 Hz, *para*), -157.96 – -158.17 (m, 4F, *meta*), -159.25 – -159.44 (m, 4F, *meta*) ppm. Other analytical data match those reported in the literature.[5]

Comments: Variations of this procedure omitting the oxidation step have been known for a long time,[6] but in our hands the main product of these reactions was a cobalt-containing complex of unknown structure. Oxidation of this complex with iodine yields the desired product.

Pentakis(pentafluorophenyl)cyclopentadienol D: 19.3 mmol (4.77 g, 2.41 mL) of bromopentafluorobenzene was slowly added at 0 °C to a solution of 19.3 mmol (6.44 mL) EtMgBr in diethyl ether (3 mol/L). All volatiles were removed under vacuum and the resulting colorless solid was redissolved in THF (10 mL). This solution was slowly added at –78 °C to a suspension of tetrakis(pentafluorophenyl)cyclopentadienone (16.1 mmol, 12.0 g) in THF (100 mL). The resulting mixture was gradually warmed to 25 °C within 4 h. Then 3 mL HCl_{aq} (37 %), 100 mL diethyl ether, and 100 mL of water were added. The aqueous phase was discarded and the organic phase was washed with 100 mL of water. The solution was dried with $MgSO_4$ and all volatiles were removed under reduced pressure using a rotary evaporator. The product was purified by column chromatography (*n*-hexane/diethyl ether 20:1; R_f = 0.30; colorless band with a blue fluorescence).

Yield 10.3 g, 11.3 mmol, 58 %. **Mp** 216 °C. **^{19}F NMR** (565 MHz, CD_2Cl_2) δ -134.96 (br s, 1F, $HOCC_6F_5$, *ortho*), -137.97 (br s, not integratable, $HOCCCC_6F_5$, *ortho*) -138.92 (m, 2F, $HOCCC_6F_5$, *ortho*), -139.53 (d, 2F, $^3J_{FF}$ = 21.7 Hz, $HOCCC_6F_5$, *ortho*), -144.02 (d, 2F, $^3J_{FF}$ = 21.3 Hz, $HOCC_6F_5$, *ortho*), -150.01(t, 2F, $^3J_{FF}$ = 20.8 Hz, $HOCCC_6F_5$ or $HOCCCC_6F_5$, *para*), -150.10 (t, 2F, $^3J_{FF}$ = 21.0 Hz, $HOCCC_6F_5$ or $HOCCCC_6F_5$, *para*), -152.60 (t, 1F, $^3J_{FF}$ = 21.2 Hz, $HOCC_6F_5$, *para*), -159.73 (td, 2F, $^3J_{FF}$ = 21.7 Hz, 7.7 Hz, $HOCCC_6F_5$, *meta*), -159.85 (td, 2F, $^3J_{FF}$ = 21.8 Hz, 7.7 Hz, $HOCCC_6F_5$, *meta*), -160.08 (td, 2F, $^3J_{FF}$ = 21.7 Hz, 7.7 Hz, $HOCCCC_6F_5$, *meta*), -160.45 (br t, 2F, $^3J_{FF}$ = 21.4 Hz, $HOCC_6F_5$, *meta*), -162.30 (br t, 2F, $^3J_{FF}$ = 20.9 Hz, $HOCC_6F_5$, *meta*). **^{1}H NMR** (400 MHz, C_6D_6) δ 3.40 (s, CpOH). **^{13}C{^{19}F} NMR** (151 MHz, CD_2Cl_2) δ 148.04 ($HOCC_6F_5$, *ortho*), 145.24 ($HOCCCC_6F_5$, *ortho*), 144.86 ($HOCC_6F_5$, *ortho*), 144.48 ($HOCCC_6F_5$, *ortho*), 144.35 ($HOCCC_6F_5$, *ortho*), 142.72 ($HOCCC_6F_5$ or $HOCCCC_6F_5$, *para*), 142.65 ($HOCCC_6F_5$ or $HOCCCC_6F_5$, *para*), 141.84, 141.83, 141.76 ($HOCC_6F_5$, *para*), 138.77 ($HOCC_6F_5$, *meta*), 138.26 ($HOCCCC_6F_5$, *meta*), 138.20 ($HOCCC_6F_5$, *meta*), 138.09 ($HOCC_6F_5$, *meta*), 137.86 ($HOCC_6F_5$, *meta*), 135.85 (HOCCC), 109.43 (HOCC), 106.76 ($HOCC_6F_5$ or $HOCCC_6F_5$, *ipso*), 106.36 ($HOCC_6F_5$ or $HOCCC_6F_5$, *ipso*), 90.36 (HOC). **ATR-IR** ν = 3601, 1646, 1514, 1484, 1341, 1305, 1118, 1088, 982, 912, 803, 731 cm^{-1}.

Pentakis(pentafluorophenyl)cyclopentadienyl hexadecafluorotriantimonate 1: Pentakis(pentafluorophenyl)cyclopentadienyl radical **2** (10 µmol, 8.6 mg) and $SbF_5{\cdot}SO_2$ (40 µmol, 11.2 mg) were suspended in 0.5 mL of hexafluorobenzene. 200 µmol (33.9 mg) of XeF_2 was added and the mixture was stirred for 30 min at 25 °C, resulting in the formation of a colorless gas, a deep blue solution, and a blue precipitate. The solution was decanted from the solid by using a glass syringe, sealed in a glass ampoule, and stored at 6 °C for three days.

The first run of this reaction gave the solvate $Cp(C_6F_5)_5Sb_3F_{16}{\cdot}2\ C_6F_5$ **1b**, all subsequent runs gave $Cp(C_6F_5)_5Sb_3F_{16}{\cdot}1.5\ C_6F_5$ **1a**. The yield varied from 8.6 mg to 15.1 mg (47-81 %) for solvate **1a** and was not determined for **1b**.

Alternative preparation: 10 µmol (9.1 mg) pentakis(pentafluorophenyl)cyclopentadienol **D** and 40 µmol (11.2 mg) $SbF_5{\cdot}SO_2$ were suspended in 0.5 mL hexafluorobenzene and stirred for 30 min at 25 °C, resulting in the formation of a deep blue solution and a blue precipitate. The solution

was decanted from the solid using a glass syringe, and further treated as above, yielding crystals with identical cell parameters and color.

In situ NMR spectroscopy: Pentakis(pentafluorophenyl)cyclopentadienol **D** (10 µmol, 9.1 mg) was dissolved in 0.5 mL of SO_2 at -78 °C in a Teflon-capped NMR tube, which also contained a capillary with acetone-d_6 and the first NMR spectrum was measured at -30 °C. The solution was again cooled to -78 °C, 50 µmol (14.0 mg) $SbF_5{\cdot}SO_2$ were sublimed into the NMR tube, and the second NMR spectrum was measured at -30 °C.

Comments: The use of a glass syringe is necessary, because **1** reacts immediately with polypropylene syringes to form **2** and unidentified other products. An excess of XeF_2 is also necessary because $SbF_5{\cdot}SO_2$ catalyzes the reaction of XeF_2 with hexafluorobenzene. For the second preparation, starting from **D**, the formation of hydroxide-containing counteranions $Sb_3(OH)_nF_{(16-n)}$ cannot be completely excluded. Crystals for sc-XRD were therefore obtained from the first reaction (oxidation of **2**).

UV-Vis (hexafluorobenzene): λ_{max} (log ε) = 678 nm (4.68).

Caution! When XeF_2 and $SbF_5{\cdot}SO_2$ are premixed and the solvent is added subsequently, a vigorous reaction with flame formation may occur even in the absence of air.

Pentakis(pentafluorophenyl)cyclopentadienyl radical 2: 1 mmol (912 mg) pentakis(pentafluorophenyl)cyclopentadienol and 20 mmol (5.33 g) $AlBr_3$ were suspended in 3 mL of benzene and 10 mmol (1.09 g, 746 µL) of bromoethane was slowly added at 0 °C. The red suspension was warmed to 25 °C, stirred for 30 min, and subsequently cooled to 0 °C. The suspension was filtered, and the filtrate was discarded. The solid was quenched with 200 mmol (3.6 g) ice and the mixture was kept at 25 °C until completely thawed. The solution was then removed by filtration and the solid was washed rapidly three times with 10 mL of water at 0 °C. All volatiles were removed under reduced pressure and the solid was sublimed at 150 °C/10^{-3} mbar over 2 days. The sublimate was crystallized three times from 1 mL of toluene and again all volatiles were removed under vacuum.

Yield 484 mg, 541 µmol, 54 %. **Mp** 236 °C, evaporates undecomposed at approx. 300 °C. **ATR-IR** ν = 1647, 1517, 1487, 1383, 1344, 1312, 1138, 1104, 1079, 983, 919, 911, 836, 730, 654, 542 cm^{-1}. **UV-Vis** (hexafluorobenzene): λ_{max} (log ε) = 546 nm (3.41).

Comments: The washing steps can be performed in a Büchner funnel without the need for an inert gas atmosphere, since crystalline **2** is stable under these conditions. The mother liquors and the liquid portion of the reaction mixture contain mainly pentakis(pentafluorophenyl)cyclopentadiene and can be used for the preparation of pyridinium pentakis(pentafluorophenyl)cyclopentadienide.

Ferrocenium pentakis(pentafluorophenyl)cyclopentadienide 3a: 5 µmol (4.5 mg) pentakis(pentafluorophenyl)cyclopentadienyl radical and 6 µmol (1.1 mg) ferrocene were dissolved in 0.3 mL 1,2-difluorobenzene. The product was crystallized by vapor phase diffusion with 3 mL *n*-hexane.

Yield 3.5 mg, 3.2 µmol, 65 %. **Mp** 232 °C. **^{19}F NMR** (565 MHz, thf-d_8) δ -142.96 (dd, 10F, $^3J_{FF}$ = 25.2 Hz, $^4J_{FF}$ = 8.3 Hz, *ortho*), -163.13 (t, 5F, $^3J_{FF}$ = 21.5 Hz, *para*), -166.38 – -166.51 (m, 10F, *meta*). **^{13}C NMR** (151 MHz, CD_2Cl_2) δ 145.1 (d, $^1J_{FC}$ = 243 Hz, *meta*), 139.2 (d, $^1J_{FC}$ = 243 Hz, *para*), 138.3zz (dt, $^1J_{FC}$ = 246 Hz, *ortho*, $^2J_{FC}$ = 14.5 Hz), 116.7 (t, $^2J_{FC}$ = 19.3 Hz, *ipso*), 108.5 ($C_5(C_6F_5)_5$). **ATR-IR** ν = 3111, 3075, 1514, 1471, 1418, 1282, 1267, 1098, 976, 915, 849, 759, 540 cm^{-1}.

Tritylium pentakis(pentafluorophenyl)cyclopentadienide 3b: 5 µmol (4.5 mg) of pentakis(pentafluorophenyl)cyclopentadienyl radical and 3 µmol (1.7 mg) of trityl$_2$·toluene were heated to 110 °C in 0.5 mL of toluene until all solids were dissolved (about 10 min). The solution was then slowly cooled to 25 °C and left undisturbed for 24 h, resulting in the formation of large yellow-green needles.

Yield 4.9 mg, 4.4 µmol, 87 %. **Mp** 227 °C. **^{19}F NMR** (565 MHz, CD_2Cl_2) δ -142.71 (dd, 10F, $^3J_{FF}$ = 25.6 Hz, $^4J_{FF}$ = 7.4 Hz, *ortho*), -161.53 (t, 5F, $^3J_{FF}$ = 21.5 Hz, *para*), -164.97 – -165.16 (m, 10F, *meta*). **^{1}H NMR** (400 MHz, CD_2Cl_2) δ 7.91 (br s). The signals in the ^{13}C NMR spectrum were too broad to be well resolved. **ATR-IR** ν = 2945, 1574, 1516, 1479, 1350, 1290, 1181, 1099, 982, 916, 839, 764, 701, cm^{-1}.

Decamethylaluminocenium pentakis(pentafluorophenyl)cyclopentadienide 3c: 5 µmol (4.5 mg) of pentakis(pentafluorophenyl)cyclopentadienyl radical and 10 µmol (1.6 mg) of Cp*Al were heated to 110 °C in 0.5 mL of toluene until all reagents dissolved (about 10 min). This process was accompanied by the formation of a gray, finely dispersed solid (probably aluminum metal). The solution was then cooled to 25 °C. The grayish solid formed was isolated by centrifugation and extracted with 0.5 mL CH_2Cl_2. The extract was evaporated to dryness at 25 °C/10^{-3} mbar.

The formation of single crystals was achieved by immersing the product in a small glass tube (5 mm diameter) containing 1 mL of benzene and heating the lower end of the solution to 80 °C, while keeping the upper end at 25 °C.

Yield 5.3 mg, 4.9 µmol, 89 % (before crystallization). **Mp** 230 °C. **^{19}F NMR** (565 MHz, CD_2Cl_2) δ -142.74 (dd, 10F, $^3J_{FF}$ = 25.5 Hz, $^4J_{FF}$ = 7.0 Hz, *ortho*), -161.57 (t, 5F, $^3J_{FF}$ = 21.0 Hz, *para*), -165.04 – -165.17 (m, 10F, *meta*). **^{1}H NMR** (600 MHz, CD_2Cl_2) δ 2.16. **^{13}C NMR** (151 MHz, CD_2Cl_2) δ 144.4 (d, $^1J_{FC}$ = 241 Hz, *meta*), 138.9 (d, $^1J_{FC}$ = 248 Hz, *para*), 137.8 (dt, $^1J_{FC}$ = 248 Hz, *ortho*, $^2J_{FC}$ = 14.0f Hz), 119.3 (C_5Me_5), 115.5 (t, $^2J_{FC}$ = 19.3 Hz, *ipso*), 107.9 ($C_5(C_6F_5)_5$) 10.4 (C_5Me_5). **ATR-IR** ν = 2952, 2914, 2867, 1514, 1481, 1098, 982, 916, 653, 623, 574, 538 cm^{-1}.

Comments: The unusual shape of the ^{1}H NMR signal has been reported previously.[7]

Pyridinium pentakis(pentafluorophenyl)cyclopentadienide 3d: The combined mother liquors of **2**, including the soluble fraction of the reaction mixture, were washed with dilute hydrochloric acid (1 mol/L), dried with $MgSO_4$, and degassed by three freeze-thaw-pump cycles. 1 mmol (79.1 mg; 80.7 µL) of pyridine was added, initiating the formation of a colorless precipitate, which was removed by filtration, washed three times with 3 mL of benzene, and dried under reduced pressure.

Yield 302 mg, 314 µmol, 31 % (with respect to reagent **D**). **Mp** 218 °C. **^{19}F NMR** (565 MHz, thf-d_8) δ -143.02 (dd, 10F, $^3J_{FF}$ = 24.6 Hz, $^4J_{FF}$ = 7.7 Hz, *ortho*), -162.62 (t, 5F, $^3J_{FF}$ = 21.3 Hz, *para*), -166.03 – -166.22 (m, 10F, *meta*). **^{1}H NMR** (400 MHz, thf-d_8) δ 8.56 – 8.53 (m, 2H, *ortho*), 7.56 (tt, 1H, $^3J_{HH}$ = 7.6 Hz, $^4J_{HH}$ = 1.l9 Hz, *para*) 7.27 – 7.23 (m, 2H, *meta*). The signals in the ^{13}C NMR spectrum were too broad to be well resolved. **ATR-IR** ν = 1516, 1474, 1099, 978, 915, 750, 691, 620, 538 cm^{-1}.

Pentakis(pentafluorophenyl)cyclopentadienylcarboxylic acid 5: 10 µmol (15.6 mg) of **1** was suspended in 0.5 mL of C_6F_6. The solution was degassed and 89 µmol (2 mL; 1.1 bar; 25 °C) of CO was added. The solution was stirred for 24 h, resulting in a color change from deep blue to pale yellow and the formation of brown solids. All volatiles were removed under vacuum. 1 mL of water and 1 mL of benzene were added to the solid residue. The phases were separated, the aqueous phase was discarded, and the organic phase was dried with $MgSO_4$. All volatiles were removed again under vacuum.

The product is a mixture of **5** and **6**, since **5** decomposes slowly to **6** under the conditions of the work-up and NMR measurement. Single crystals of **5** were obtained by vapor phase diffusion of *n*-hexane into a concentrated solution of **5** in hexafluorobenzene at 6 °C.

Yield 7 mg. **^{19}F NMR** (565 MHz, C_6D_6) δ -132.34 (br s, 1F, *ortho*), -135.05 (br s, 1F, *ortho*), -138.42 (d, 2F, $^3J_{FF}$ = 21.6 Hz, *ortho*), -139.28 – -139.48 (m, not integratable due to overlap and uneven baseline, *ortho*), -145.35 (t, 2F, $^3J_{FF}$ = 21.7 Hz, *para*), -146.33 (d, 2F, $^3J_{FF}$ = 21.7 Hz, *para*), -148.23 (d, 2F, $^3J_{FF}$ = 21.7 Hz, *para*), 158.0 – 158.41 (m, 9F, *meta*) 160.05 (td, 1H, $^3J_{FF}$ = 21.7 Hz, $^4J_{FF}$ = 6.1 Hz, *meta*).

Comment: Because **5** decomposes during column chromatography and on prolonged standing, only the ^{19}F NMR spectrum and sc-XRD data are reported.

Pentakis(pentafluorophenyl)cyclopentadiene 6: 5 µmol of **3a**, **3b**, or **3c** are suspended in 1 mL of hydrochloric acid (1 mol/L). The suspension is extracted three times with 1 mL of dichloromethane (DCM). The combined extracts are dried with $MgSO_4$ and all volatiles are removed under reduced pressure (3 h to ensure the removal of ferrocene, Cp*H, and pyridine). The yield is almost quantitative.

If larger amounts of **6** are desired, the following procedure is advantageous: 0.5 mmol (456 mg) pentakis(pentafluorophenyl)cyclopentadienol and 10 mmol (2.67 g) $AlBr_3$ were suspended in 1.5 mL benzene and 5 mmol (0.55 g, 373 µL) bromoethane was slowly added at 0 °C. The red suspension was warmed to 25 °C and stirred for 30 min. The suspension was quenched with 100 mmol (1.8 g) ice and the mixture was kept at 25 °C until completely thawed. 0.5 mmol (93 mg) ferrocene and 1.5 mL hydrochloric acid (1 mol/L) were added and the suspension was stirred for 30 min. It was then diluted with 10 mL DCM and the phases were separated. The aqueous phase was discarded and the organic phase was dried with $MgSO_4$. All volatiles were removed under vacuum. The crude product was dissolved in 5 mL hot toluene and filtered while hot. 0.5 mmol (39.6 mg; 40.6 µL) pyridine was added to the filtrate and the solution was stored at 25 °C for 24 h. The separated solids were isolated by filtration and dissolved in a mixture of 1.5 mL

hydrochloric acid (1 mol /L) and 10 mL DCM. The aqueous phase was discarded and the organic phase was dried with $MgSO_4$. All volatiles were removed under vacuum.

Yield 309 mg, 345 mmol, 69 %. **Mp** 188 °C (dec.). **^{19}F NMR** (565 MHz, C_6D_6) δ -139.13 (d, 2F, $^3J_{FF}$ = 21.0 Hz, $HCCC_6F_5$, *ortho*), -140.00 (d, 4F, $^3J_{FF}$ = 21.2 Hz, $HCCCC_6F_5$, *ortho*) -140.62 (d, 2F, $^3J_{FF}$ = 23.0 Hz, $HCCC_6F_5$, *ortho*), -141.18 (d, 1F, $^3J_{FF}$ = 18.2 Hz, HCC_6F_5, *ortho*), -143.18 (d, 2F, $^3J_{FF}$ = 21.6 Hz, HCC_6F_5, *ortho*), -147.69 (t, 2F, $^3J_{FF}$ = 21.7 Hz, $HCCC_6F_5$ or $HCCCC_6F_5$, *para*), -148.14 (t, 2F, $^3J_{FF}$ = 21.3 Hz, $HCCC_6F_5$ or $HCCCC_6F_5$, *para*), -149.62 (t, 1F, $^3J_{FF}$ = 21.5 Hz, HCC_6F_5, *para*), -158.72 – 158.93 (m, 6F, *meta*), -159.18 – 159.42 (m, 3F, *meta*), -159.67 (td, 1F, $^3J_{FF}$ = 21.6 Hz, $^4J_{FF}$ = 8 Hz, HCC_6F_5, *meta*). **^{1}H NMR** (400 MHz, C_6D_6) δ 5.91 (s, CpH). **^{13}C{^{19}F} DEPT-135 NMR** (151 MHz, C_6D_6) δ 146.41 (d, $^3J_{HC}$ = 7.1 Hz HCC_6F_5, *ortho*), 145.94 (d, $^3J_{HC}$ = 5.7 Hz HCC_6F_5, *ortho*), 144.86 (s, $HCCC_6F_5$, *ortho*), 144.67 (s, $HCCCC_6F_5$, *ortho*), 144.31 (s, $HCCC_6F_5$, *ortho*), 142.47 (s, $HCCC_6F_5$ or $HCCCC_6F_5$, *para*), 142.31 (s, $HCCCC_6F_5$ or $HCCC_6F_5$, *para*), 142.08 (s, HCC_6F_5, *para*), 138.24 (s, $HCCC_6F_5$, *meta*), 138.21 (s, HCC_6F_5, *meta*), 138.18 (s, $HCCCC_6F_5$, *meta*), 138.17 (s, $HCCC_6F_5$, *meta*), 138.04 (s, $HCCCC_6F_5$, *meta*), 137.06 (s, HCC_6F_5, *meta*). **^{13}C{^{1}H} NMR** (151 MHz, C_6D_6) δ 146 – 136 (several multiplets) 107.84 – 106.83 (m, *ipso*), 53.56 (s, H*C*). **ATR-IR** ν = 1656, 1522, 1491, 1445, 1315, 1105, 1080, 982, 935, 916, 841, 735, 652, cm^{-1}.

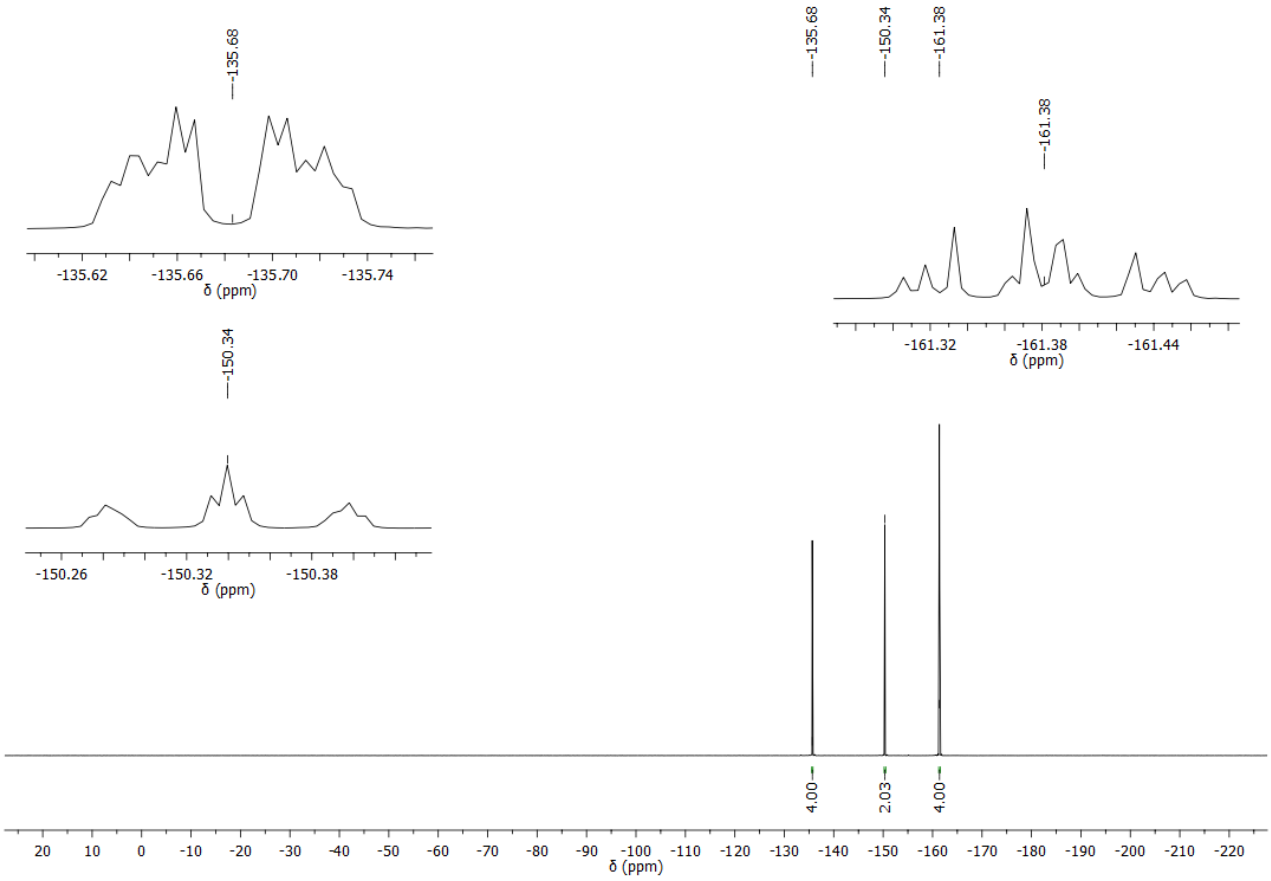

Figure S1. ^{19}F NMR spectrum of bis(pentafluorophenyl)ethyne **B** in C_6D_6 at 25 °C.

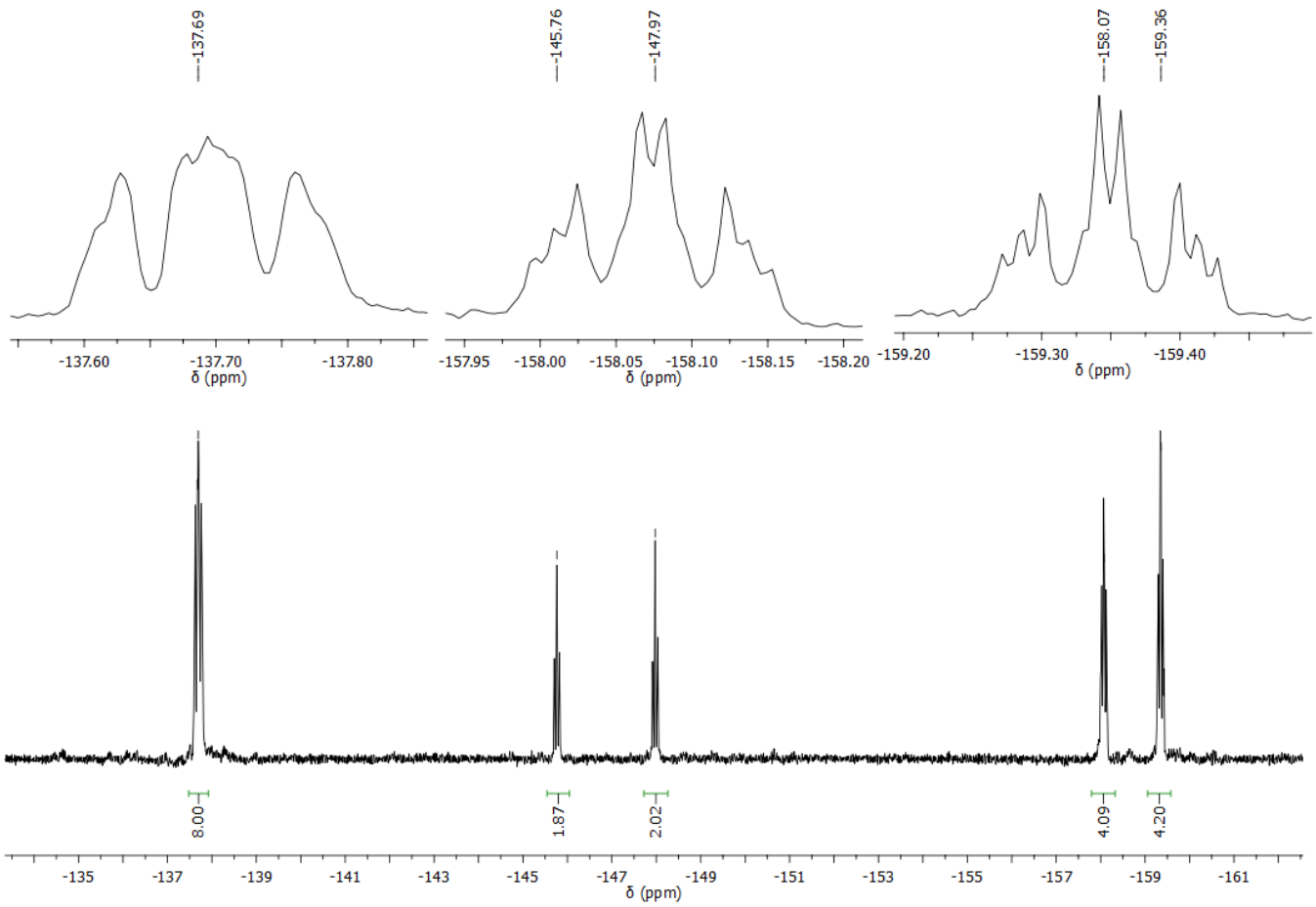

Figure S2. ^{19}F NMR spectrum of tetrakis(pentafluorophenyl)cyclopentadienone **C** in C_6D_6 at 25 °C.

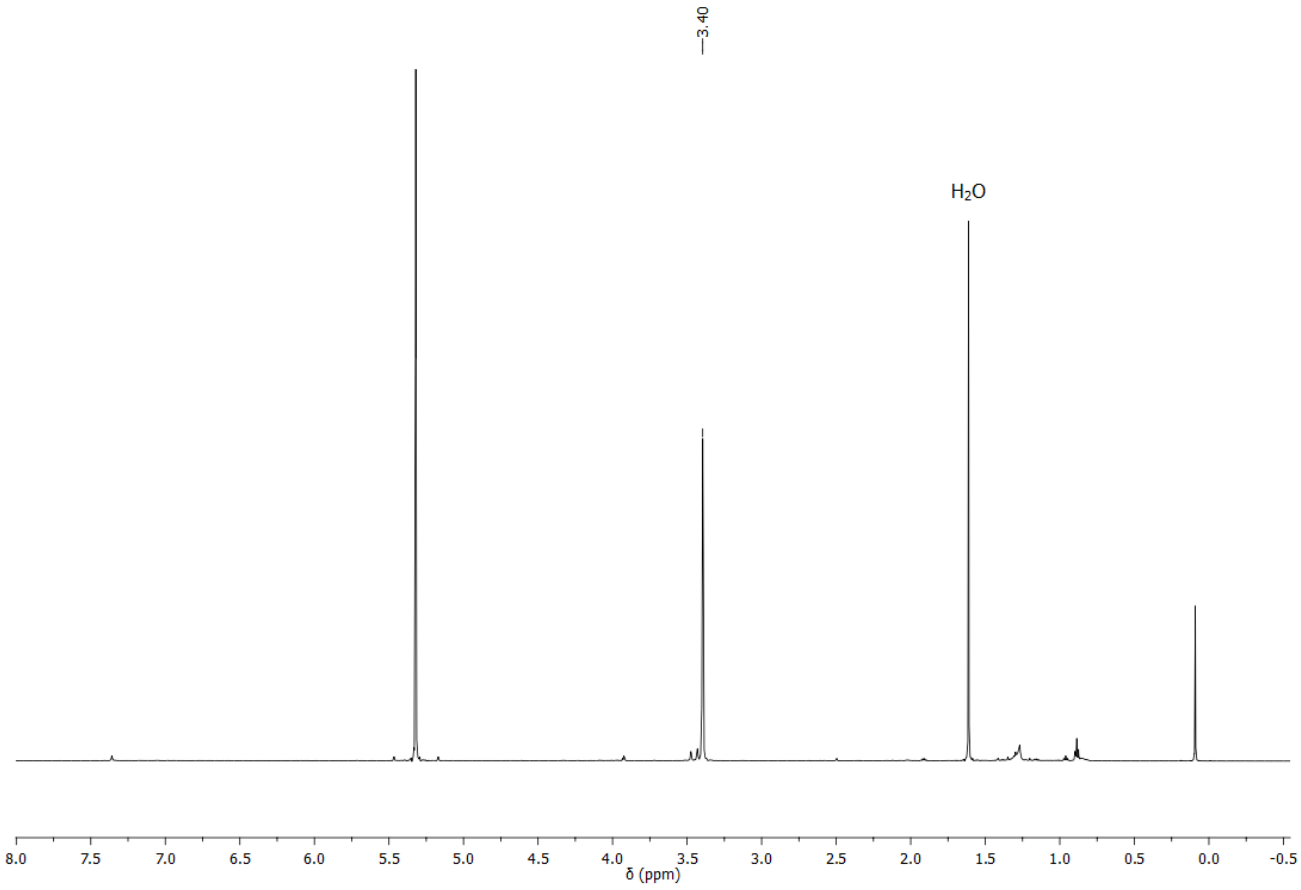

Figure S3. ^{1}H NMR spectrum of pentakis(pentafluorophenyl)cyclopentadienol **D** in CD_2Cl_2 at 25 °C.

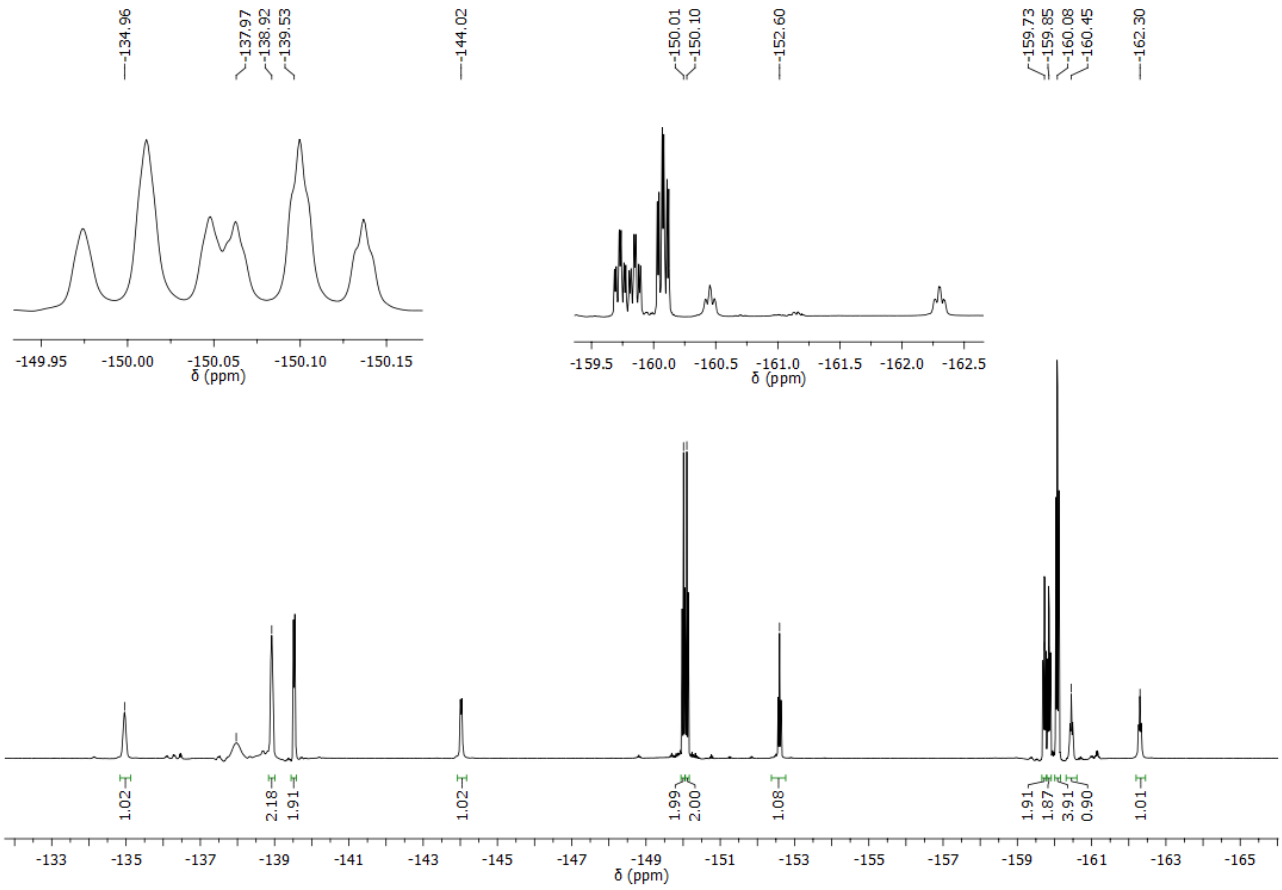

Figure S4. ^{19}F NMR spectrum of pentakis(pentafluorophenyl)cyclopentadienol **D** in CD_2Cl_2 at 25 °C.

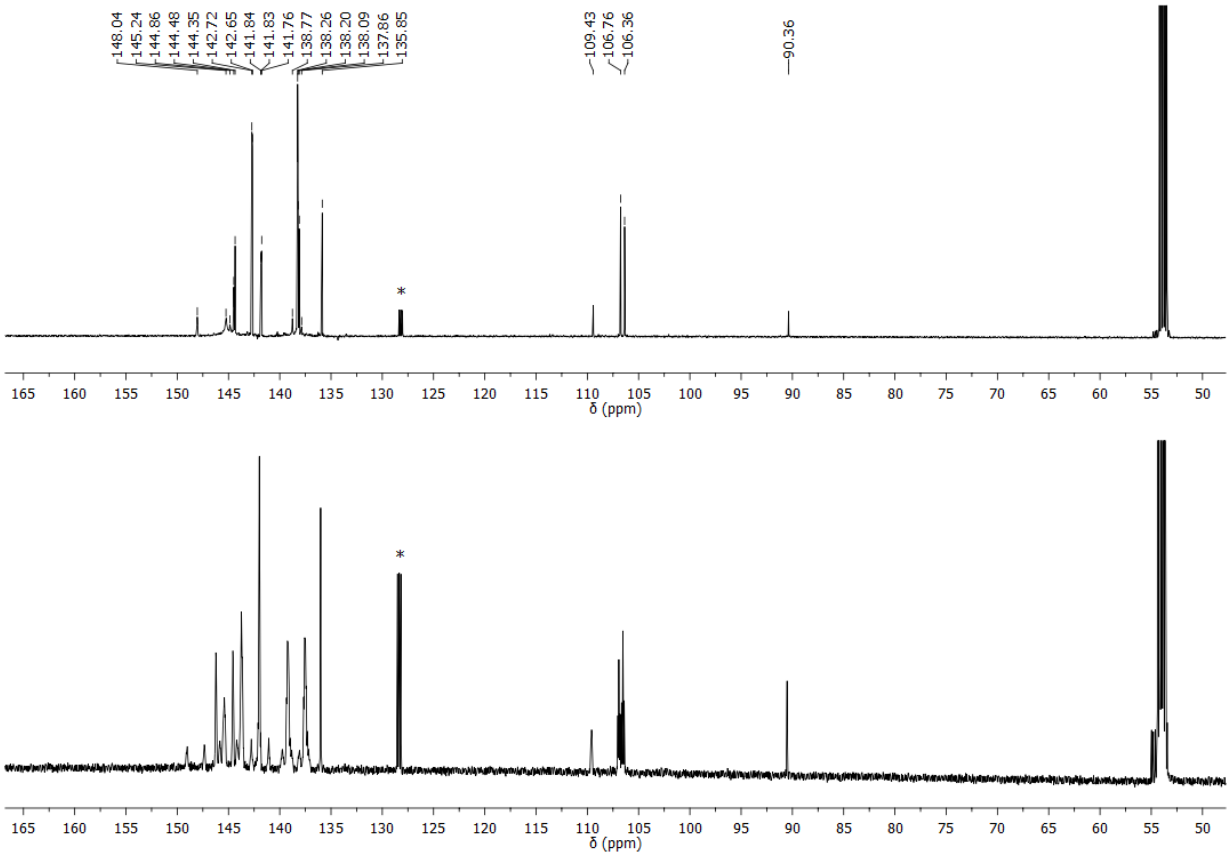

Figure S5. $^{13}C\{^{19}F\}$ NMR and $^{13}C\{^{1}H\}$ NMR spectrum of pentakis(pentafluorophenyl)cyclopentadienol **D** in CD_2Cl_2 at 25 °C (containing traces of C_6D_6 (*) from a previous measurement which was hindered by the low solubility in this solvent).

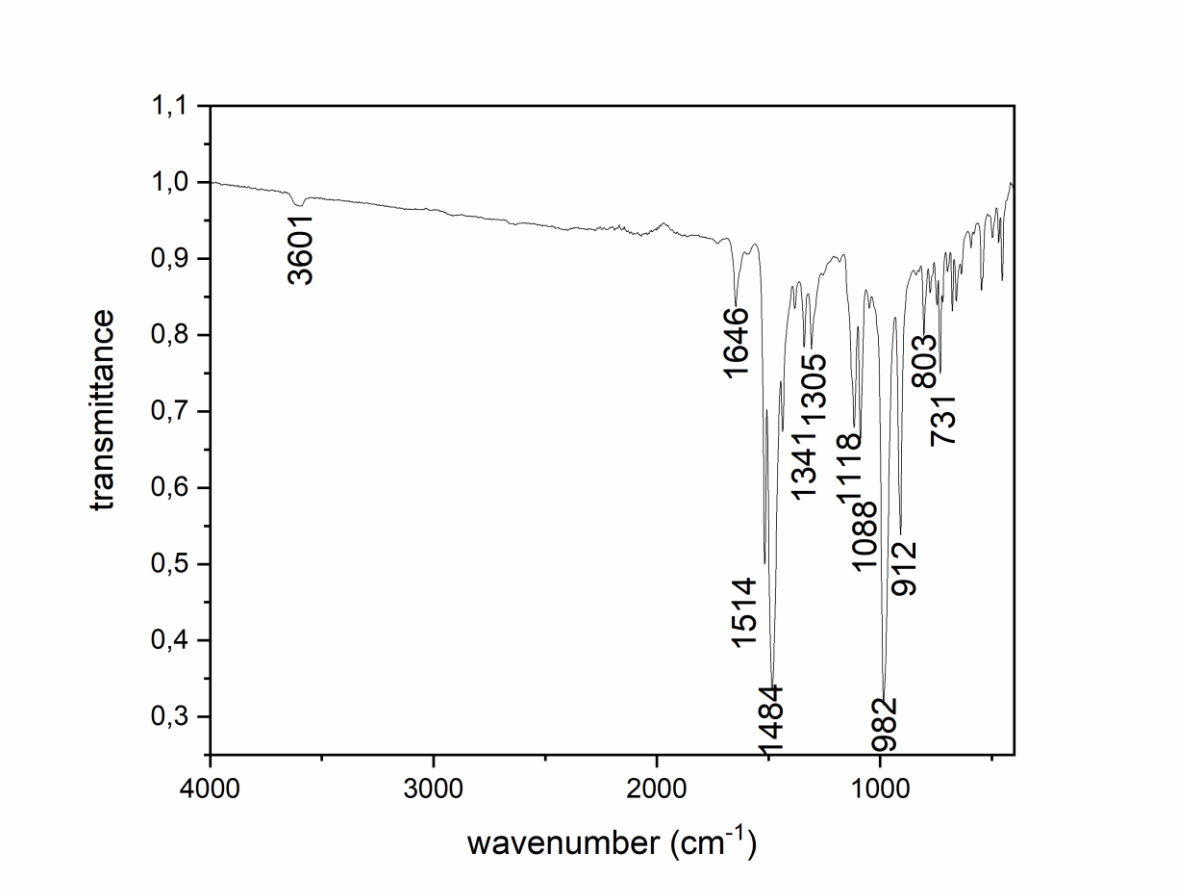

Figure S6. ATR-IR spectrum of pentakis(pentafluorophenyl)cyclopentadienol **D**.

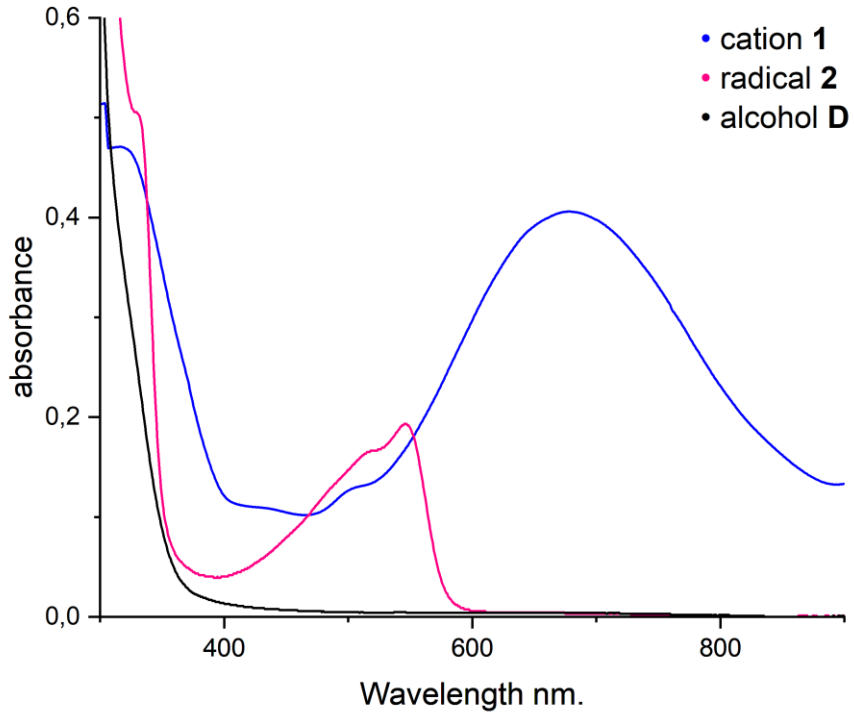

Figure S7. UV-vis spectra of cation **1**, radical **2**, and alcohol **D** (50 µmol/L in hexafluorobenzene). The solution of **1** contained an excess (250 µmol/L) of $SbF_5 \cdot SO_2$ to scavange traces of reducing agents or nucleophiles. Quantitative results for **1** may be imprecise because the concentration of **1** was not accurately known due to difficulties in the handling of its solution.

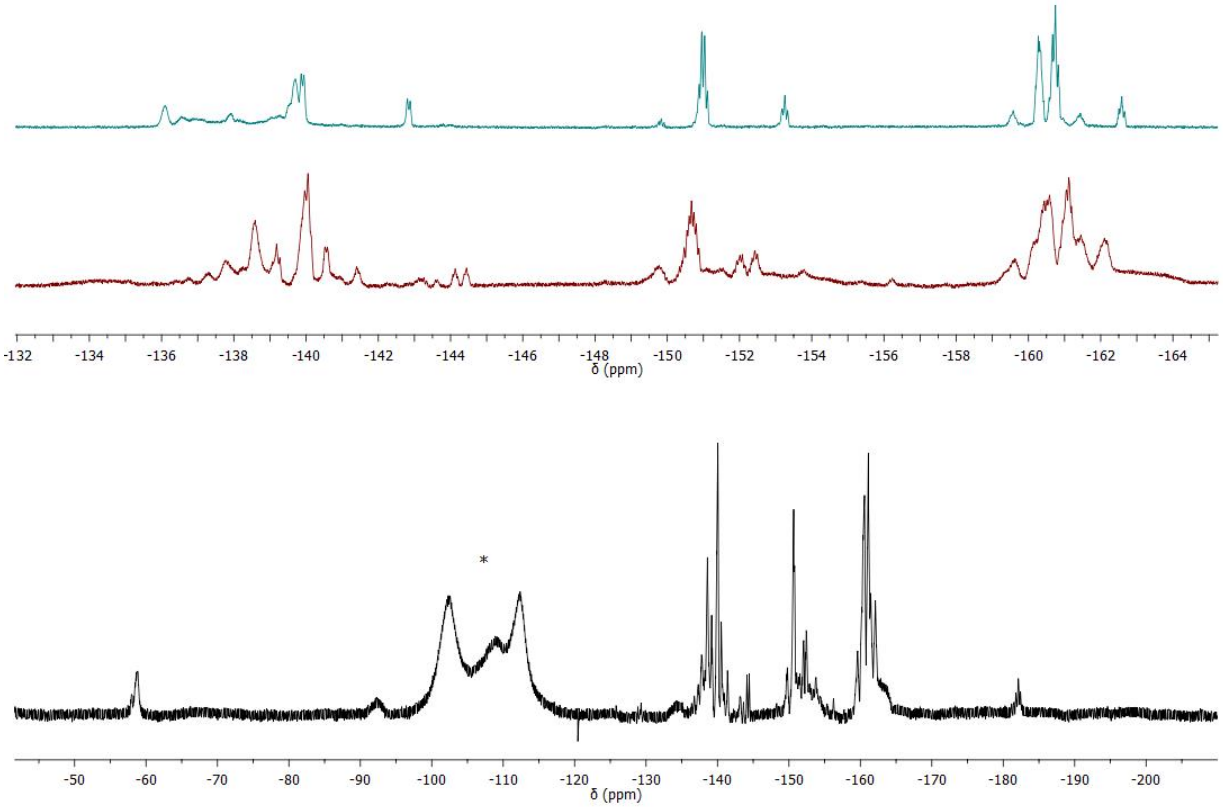

Figure S8. ^{19}F NMR spectra in liquid SO_2 at -30 °C of pentakis(pentafluorophenyl)cyclopentadienol **D** before (top, cyan) and after (middle, red and bottom, black) the addition of 5 equivalents of $SbF_5 \cdot SO_2$ using a glass capillary with acetone-d_6 as reference. The multiplet marked with an asterisk arises from $Sb_nF_mOH_o$ species.

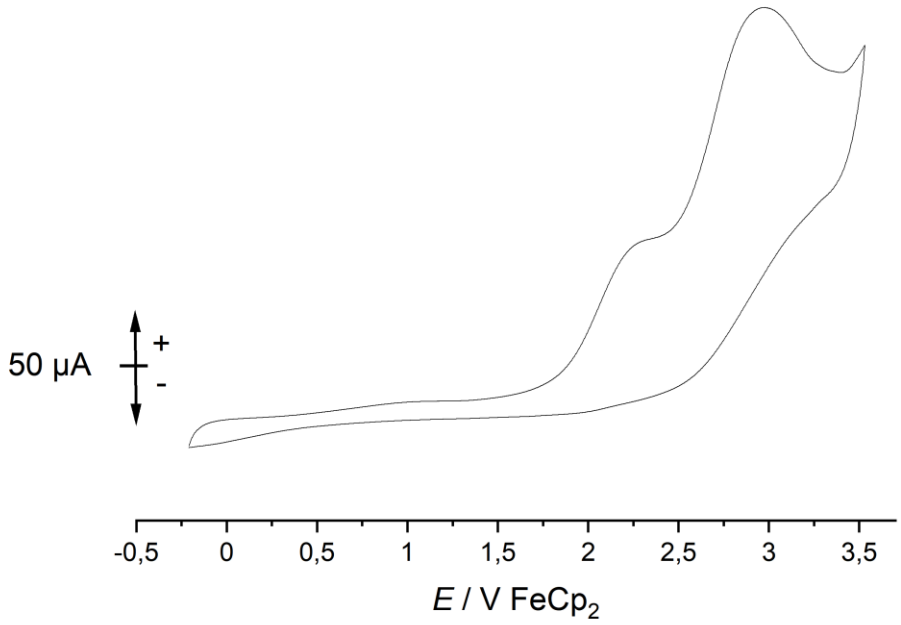

Figure S9. Cyclovoltammogram of the pentakis(pentafluorophenyl)cyclopentadienyl radical **2** at -20 °C in SO_2. We assign the first redox event at E_{pa} = 2.30 V to its oxidation to cation **1** and the second redox event at E_{pa} = 3.55 V to the subsequent oxidation of the aryl groups.

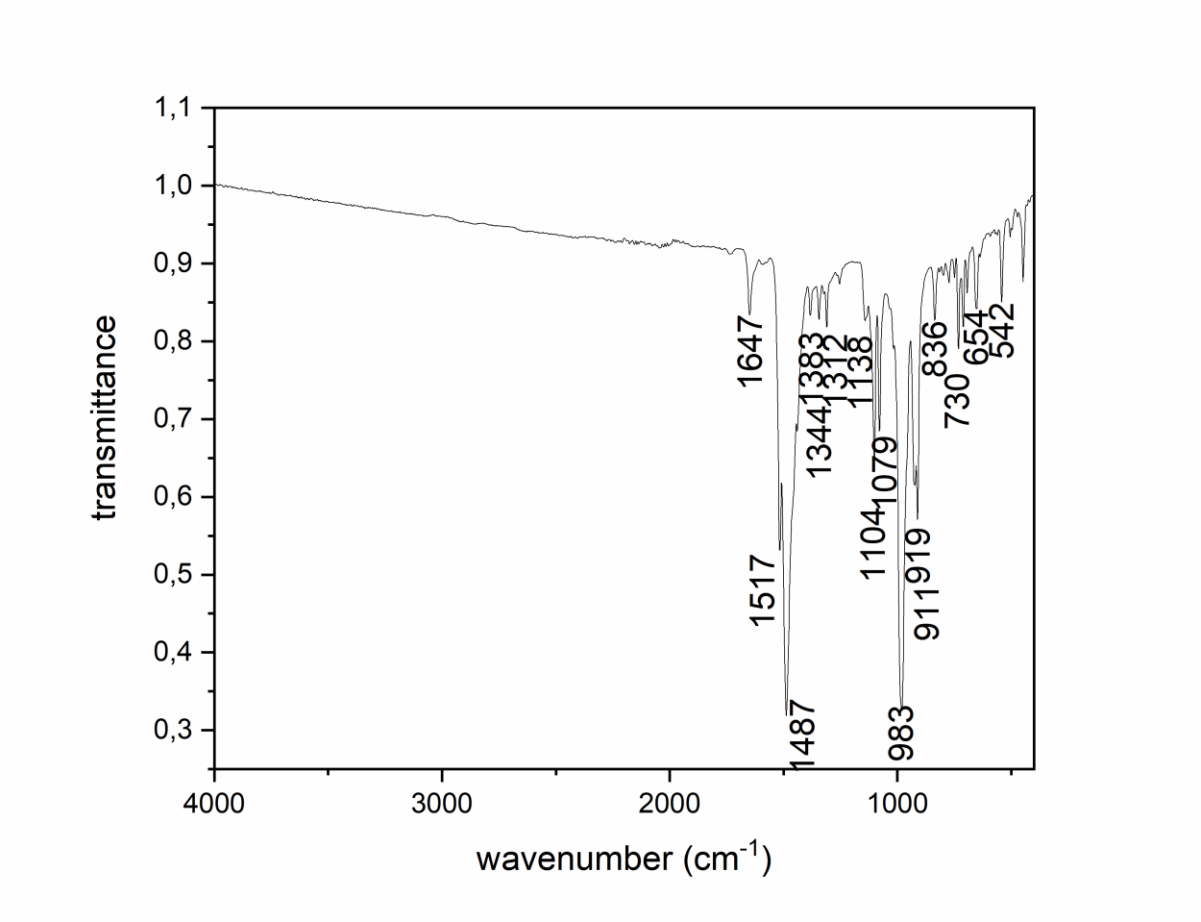

Figure S10. ATR-IR spectrum of the pentakis(pentafluorophenyl)cyclopentadienyl radical **2**.

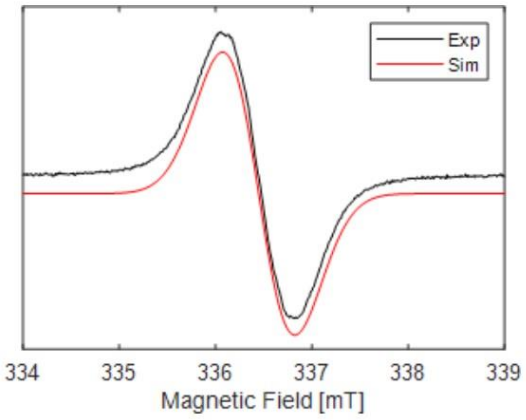

Figure S11. EPR spectrum of the pentakis(pentafluorophenyl)cyclopentadienyl radical **2**. For the simulation, a g value of 2.0033 and a linewidth (peak-to-peak) of 0.75 mT were used.

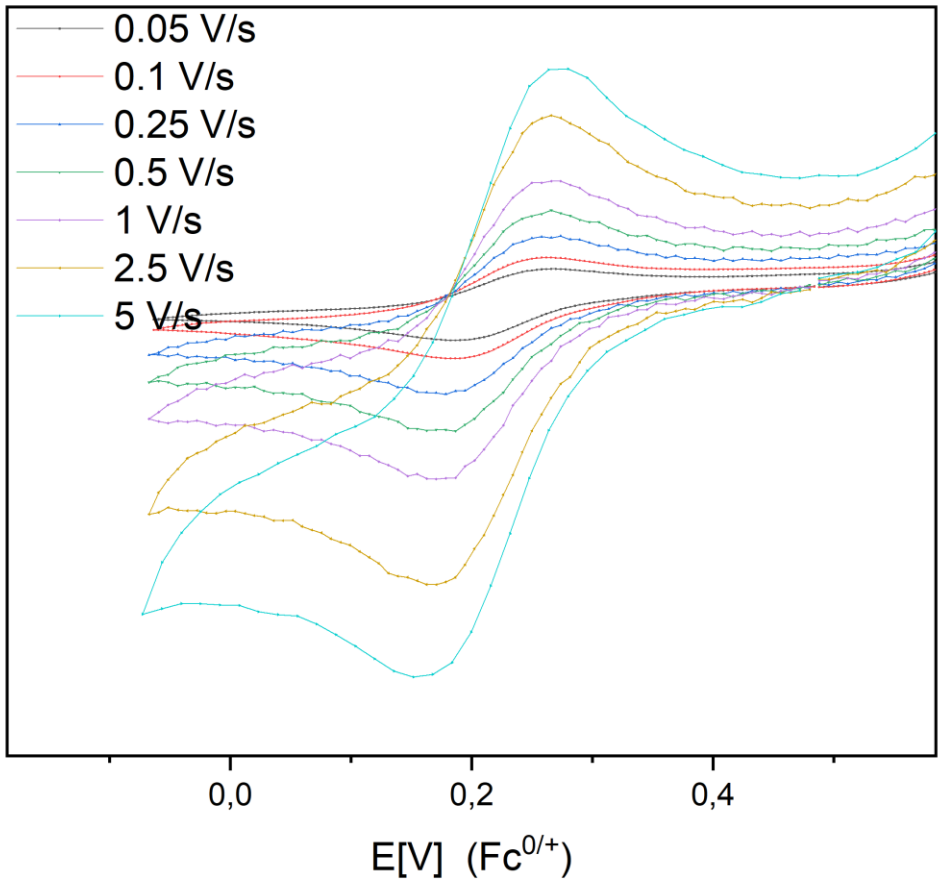

Figure S12. Cyclovoltammogramm of the pentakis(pentafluorophenyl)cyclopentadienyl radical **2** at 25 °C in 1,2-difluorobenzene. The reversible reduction to the corresponding anion **3** occurs at a half wave potential of $E_{1/2}$ = 0.48 V.

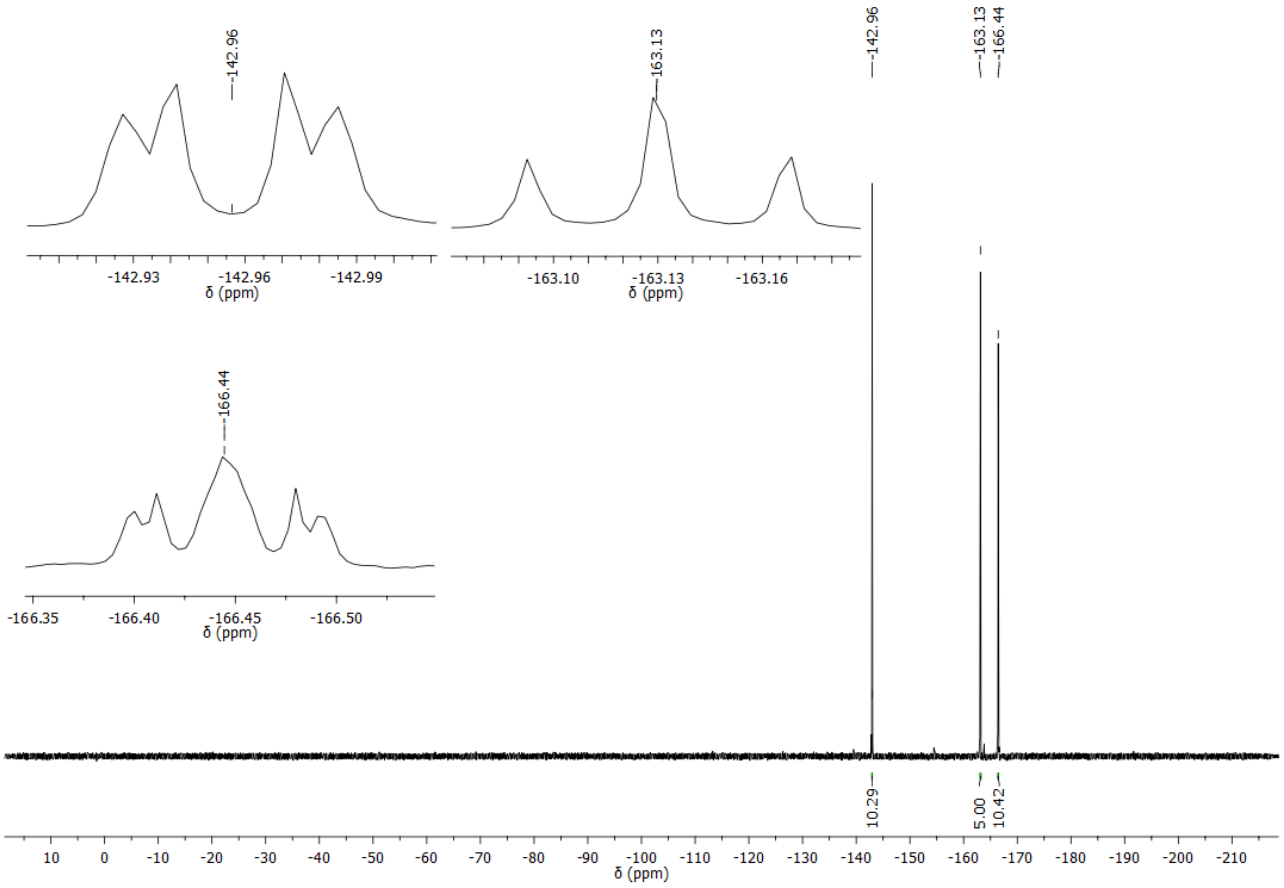

Figure S13. ^{19}F NMR spectrum of ferrocenium pentakis(pentafluorophenyl)cyclopentadienide **3a** in THF-d_8 at 25 °C.

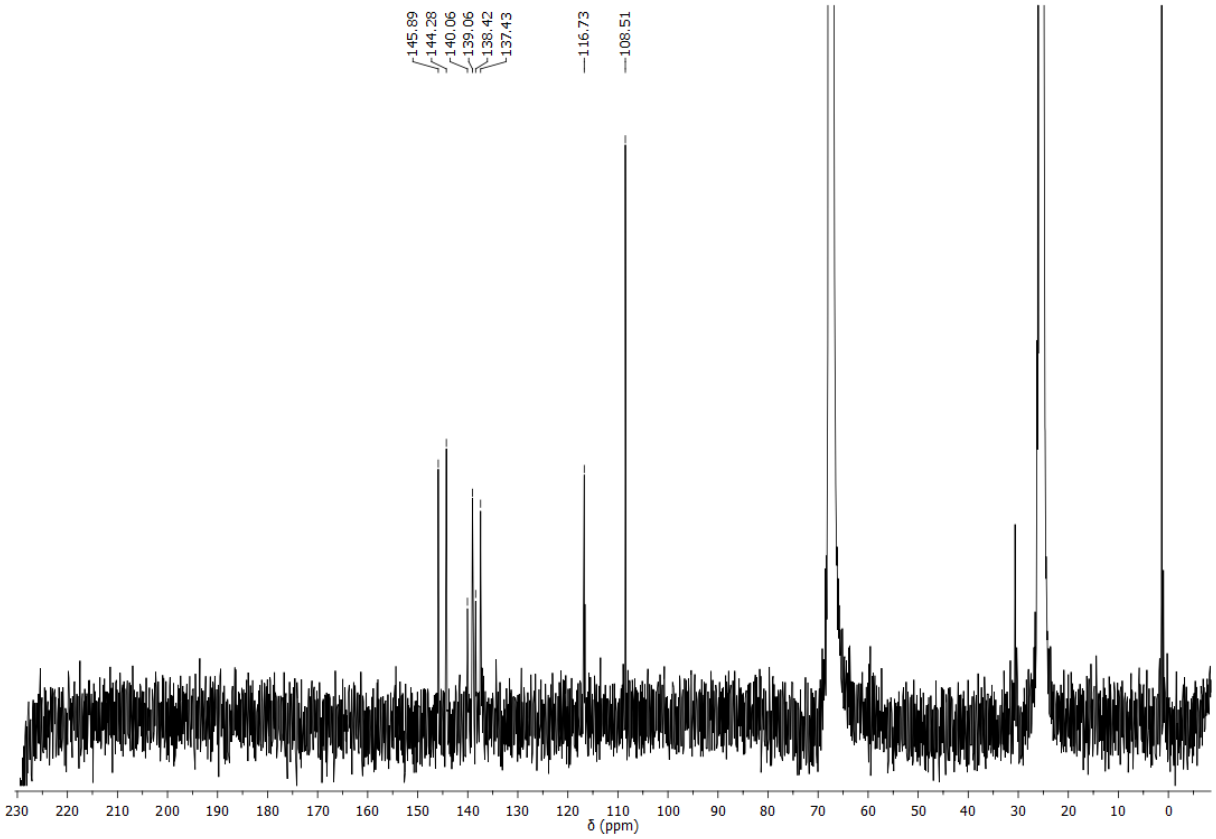

Figure S14. ^{13}C NMR spectrum of ferrocenium pentakis(pentafluorophenyl)cyclopentadienide **3a** in THF-d_8 at 25 °C.

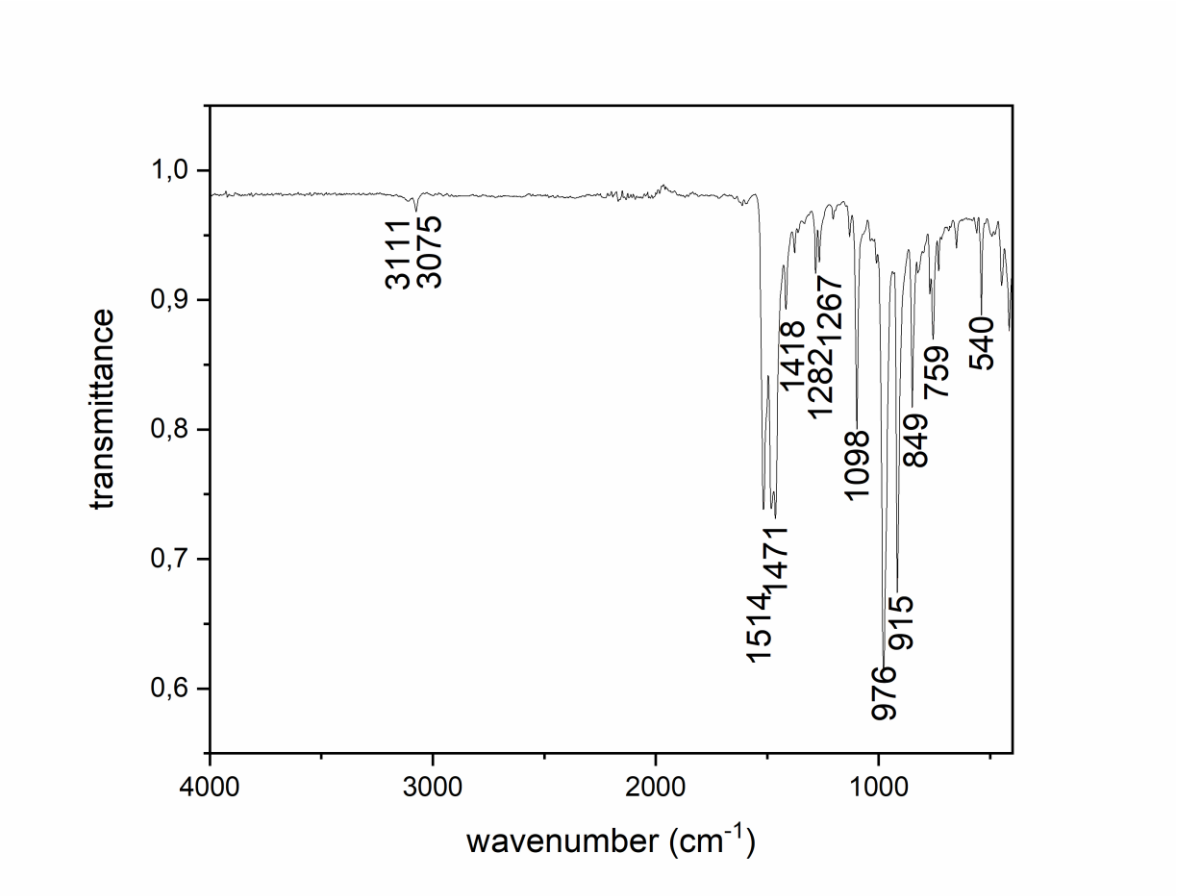

Figure S15. ATR-IR spectrum of ferrocenium pentakis(pentafluorophenyl)cyclopentadienide **3a**.

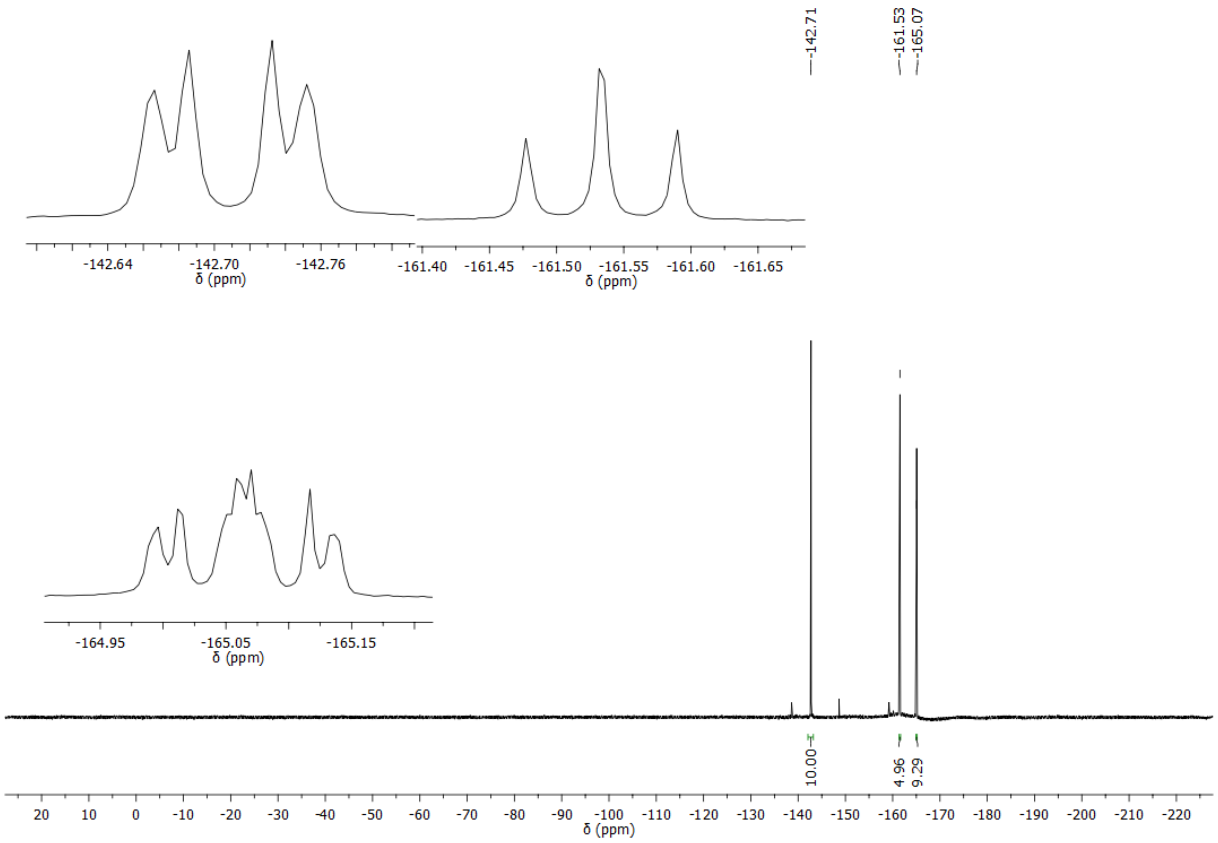

Figure S16. ^{19}F NMR spectrum of tritylium pentakis(pentafluorophenyl)cyclopentadienide **3b** in CD_2Cl_2 at 25 °C.

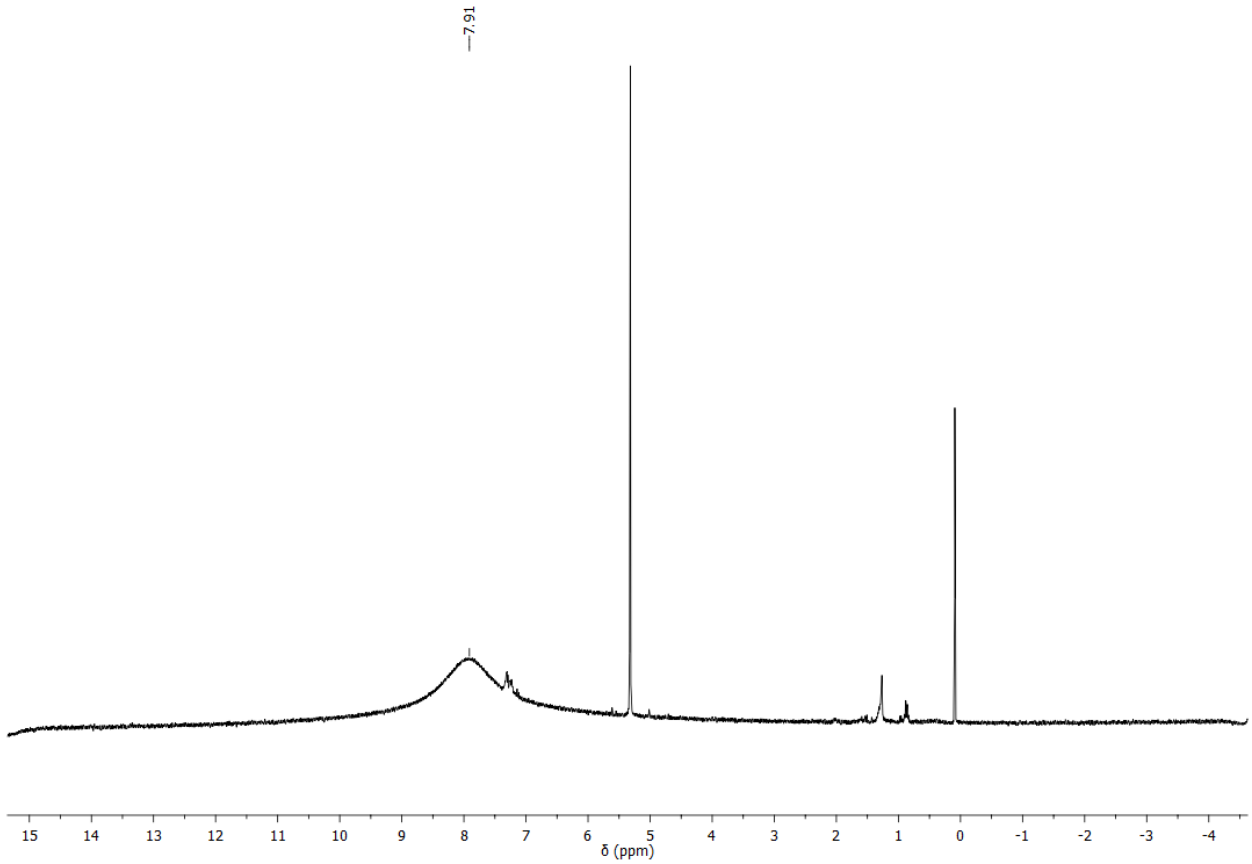

Figure S17. ^{1}H NMR spectrum of tritylium pentakis(pentafluorophenyl)cyclopentadienide **3b** in CD_2Cl_2 at 25 °C.

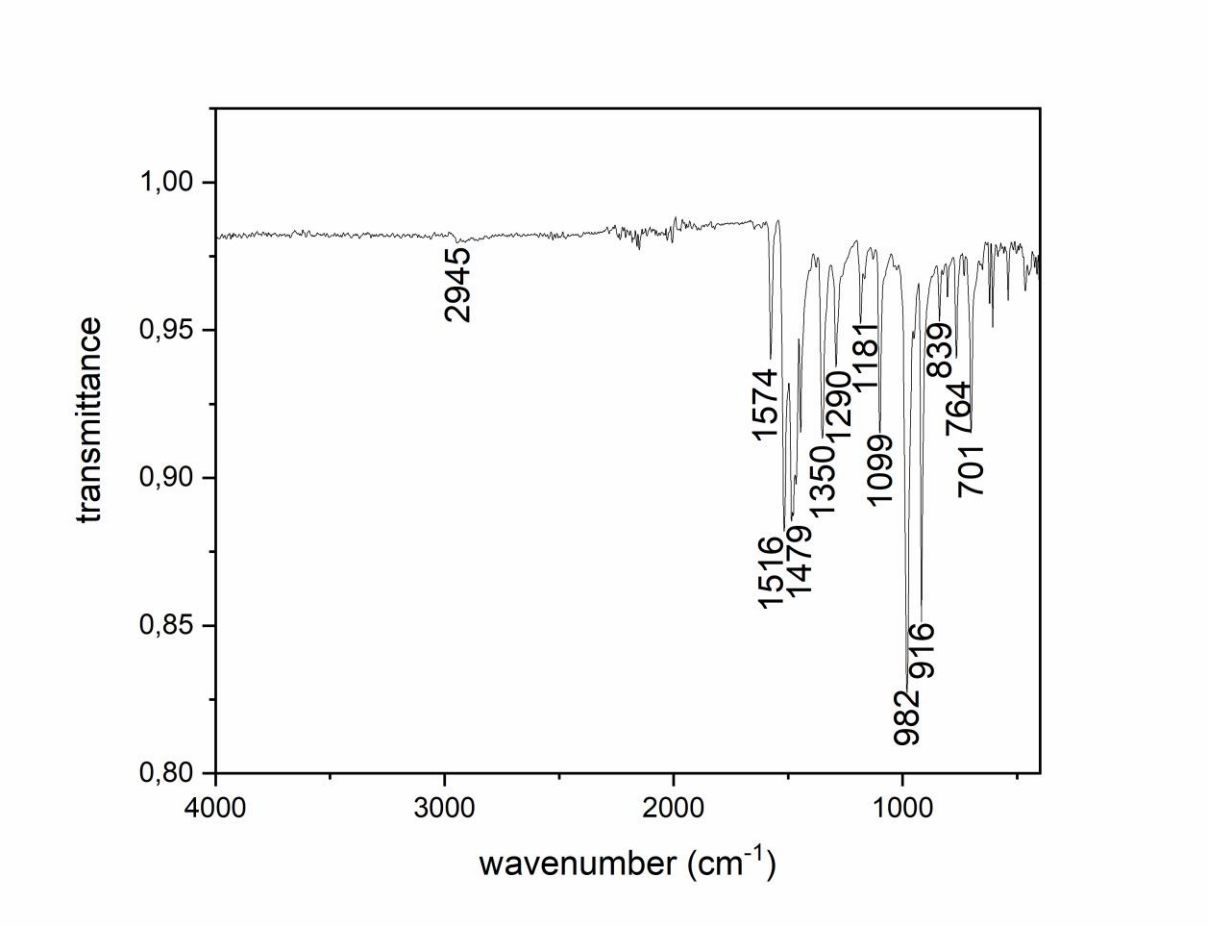

Figure S18. ATR-IR spectrum of tritylium pentakis(pentafluorophenyl)cyclopentadienide **3b**.

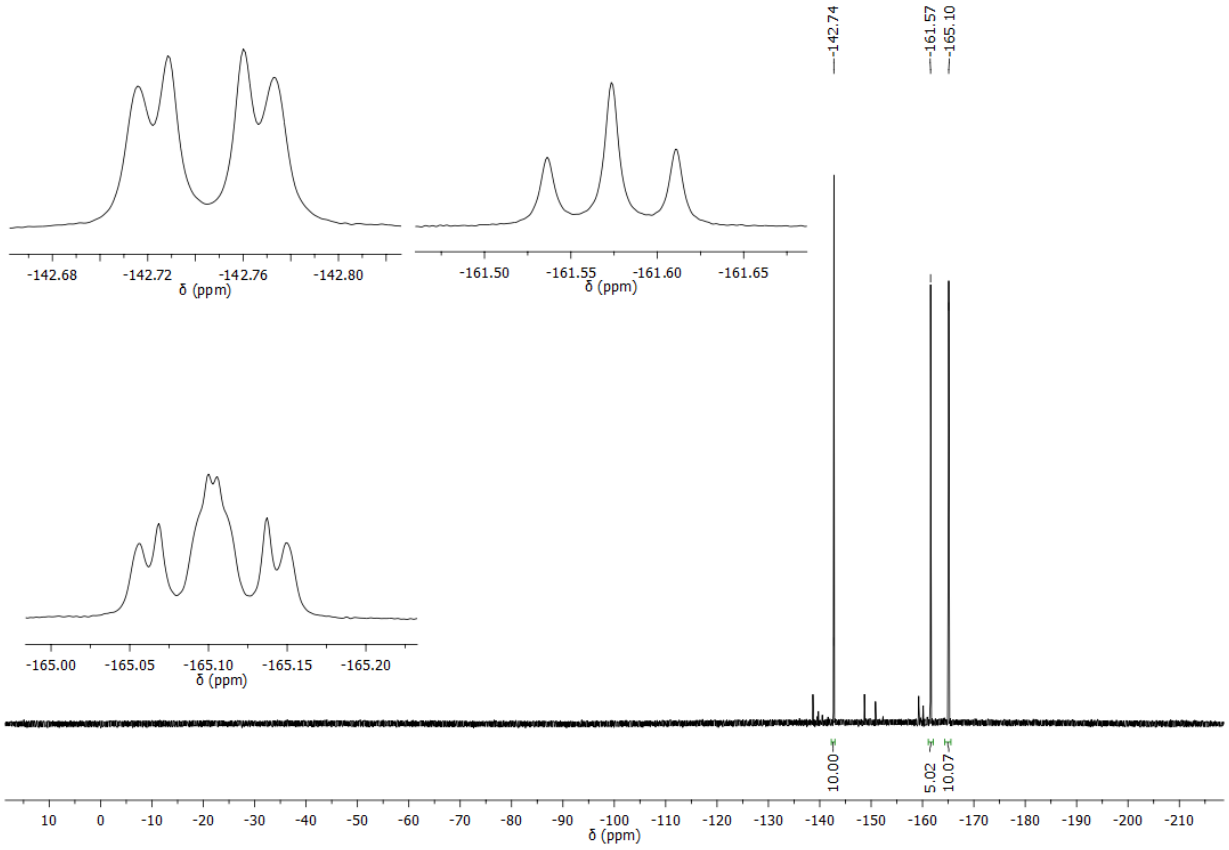

Figure S19. ^{19}F NMR spectrum of decamethylalumocenium pentakis(pentafluorophenyl)cyclopentadienide **3c** in CD_2Cl_2 at 25 °C.

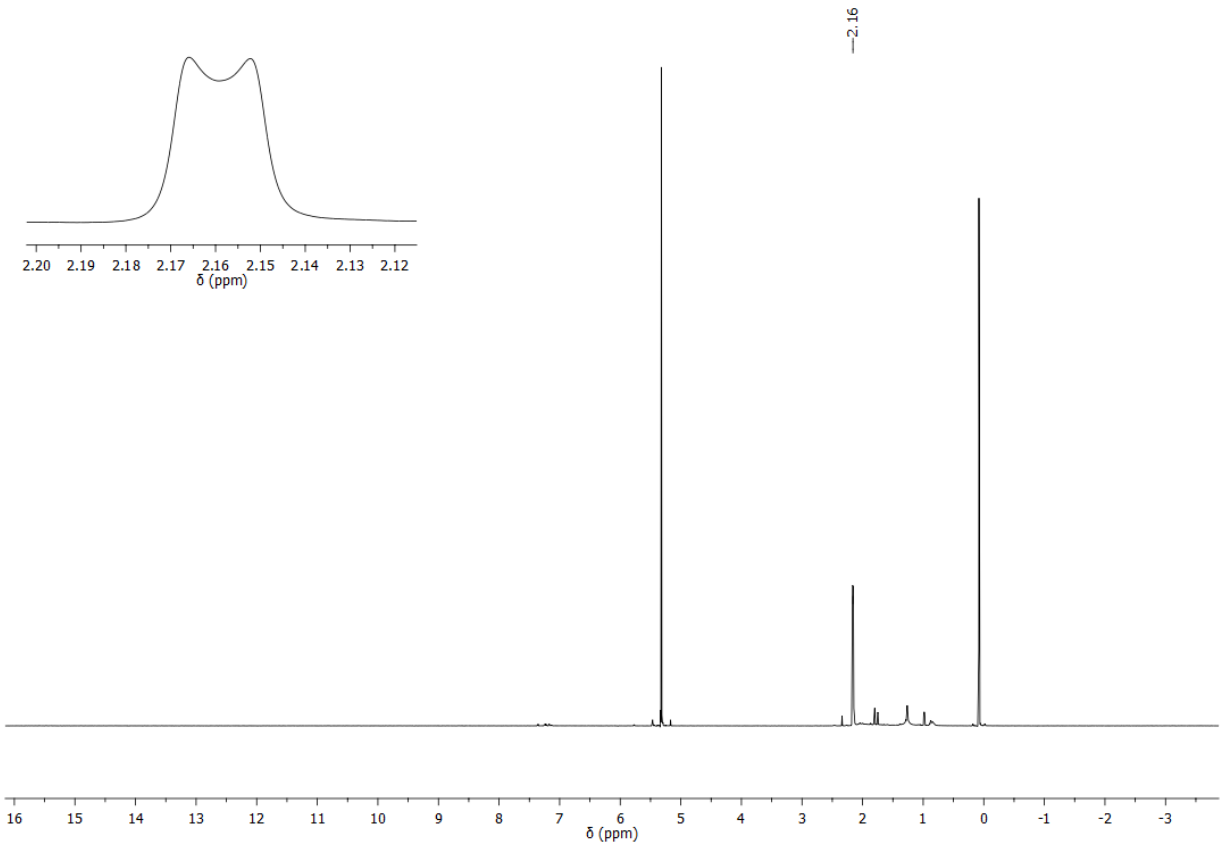

Figure S20. ^{1}H NMR spectrum of decamethylalumocenium pentakis(pentafluorophenyl)cyclopentadienide **3c** in CD_2Cl_2 at 25 °C.

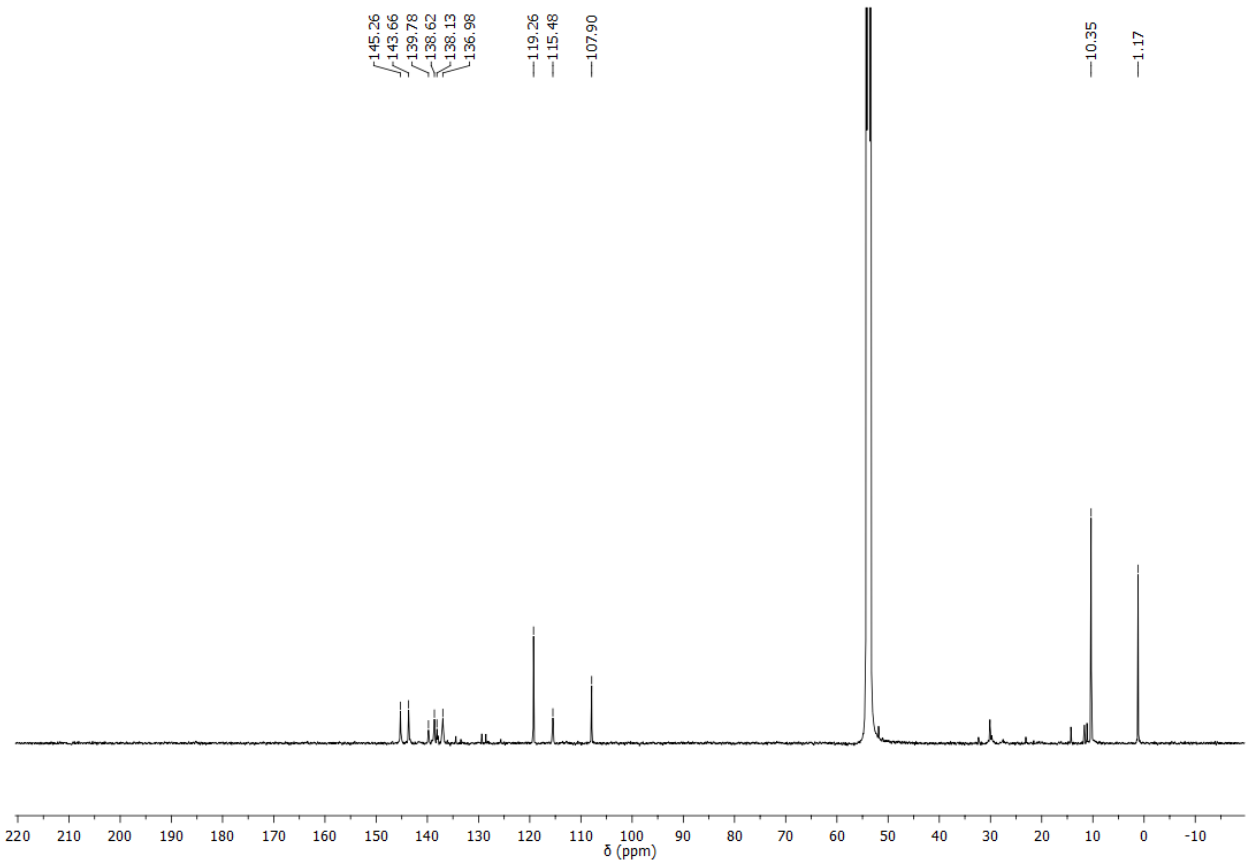

Figure S21. ^{13}C NMR spectrum of decamethylalumocenium pentakis(pentafluorophenyl)cyclopentadienide **3c** in CD_2Cl_2 at 25 °C.

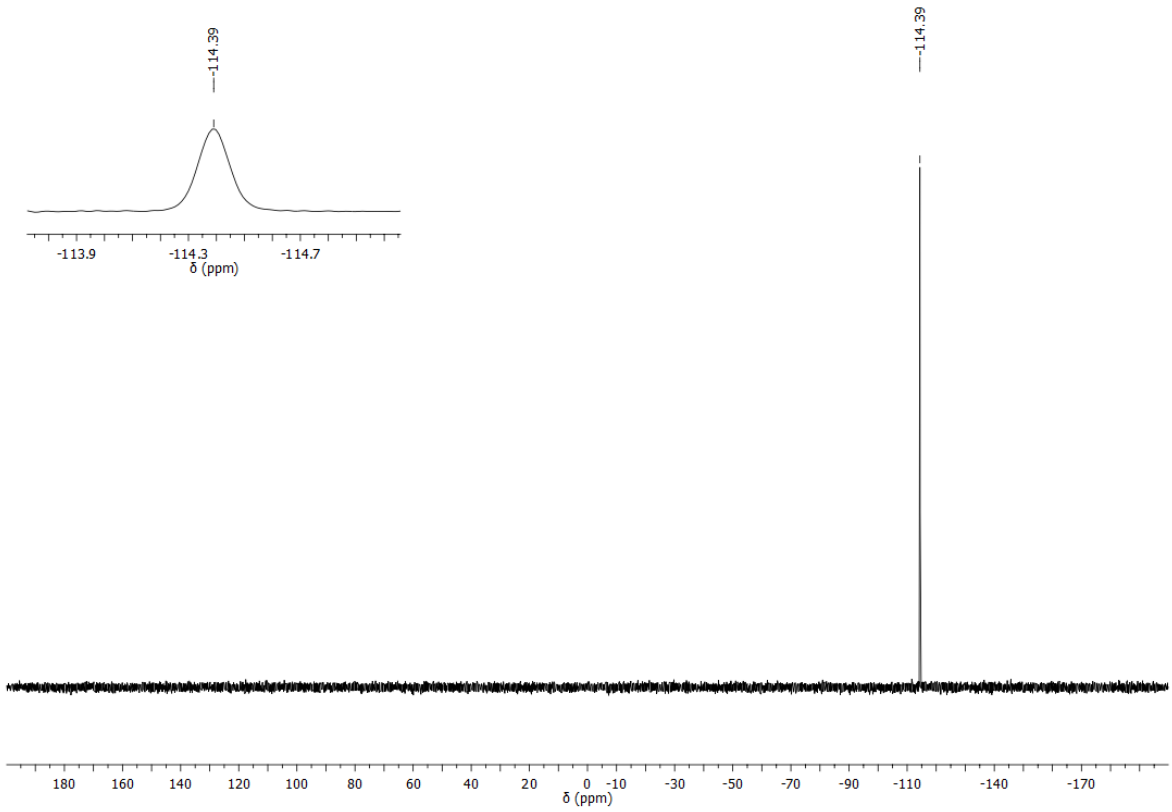

Figure S22. ^{27}Al NMR spectrum of decamethylalumocenium pentakis(pentafluorophenyl)cyclopentadienide **3c** in CD_2Cl_2 at 25 °C.

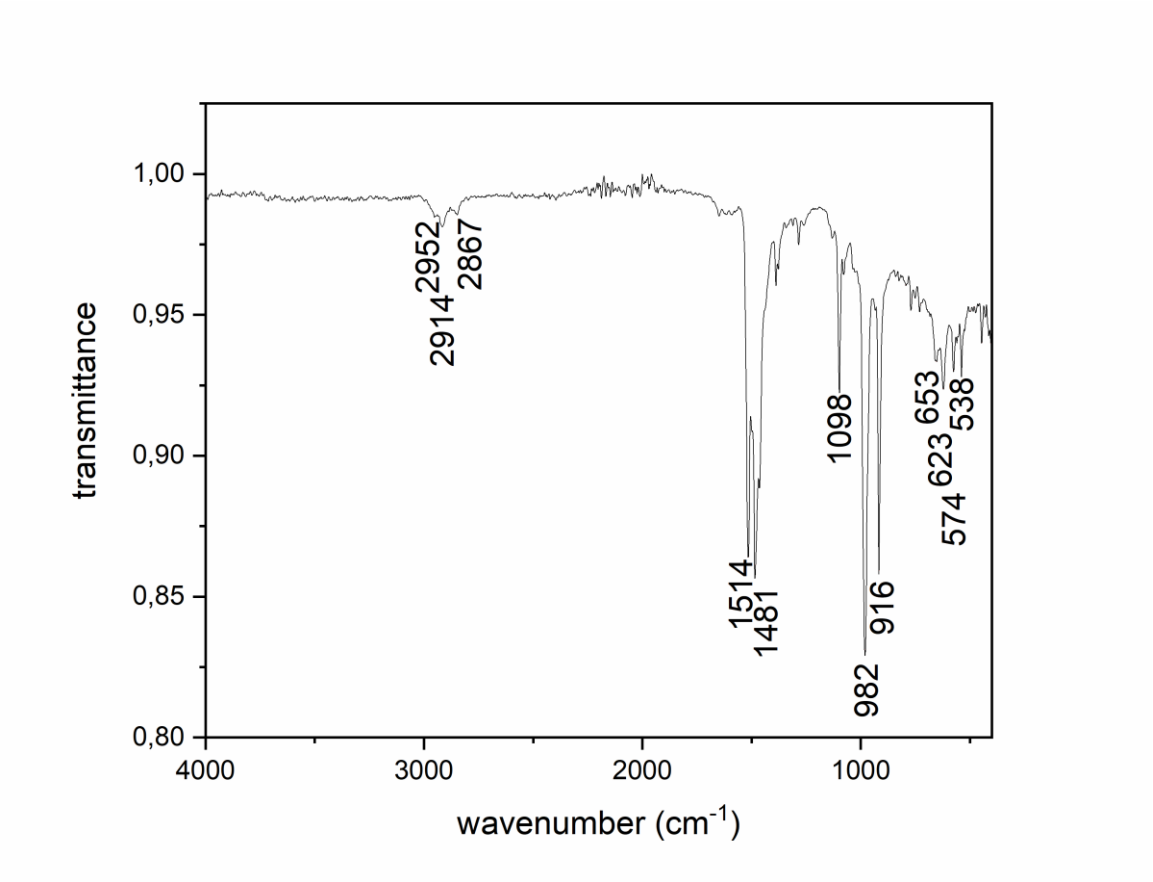

Figure S23. ATR-IR spectrum of decamethylalumocenium pentakis(pentafluorophenyl)cyclopentadienide **3c**.

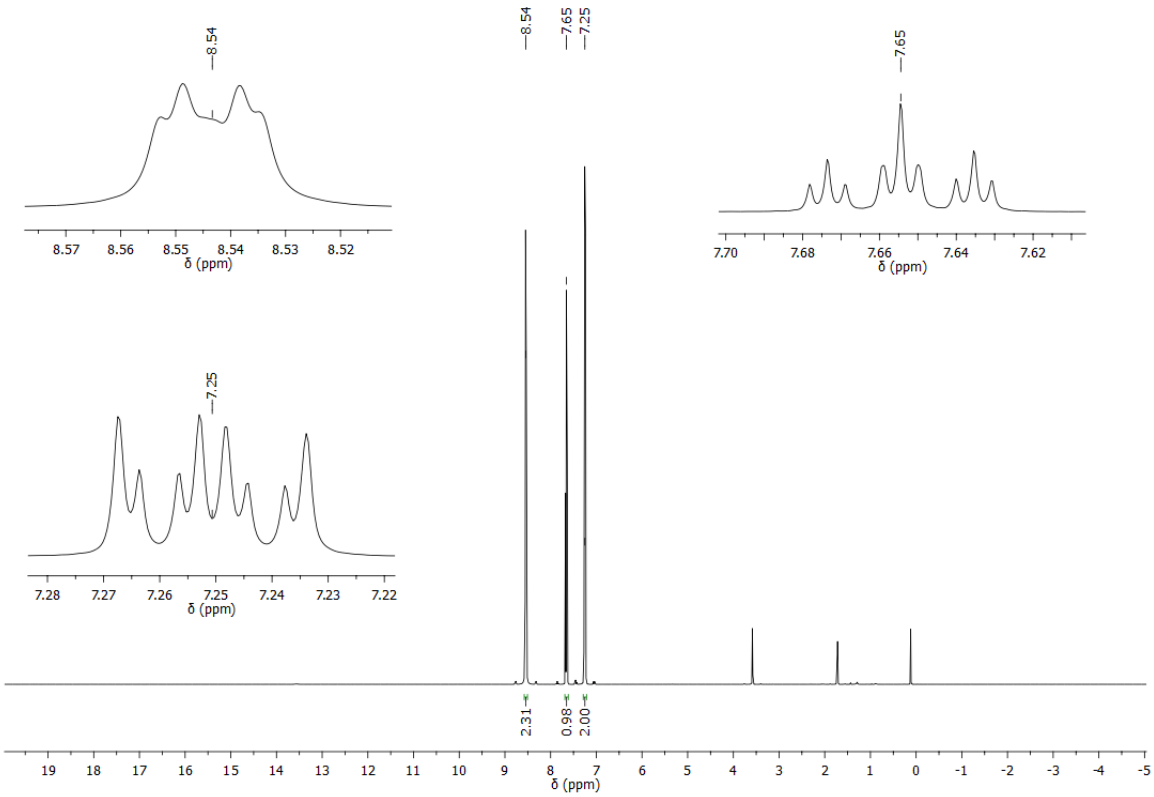

Figure S24. ^{1}H NMR spectrum of pyridinium pentakis(pentafluorophenyl)cyclopentadienide **3d** in thf-d_8 at 25 °C.

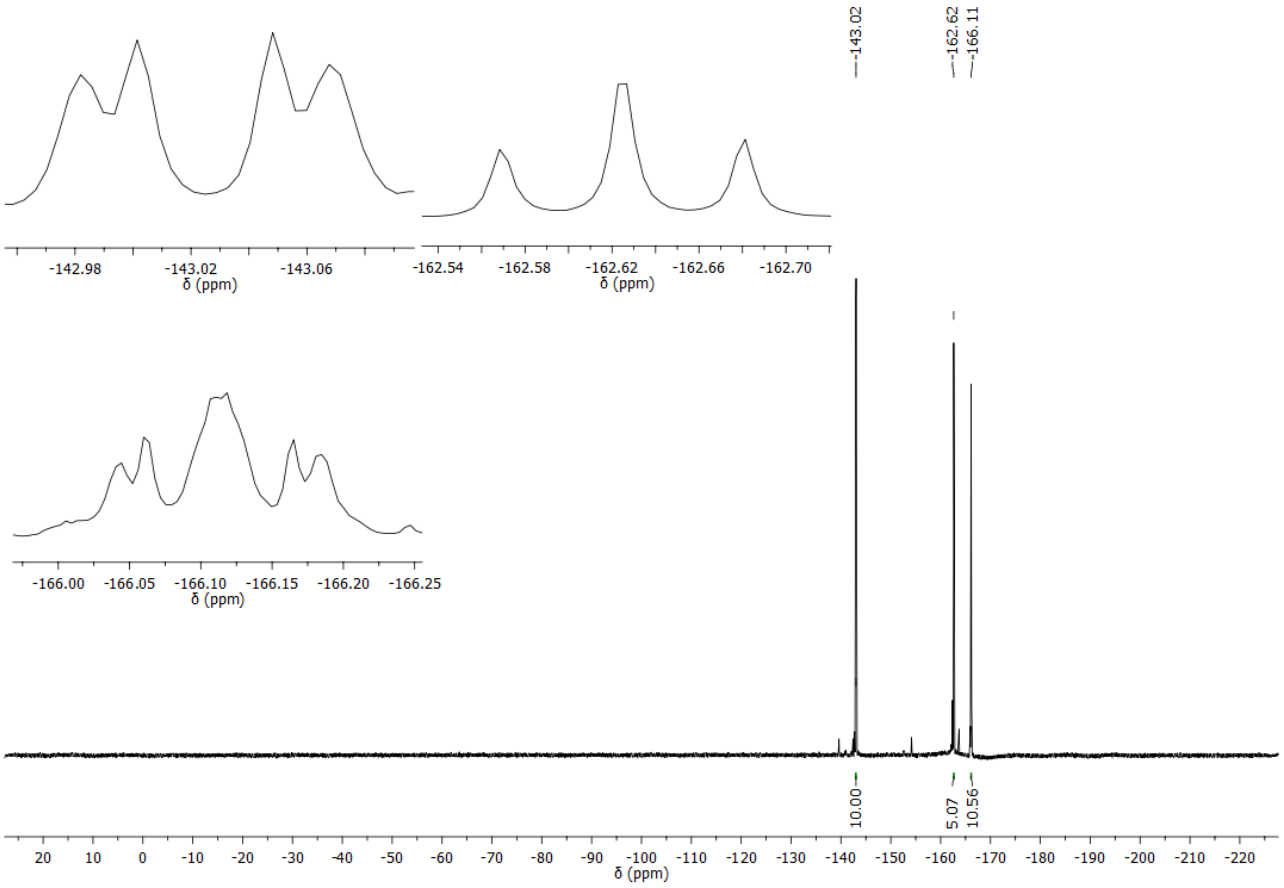

Figure S25. ^{19}F NMR spectrum of pyridinium pentakis(pentafluorophenyl)cyclopentadienide **3d** in thf-d_8 at 25 °C.

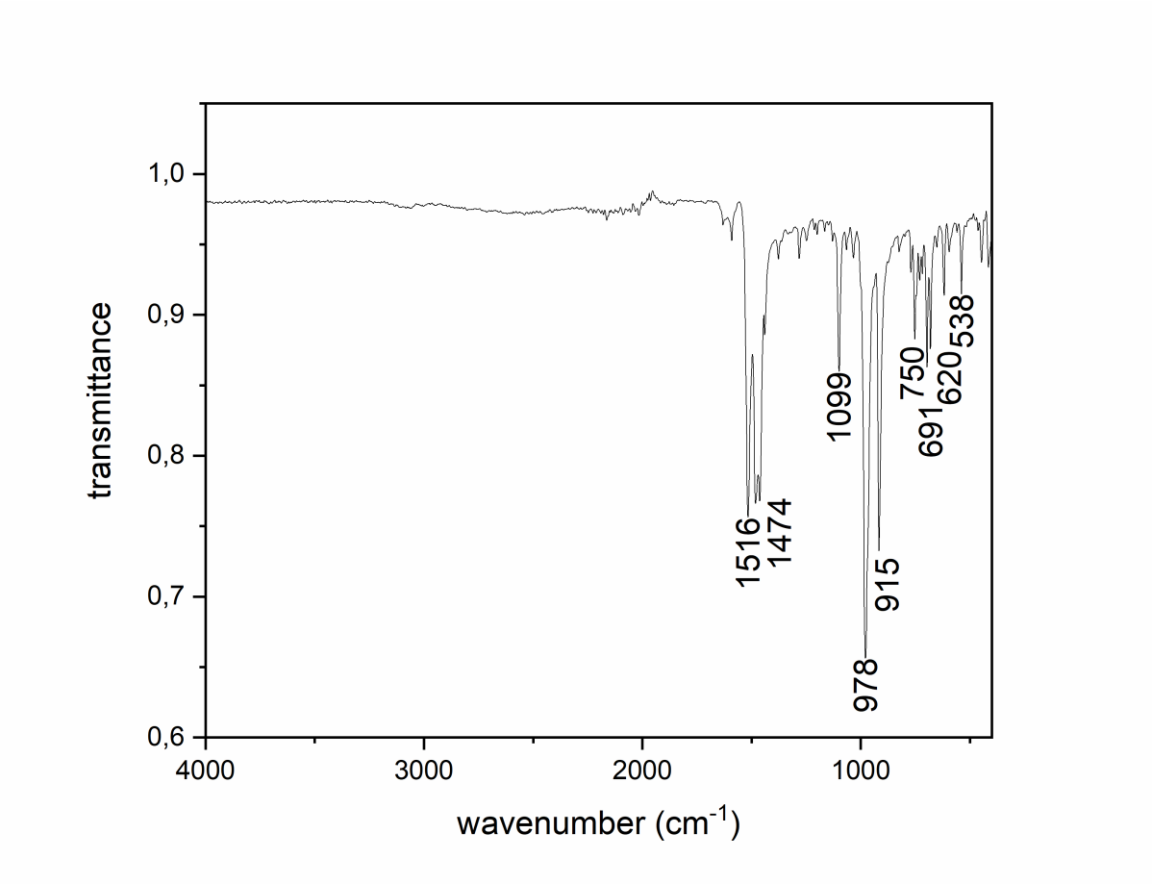

Figure S26. ATR-IR spectrum of pyridinium pentakis(pentafluorophenyl)cyclopentadienide **3d**.

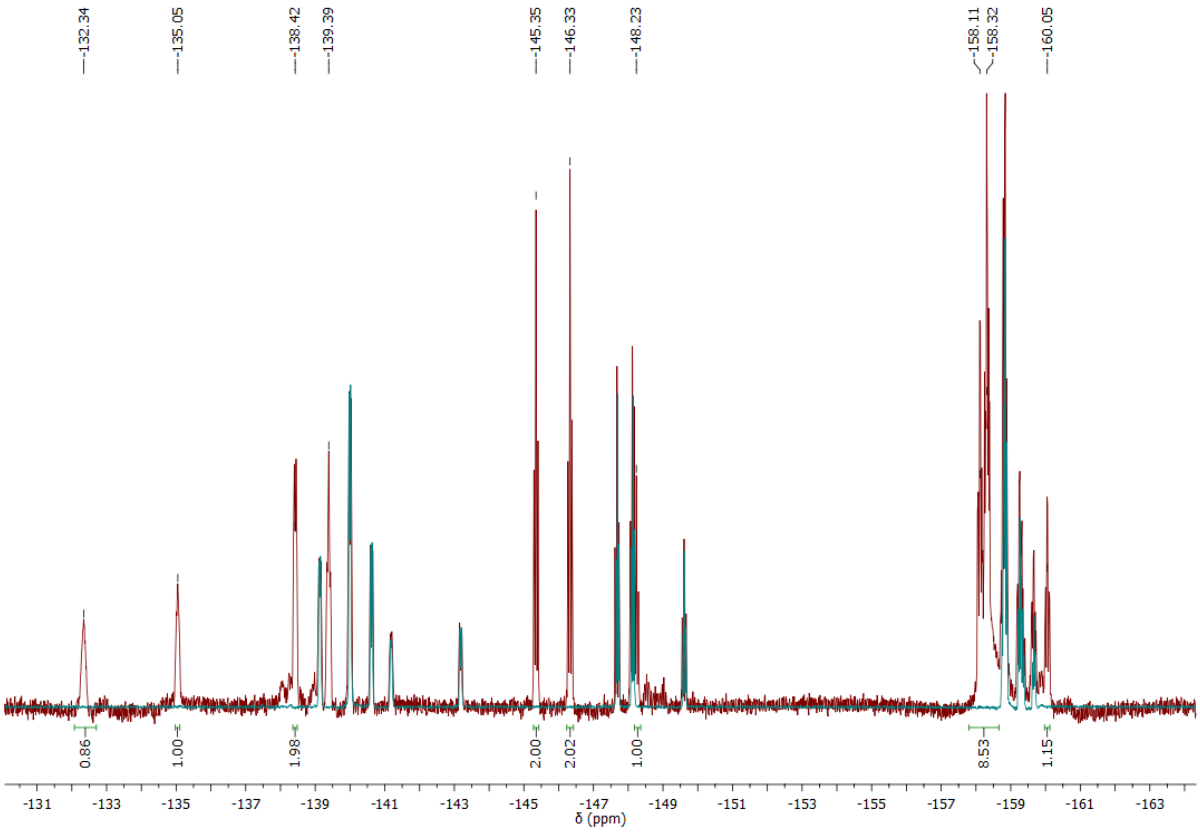

Figure S27. ^{19}F NMR spectrum of pentakis(pentafluorophenyl)cyclopentadienyl carboxylic acid **5** and pentakis(pentafluorophenyl)cyclopentadiene **6** (red) and pure pentakis(pentafluorophenyl)cyclopentadiene **6** (cyan) in C_6D_6 at 25 °C.

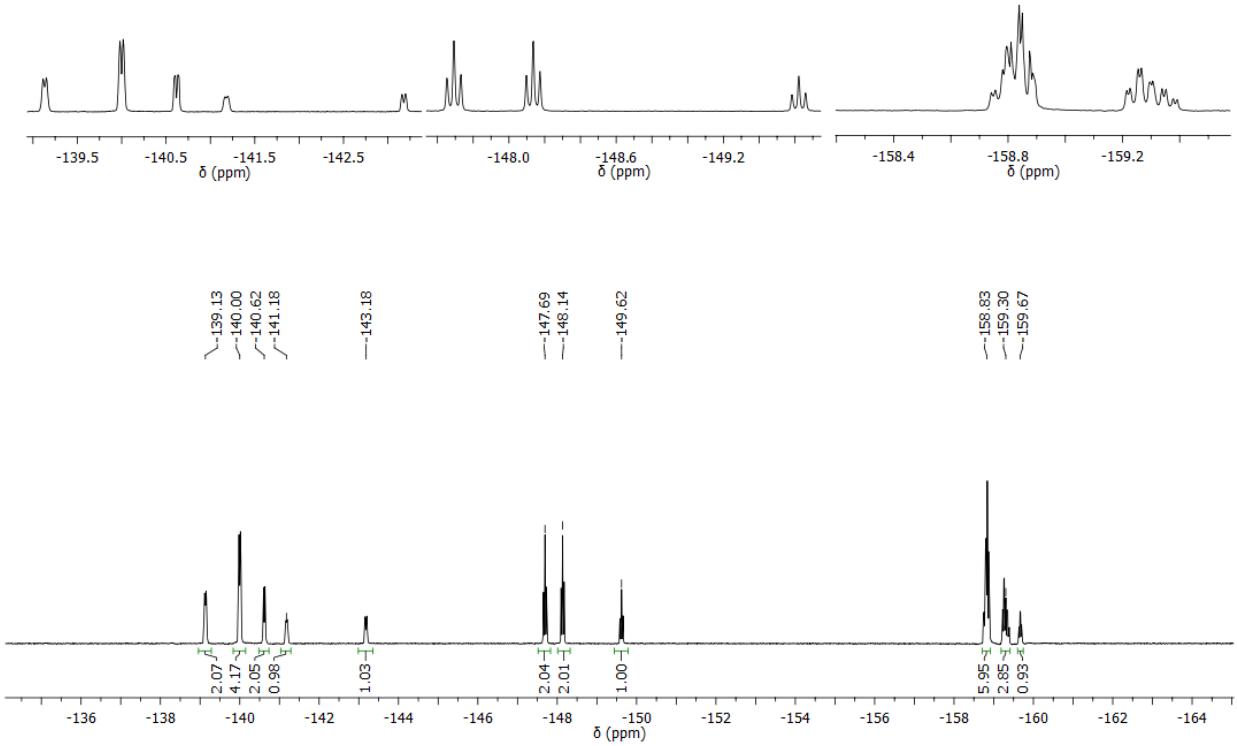

Figure S28. ^{19}F NMR spectrum of pentakis(pentafluorophenyl)cyclopentadiene **6** in C_6D_6 at 25 °C.

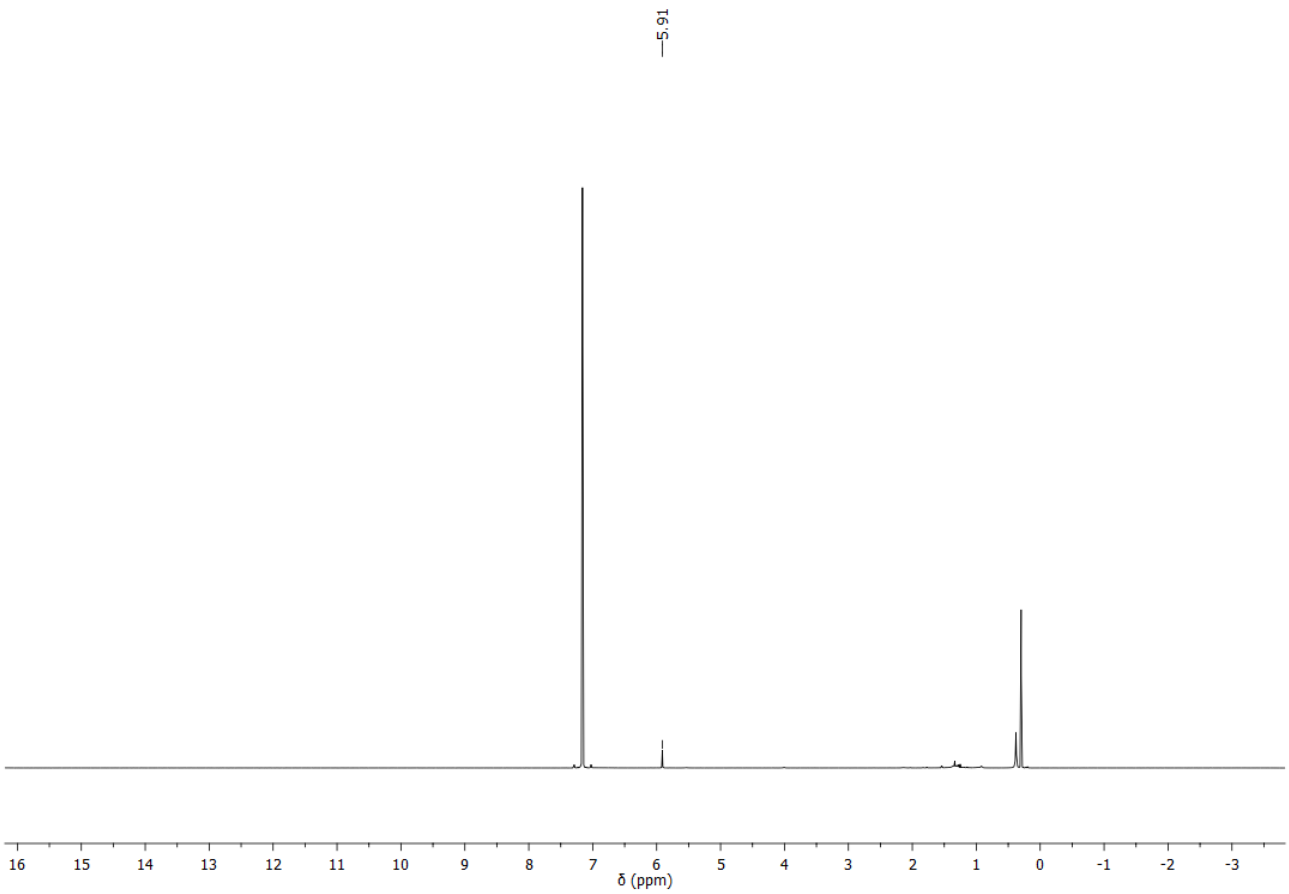

Figure S29. ^{1}H NMR spectrum of pentakis(pentafluorophenyl)cyclopentadiene **6** in C_6D_6 at 25 °C.

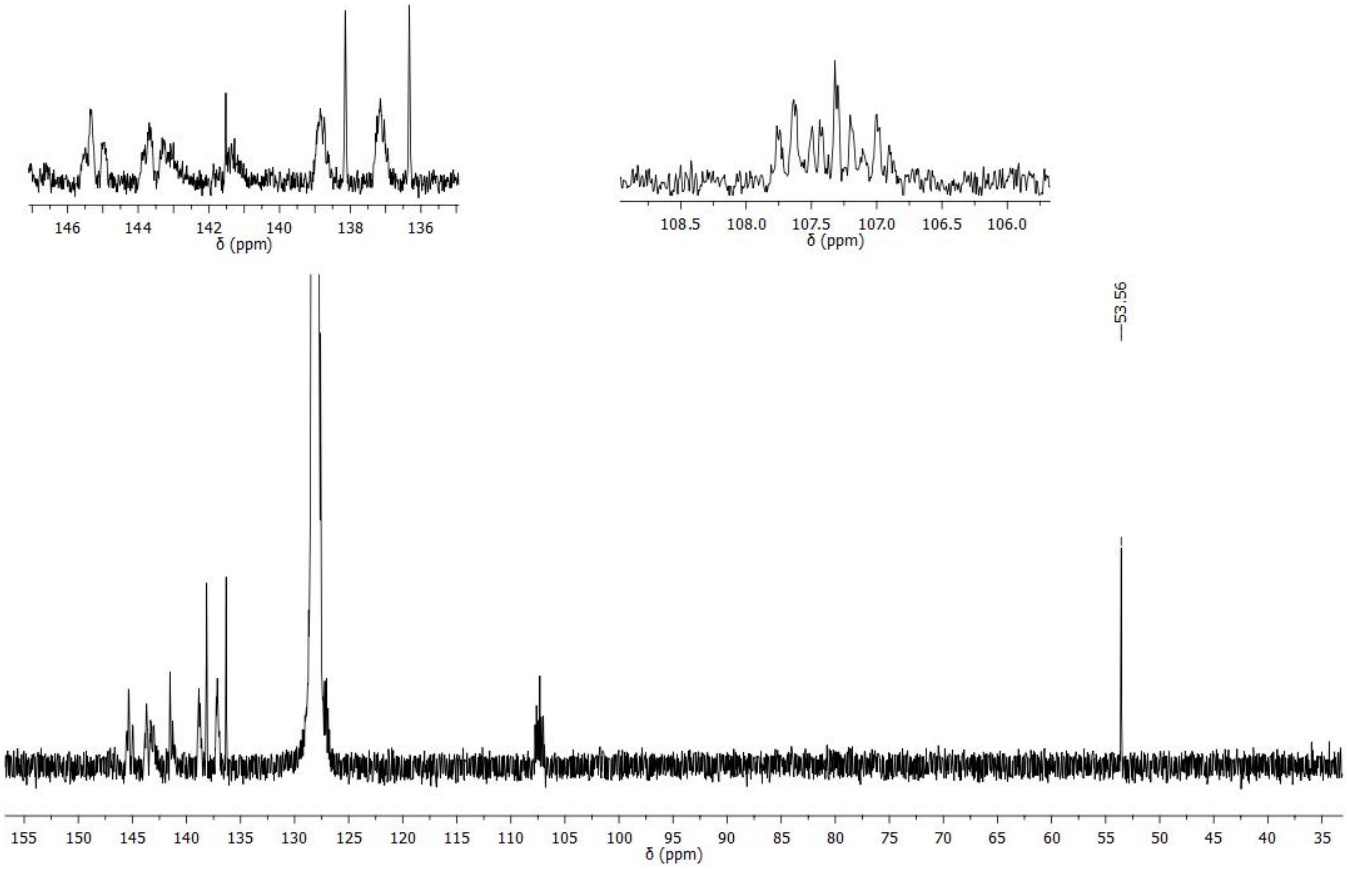

Figure S30. $^{13}C\{^{1}H\}$ NMR spectrum of pentakis(pentafluorophenyl)cyclopentadiene **6** in C_6D_6 at 25 °C.

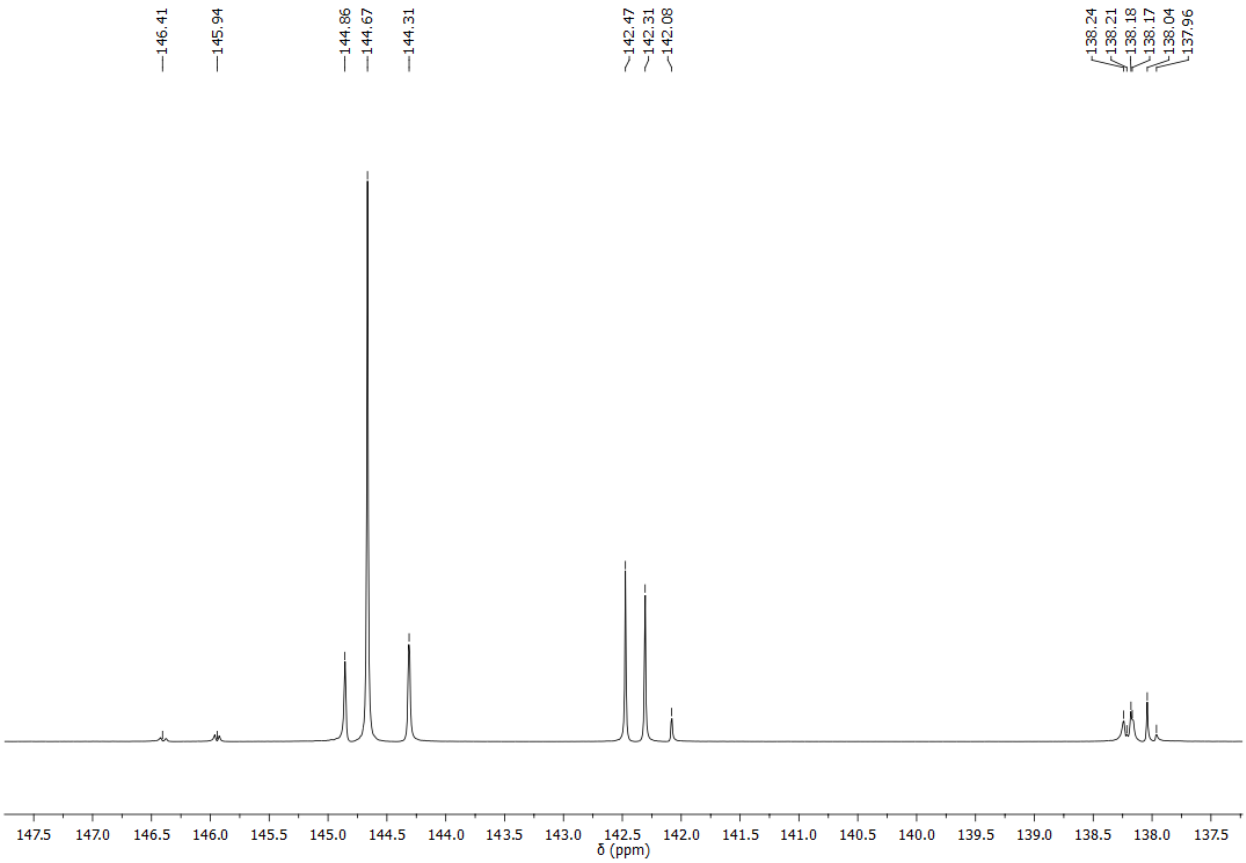

Figure S31. $^{13}C\{^{1}H\}$ DEPT-135 NMR spectrum of pentakis(pentafluorophenyl)cyclopentadiene **6** in C_6D_6 at 25 °C.

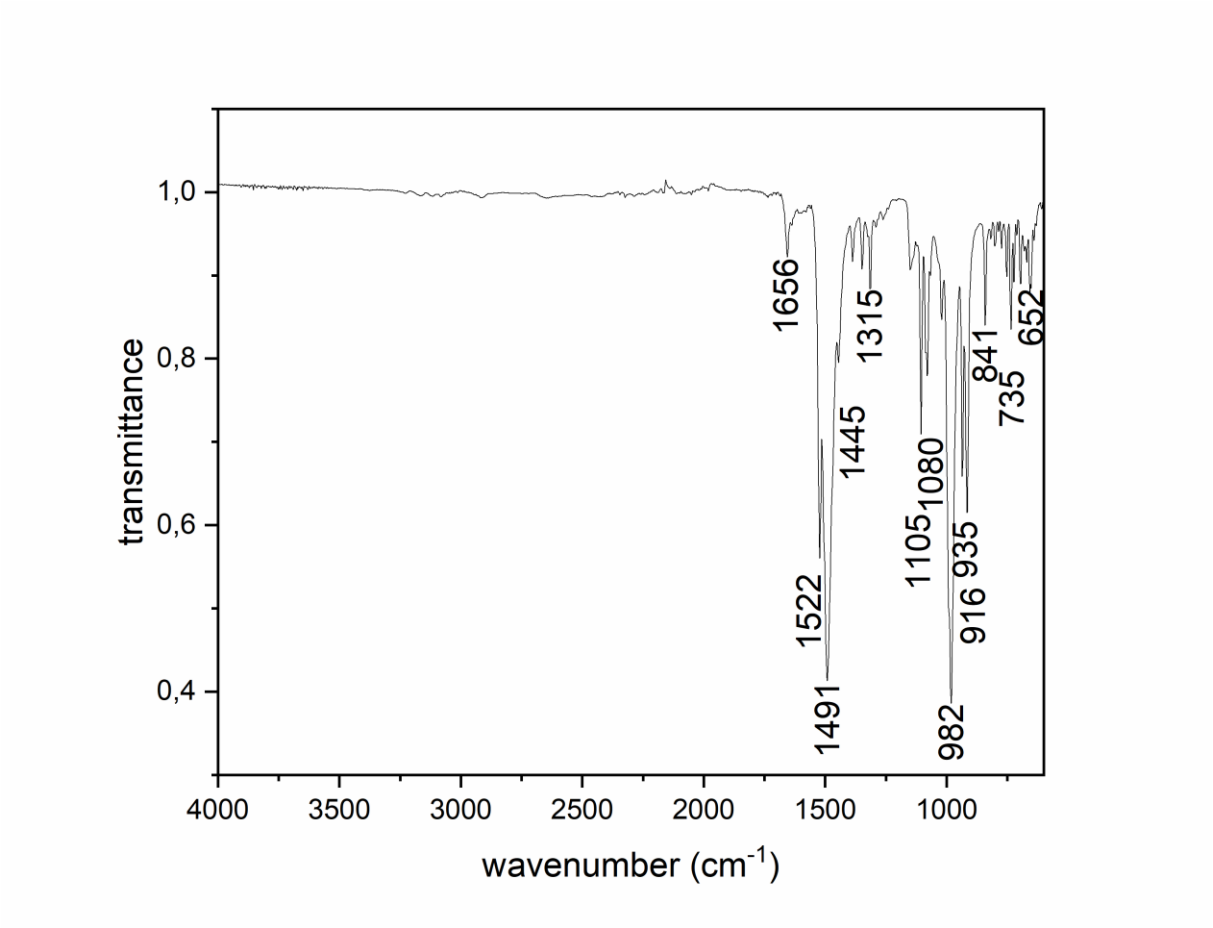

Figure S32. ATR-IR spectrum of pentakis(pentafluorophenyl)cyclopentadiene **6**.

Single-crystal X-ray analyses. Crystals were mounted on nylon loops in inert oil. Data of **1b** (ys_712m) were collected on a Bruker AXS D8 Kappa diffractometer with APEX2 detector (monochromated Mo$_{K\alpha}$ radiation, λ = 0.71073 Å) at 100(2) K. Data of **B** (ys_584m), (**ys_586m), 1a** (ys_712am), **2a** (ys_631a_tw4)**, 2b** (ys_681m), **3a** (ys_679a), **3b** (ys_682am_sq), **3c** (ys_695cm), **5** (ys_719m_sq), and **6** (ys_705m) were collected on a Bruker AXS D8 Venture diffractometer with Photon II detector (monochromated Cu$_{K\alpha}$ radiation, λ = 1.54178 Å, microfocus source) at 100(2) K. The structures were solved by Direct Methods (SHELXS-2013)[8] and refined anisotropically by full-matrix least-squares on F^2 (SHELXL-2017)[9,10]. Absorption corrections were performed semi-empirically from equivalent reflections on basis of multi-scans or numerical from indexed faces (**1b** (ys_712m)) (Bruker AXS APEX3). Hydrogen atoms were refined using a riding model or rigid methyl groups.

In **ys_586** a –C_6F_5 is disordered over two positions. The bond lengths and angles of the phenyl ring were restrained to be equal (SADI). SIMU and RIGU restraints were applied to the displacement parameters of the group. The displacement parameters of the carbon atoms were constrained to be equal for the alternate positions (EADP).

In **1a** (ys_712am) one solvent molecule is disordered over a center of inversion. The local symmetry was ignored in the refinement and the C–C bond lengths and angles of the solvent molecule were restrained to be equal as well as the F/F distances (SADI). RIGU restraints were applied to the displacement parameters of the solvent molecules' atoms.

The only available specimen of **1b** (ys_712m) was too large for the X-ray beam and we did not want to risk losing it by trying to cut it. Any attempts to obtain a more suitable one yielded the other polymorph. The uneven irradiation of the crystal led to distortions of the reflection intensities and consequently to problems with the absorption correction. Several methods and setting were tried but the residual electron density could not be reduced any further. Quantitative results should be carefully assessed. The solvent molecule is disordered over two positions. Its C–C bond lengths and C–C–C bond angles were restrained to be equal (SADI) as well as the F/F distances. All atoms of the molecule were restrained to lie on a common plane (FLAT).

The crystal of **2a** (ys_631a_tw4) was a non-merohedral twin and the model was refined against de-twinned HKLF4 data. Due to overlaps, the R_{int} value is rather high.

One of the SO_2 molecules in **2b** (ys_681m) is disordered over two alternate sites. The bond lengths and angles of the SO_2 molecules were restrained to be equal (SADI), and RIGU restraints were applied to their displacement parameters. The residual electron density suggests that two of the C_6F_5 rings may be disordered, however a refinement failed due to the low occupancy.

3a (ys_679a) was refined as an inversion twin.

In **3b** (ys_682am_sq) a C_6F_5 is disordered over two positions. SIMU and RIGU restraints were applied to the displacement parameters of the corresponding atoms. Due to their close proximity F35 and F35' were refined with common displacement parameters (EADP). The structure also contains highly disordered solvent – possibly toluene. The final refinement was done with a solvent free dataset from a PLATON/SQUEEZE run. (For details see: A. L. Spek, *Acta Cryst. A46* **(1990)**, 194–201). Since the nature and amount of the solvent is not clear it was not included in the sum formula.

The quality of the diffraction data of **3c** (ys_695cm) was rather low (high *Rint*). To check the correct assignment of the Laue group the frames were integrated with a triclinic unit cell. This lead to an equally poor R_{int}. Considering the low quality of the data quantitative results should be carefully assessed.

The hydrogen atom of **5** (ys_719m_sq) was refined freely. The structure contains highly disordered solvent molecules: one hexafluoro benzene and two *n*-hexane disordered over special positions (2, -1 and 222). The final refinement was done with a solvent free data set from a PLATON/SQUEEZE run. (For details see: A. L. Spek, *Acta Cryst. A46* **(1990)**, 194–201). The molecules were included in the sum formula for completeness. The quality of the best specimen available was still rather poor and consequently results beyond the connectivity may be unreliable and should be carefully assessed.

CCDC-2246848 (ys_712a, **1a**), -2246849 (ys_712, **1b**), -2246850 (ys_631a_tw4, **2a**), -2246851 (ys_681, **2b**), -2246852 (ys_679a, **3a**), -2246853 (ys_682am_sq, **3b**), -2246854 (ys_695c, **3c**), -2246857 (ys_719m_sq, **5**), -2246858 (ys_705, **6**), -2246859 (ys_584, **B**), and -2246860 (ys_586 hexakis(pentafluorophenyl)benzene) contain the supplementary crystallographic data for this

paper. These data can be obtained free of charge from The Cambridge Crystallographic Data Centre via www.ccdc.cam.ac.uk/data_request/cif.

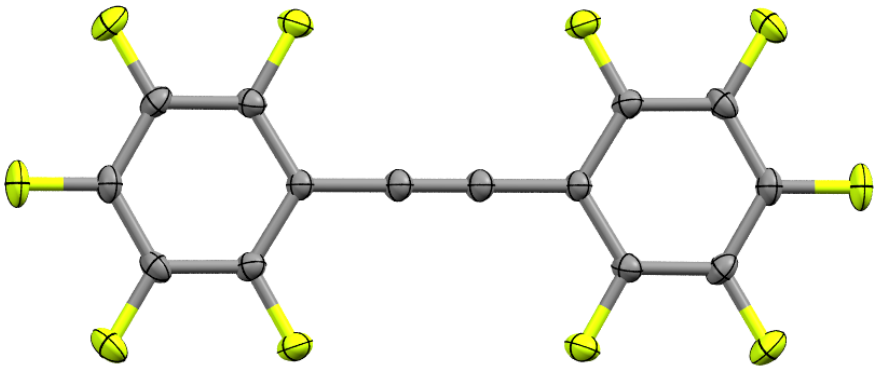

Figure S33. Molecular structure of bis(pentafluorophenyl)ethyne **B** in the solid state, crystallized from benzene. Ellipsoids are drawn at a probability level of 50%.

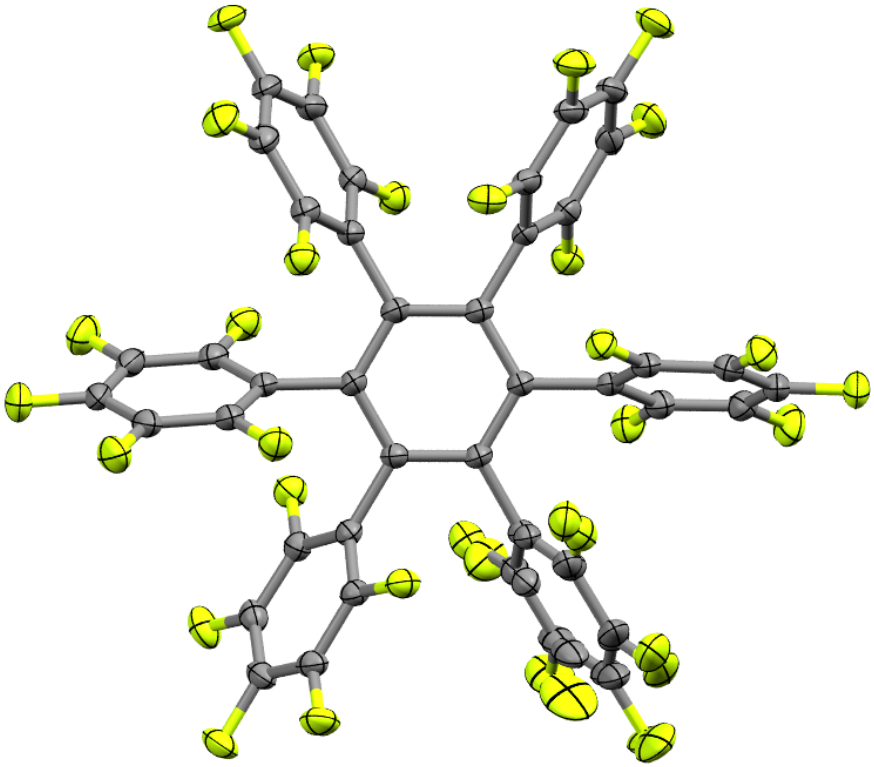

Figure S34. Molecular structure of hexakis(pentafluorophenyl)benzene in the solid state. Ellipsoids are drawn at a probability level of 50%. Hexakis(pentafluorophenyl)benzene (ys_586m) was obtained as a by-product in the synthesis of **C** and crystallized from toluene/DCM.

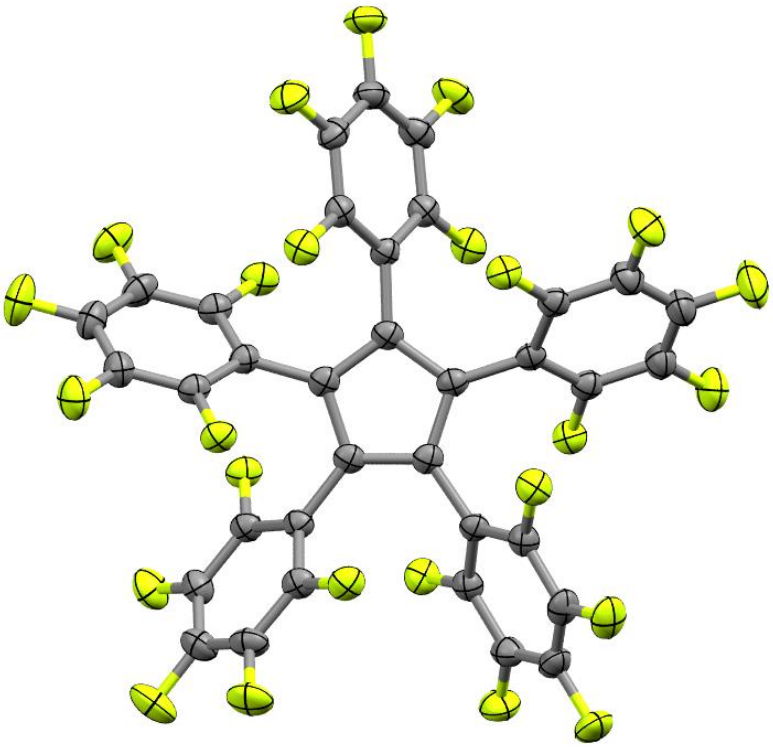

Figure S35. Molecular structure of pentakis(pentafluorophenyl)cyclopentadienyl radical **2** in the solid state, crystallized from benzene. Ellipsoids are drawn at a probability level of 50%.

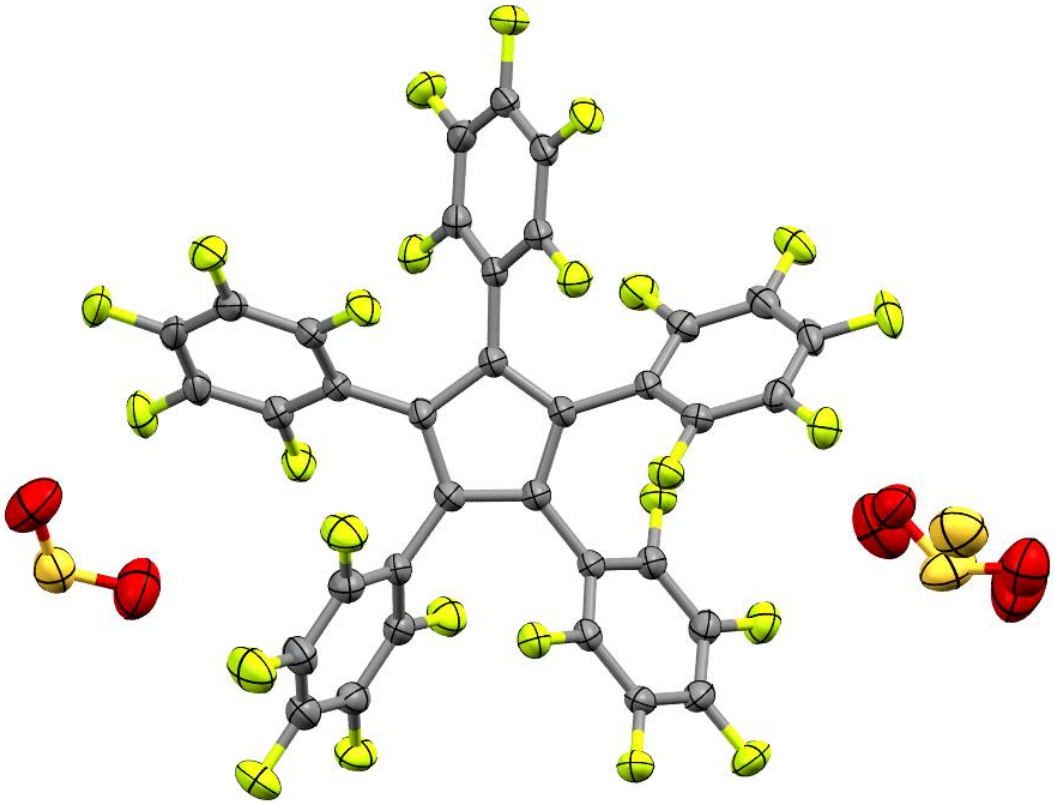

Figure S36. Molecular structure of pentakis(pentafluorophenyl)cyclopentadienyl radical **2** in the solid state, crystallized from SO_2. Ellipsoids are drawn at a probability level of 50%.

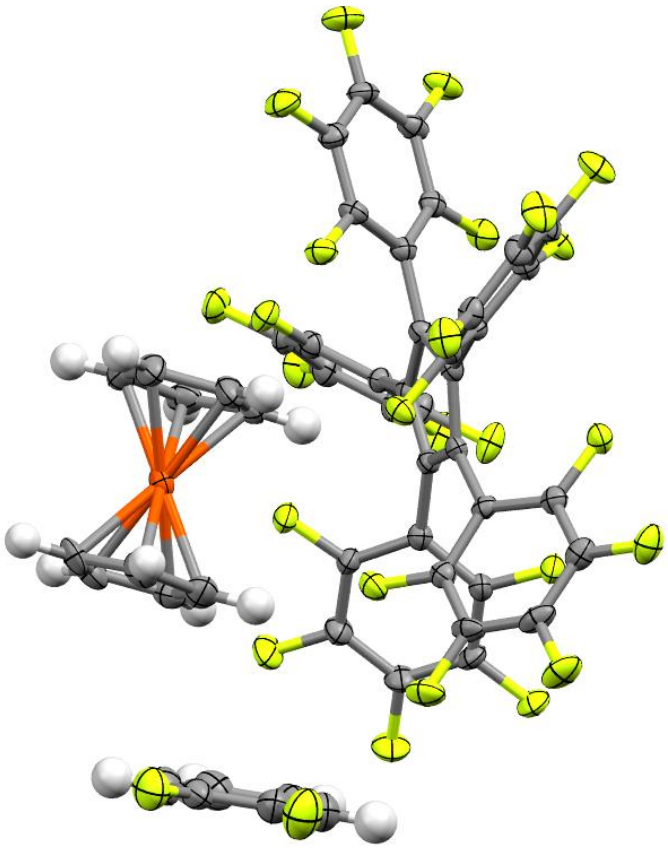

Figure S37. Molecular structure of ferrocenium pentakis(pentafluorophenyl)cyclopentadienide **3a** in the solid state, crystallized from 1,2-difluorobenzene/hexane. Ellipsoids are drawn at a probability level of 50%.

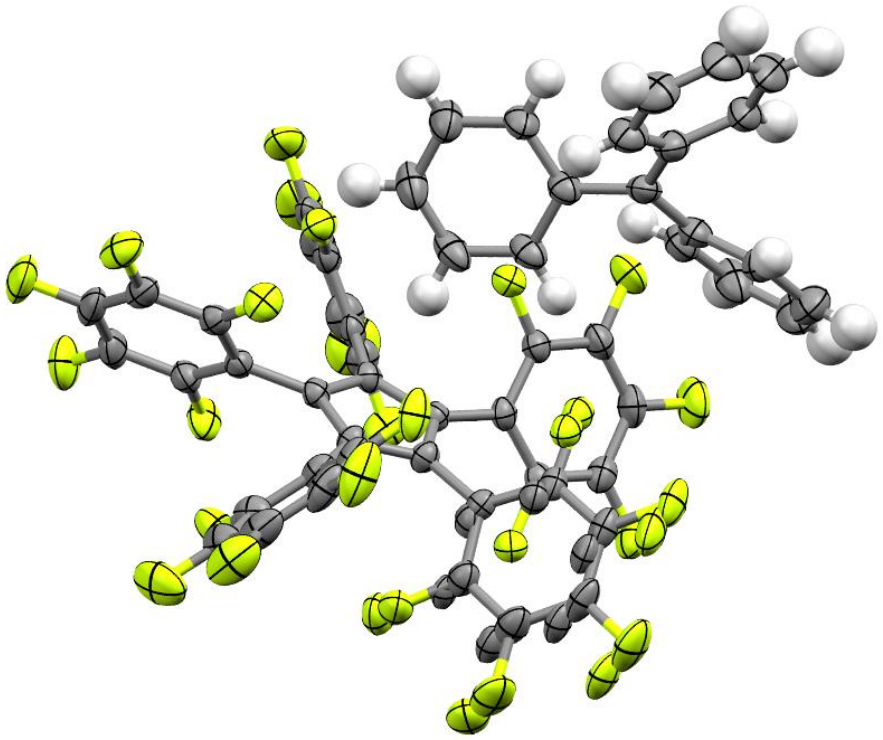

Figure S38. Molecular structure of tritylium pentakis(pentafluorophenyl)cyclopentadienide **3b** in the solid state, crystallized from toluene. Ellipsoids are drawn at a probability level of 50%.

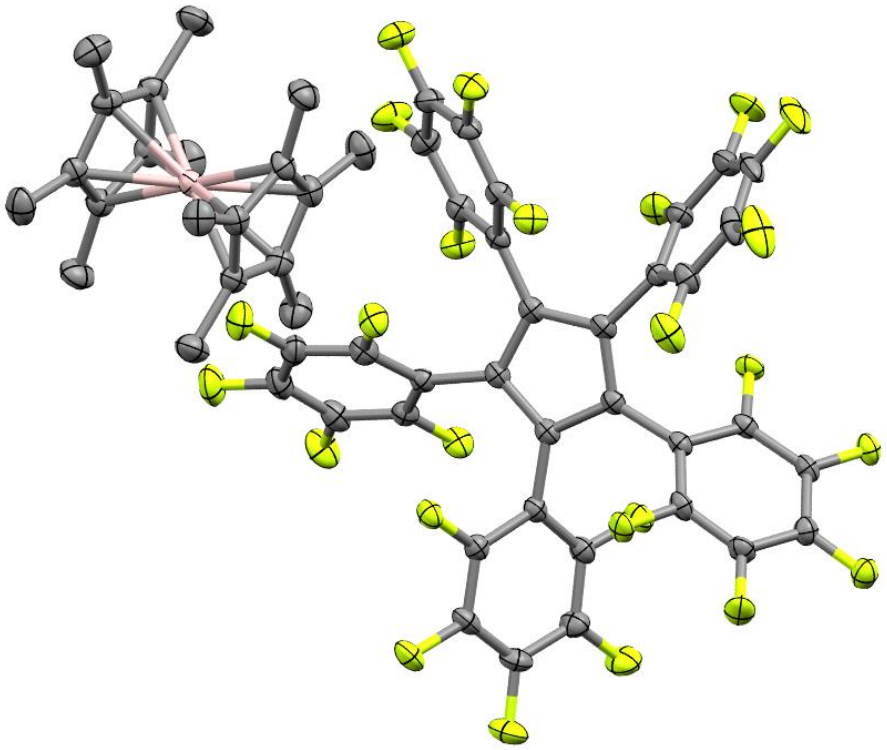

Figure S39. Molecular structure of tritylium pentakis(pentafluorophenyl)cyclopentadienide **3c** in the solid state, crystallized from benzene. Ellipsoids are drawn at a probability level of 50%. Hydrogen atoms are omitted for clarity.

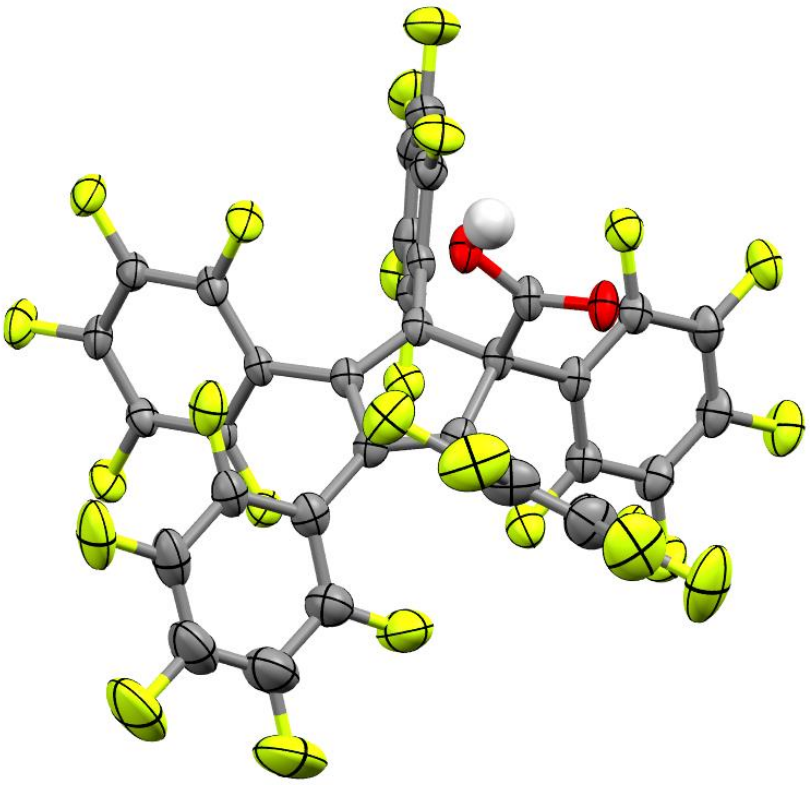

Figure S40. Molecular structure of pentakis(pentafluorophenyl)cyclopentadienylcarboxylic acid **5** in the solid state, crystallized from hexafluorobenzene/hexane. Ellipsoids are drawn at a probability level of 50%.

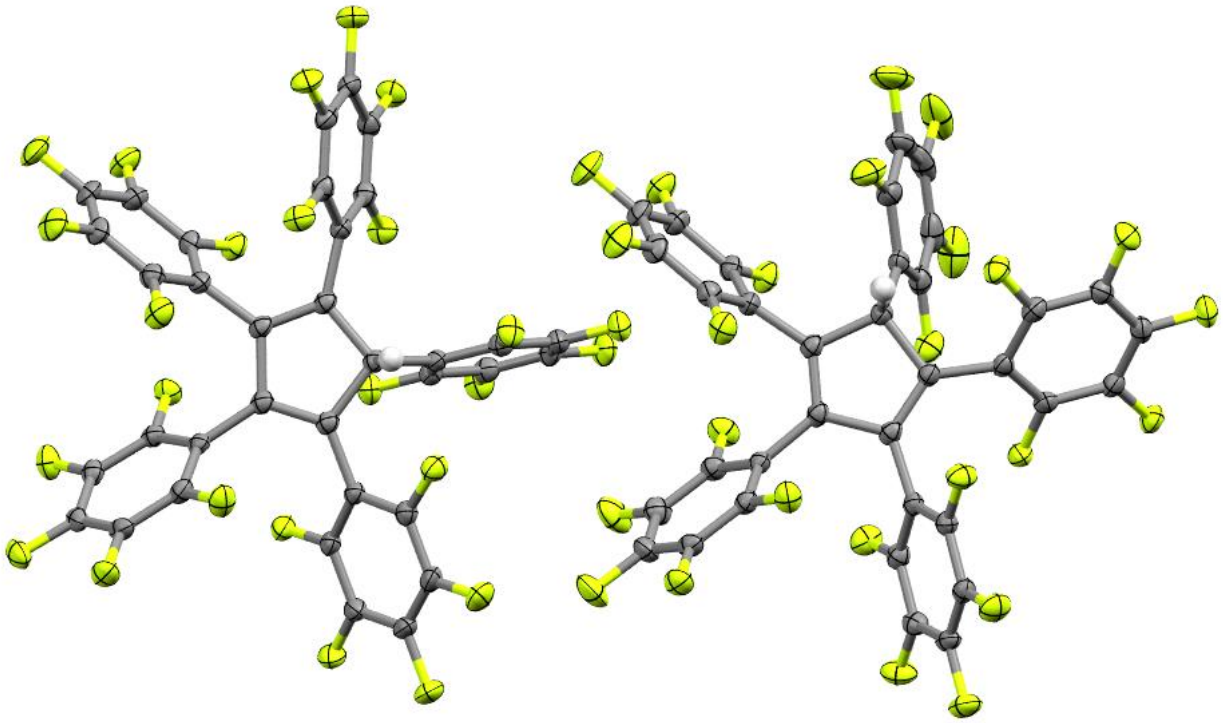

Figure S41. Asymmetric unit of pentakis(pentafluorophenyl)cyclopentadiene **6** in the solid state, featuring two independent molecules, crystallized from acetonitrile/hexane. Ellipsoids are drawn at a probability level of 50%.

Table S1. Bond lengths in the Cp ring and shortest distance of the Cp centroid to an adjacent hydrogen atom for **3a-c**.

	3a	**3b**	**3c**
bond length (Å) of C1-C2	1.405(5)	1.406(3)	1.409(3)
bond length (Å) of C2-C3	1.408(5)	1.409(3)	1.420(3)
bond length (Å) of C3-C4	1.415(6)	1.412(3)	1.401(3)
bond length (Å) of C4-C5	1.411(5)	1.409(3)	1.414(3)
bond length (Å) of C5-C1	1.405(5)	1.411(3)	1.411(3)
distance (Å) between centroid(Cp)-H	2.546	2.683	3.131

Table S2. Crystal and structure refinement data.

Identification code	ys_584m	ys_586m	ys_631a_tw4	ys_679am
Empirical formula	$C_{14}F_{10}$	$C_{42}F_{30}$	$C_{35}F_{25}$	$C_{51}H_{14}F_{27}Fe$
M	358.14	1074.42	895.35	1195.47
Crystal size [mm]	0.541 × 0.461 × 0.072	0.252 × 0.136 × 0.074	0.211 × 0.062 × 0.036	0.258 × 0.068 × 0.049
T [K]	100(2)	100(2)	100(2)	100(2)
Crystal system	monoclinic	orthorhombic	monoclinic	monoclinic
Space group	*C*2/*m*	*Pna*2$_1$	*C*2/*c*	*Cc*
a [Å]	8.9583(11)	12.8398(12)	22.3002(17)	10.7524(4)
b [Å]	7.6581(10)	22.205(2)	13.5353(11)	20.8342(7)
c [Å]	9.2374(12)	13.0139(11)	11.4185(9)	20.0712(7)
α [°]	90	90	90	90
β [°]	110.222(3)	90	116.061(3)	96.603(2)
γ [°]	90	90	90	90
V [Å^3]	594.65(13)	3710.3(6)	3096.1(4)	4466.5(3)
Z	2	4	4	4
D_{calc} [g·cm^{-3}]	2.000	1.923	1.921	1.778
μ(CuK_α [mm^{-1}])	2.098	2.018	2.015	4.123
Transmissions	0.75/0.44	0.75/0.58	0.75/0.47	0.75/0.53
F(000)	348	2088	1740	2356
Index ranges	$-11 \le h \le 9$	$-16 \le h \le 16$	$-28 \le h \le 25$	$-13 \le h \le 10$
	$-9 \le k \le 9$	$-22 \le k \le 28$	$0 \le k \le 17$	$-26 \le k \le 26$
	$-11 \le l \le 11$	$-16 \le l \le 16$	$0 \le l \le 14$	$-25 \le l \le 25$
θ_{max} [°]	79.642	80.740	80.306	81.190
Reflections collected	9187	80749	53232	65031
Independent reflections	699	7972	3359	8679
R_{int}	0.0491	0.0462	0.1450	0.0976
Refined parameters	61	713	273	713
R_1 [$I > 2\sigma(I)$]	0.0398	0.0277	0.0619	0.0360
wR_2 [all data]	0.1368	0.0737	0.1543	0.0799

x(Flack)	–	0.00(2)	–	0.362(5)
GooF	1.240	1.039	1.090	1.040
$\Delta\rho_{final}$ (max/min) [e·Å^{-3}]	0.262/-0.304	0.322/-0.152	0.320/-0.243	0.269/-0.393

Table S2. Crystal and structure refinement data (continuation).

Identification code	ys_681m	ys_682am_sq	ys_695cm	ys_705m
Empirical formula	$C_{35}F_{25}O_4S_2$	$C_{54}H_{15}F_{25}$	$C_{55}H_{30}Al\ F_{25}$	$C_{35}HF_{25}$
M	1023.47	1138.66	1192.77	896.36
Crystal size [mm]	0.390 × 0.172 × 0.070	0.345 × 0.183 × 0.092	0.162 × 0.064 × 0.055	0.152 × 0.116 × 0.083
T [K]	100(2)	100(2)	100(2)	100(2)
Crystal system	triclinic	monoclinic	monoclinic	triclinic
Space group	*P*-1	$P2_1/c$	$P2_1/c$	*P*-1
a [Å]	11.1864(13)	14.2425(7)	15.6538(10)	12.7006(9)
b [Å]	11.3372(10)	20.3955(10)	14.8935(9)	13.3258(8)
c [Å]	16.478(3)	20.0632(10)	21.2611(14)	18.1289(17)
α [°]	106.938(9)	90	90	91.743(6)
β [°]	91.037(10)	99.626(3)	101.546(4)	95.967(6)
γ [°]	117.347(8)	90	90	90.570(5)
V [Å^3]	1747.1(4)	5746.0(5)	4856.5(5)	3049.9(4)
Z	2	4	4	4
D_{calc} [g·cm^{-3}]	1.946	1.316	1.631	1.952
μ(CuK_α [mm^{-1}])	3.063	1.205	1.617	2.046
Transmissions	0.75/0.51	0.75/0.54	0.75/0.59	0.75/0.63
F(000)	998	2256	2392	1744
Index ranges	$-14 \le h \le 12$	$-17 \le h \le 12$	$-19 \le h \le 19$	$-16 \le h \le 14$
	$-14 \le k \le 14$	$-26 \le k \le 25$	$-18 \le k \le 18$	$-17 \le k \le 17$
	$-20 \le l \le 20$	$-25 \le l \le 25$	$-23 \le l \le 26$	$-22 \le l \le 23$
θ_{max} [°]	75.114	81.806	80.572	81.119
Reflections collected	94339	134589	196985	169427
Independent reflections	7163	12546	10504	13260
R_{int}	0.0509	0.0788	0.1482	0.0485
Refined parameters	623	806	740	1081
R_1 [$I > 2\sigma(I)$]	0.0550	0.0672	0.0540	0.0366
wR_2 [all data]	0.1684	0.1670	0.1485	0.0987
GooF	1.049	1.095	1.026	1.017

$\Delta\rho_{final}$ (max/min) [e·Å^{-3}]	0.754/-0.480	0.446/-0.253	0.466/-0.392	0.533/-0.271

Table S2. Crystal and structure refinement data (continuation).

Identification code	ys_712m	ys_712am	ys_719m_sq
Empirical formula	$C_{47}F_{53}Sb_3$	$C_{44}F_{50}Sb_3$	$C_{43.50}H_{11.50}F_{28}O_2$
M	1936.72	1843.69	1098.03
Crystal size [mm]	1.008 × 0.255 × 0.212	0.213 × 0.138 × 0.073	0.380 × 0.125 × 0.100
T [K]	100(2)	100(2)	100(2)
Crystal system	orthorhombic	monoclinic	orthorhombic
Space group	$Pna2_1$	$P2_1/c$	*Fddd*
a [Å]	27.1610(13)	23.1788(8)	11.6321(6)
b [Å]	15.5739(8)	10.9694(4)	47.785(2)
c [Å]	13.0018(6)	22.1030(8)	60.097(3)
α [°]	90	90	90
β [°]	90	113.0712(15)	90
γ [°]	90	90	90
V [Å^3]	5499.8(5)	5170.4(3)	33405(3)
Z	4	4	32
D_{calc} [g·cm^{-3}]	2.339	2.369	1.747
μ(CuK_α [mm^{-1}])	1.682 (MoK_α)	14.417	1.769
Transmissions	0.27/0.16	0.49/0.12	0.75/0.57
F(000)	3648	3468	17296
Index ranges	$-45 \le h \le 45$	$-29 \le h \le 29$	$-14 \le h \le 14$
	$-26 \le k \le 26$	$-13 \le k \le 14$	$-60 \le k \le 61$
	$-21 \le l \le 21$	$-27 \le l \le 20$	$-76 \le l \le 73$
θ_{max} [°]	36.455	80.949	81.008
Reflections collected	144720	139588	146520
Independent reflections	26619	11292	9180
R_{int}	0.0421	0.0764	0.0654
Refined parameters	1039	928	573
R_1 [$I > 2\sigma(I)$]	0.0639	0.0417	0.0770
wR_2 [all data]	0.1681	0.1170	0.2211
x(Flack)	0.33(2)	–	–
GooF	1.099	1.042	1.064

$\Delta\rho_{final}$ (max/min) [e·Å^{-3}]	5.049/-1.355	2.308/-1.889	0.484/-0.524

Computational Details

All calculations were performed by using the program packages Gaussian 16[11] and Amsterdam Density Functional (ADF)[12-13]. DFT geometry optimizations were carried out using B3LYP[14-16] and CAM-B3LYP[17] for closed-shell species and the corresponding unrestricted versions UB3LYP and UCAM-B3LYP for open-shell species. To consider the dispersion interaction in an appropriate way, the additional dispersion correction with Becke-Johnson damping (D3BJ)[18] was employed. As basis sets 6-31G(d), 6-311++G(d,p) and TZP were applied. Furthermore, the open-shell singlet states were calculated using UB3LYP-D3BJ/6-31G(d), UCAM-B3LYP-D3BJ/6-31G(d) and UB3LYP-D3BJ/6-311++G(d,p) and the "guess = mix" keyword. In all cases these calculations converged into the closed-shell states. To treat relativistic effects the zeroth order regular approximation (ZORA)[19] to the Dirac equation was used for the B3LYP-D3BJ/TZP calculations. Frequency calculations were carried out at each of the structures to verify the nature of the stationary point. It turned out that all structures have none.

A NICS-based scan was used as a magnetic criterion of aromaticity. Therefore, the NICS values were calculated using CAM-B3LYP/def2-TZVP//CAM-B3LYP-D3BJ/6-311++G(d,p) along a line perpendicular from the center of the ring plane to 5 Å, with a step size of 0.1 Å (Figure S43). Magnetic shieldings were calculated by employing the GIAO method[20].

The degree of (anti)aromaticity was further evaluated by using the harmonic oscillator model of aromaticity (HOMA)[21-22] index:

$$HOMA = 1 - \frac{\alpha}{n}\sum_{i}^{n}\left(R_{opt} - R_i\right)^2$$

In this equation, R_{opt} corresponds to the optimal bond length taken as 1.388 Å for a CC bond. R_i represents an individual bond length; n is the number of bonds taken up in the summation and α is an empirical constant (257.7 $Å^{-2}$).[22]

Single-point calculations were performed using the double hybrid method B2PLYP-D3BJ[23] and the TZ2P[24] basis set. Furthermore, the zeroth order regular approximation (ZORA)[19] to the Dirac

equation was employed. The geometrical data for these single point calculations stem from the B3LYP-D3BJ/TZP calculations as well as from the X-ray structure analyses.

Table S3. Energy (Δ*E*) and Gibbs energy (Δ*G*) of the triplet state of **1** and **1 SbF_6** relative to the singlet state. The values are given in kcal/mol.

method	molecule	Δ*E*	Δ*G*
cam-B3LYP-D3BJ/6-31G(d)	**1**	-6.20	-5.43
cam-B3LYP-D3BJ/6-311++G(d,p)	**1**	-5.55	-4.58
B3LYP-D3BJ/6-31G*	**1**	-5.62	-5.39
B3LYP-D3BJ/TZP[a]	**1**	-4.96	-5.45
B3LYP-D3BJ/TZP[a]	**1 SbF_6**	-3.65	-2.54
B2PLYP-D3BJ/TZ2P//B3LYP-D3BJ/TZP[a]	**1**	-2.27	-2.77
B2PLYP-D3BJ/TZ2P//B3LYP-D3BJ/TZP[a]	**1 SbF_6**	-0.75	+0.36

[a] The zeroth order regular approximation (ZORA) to the Dirac equation was used.

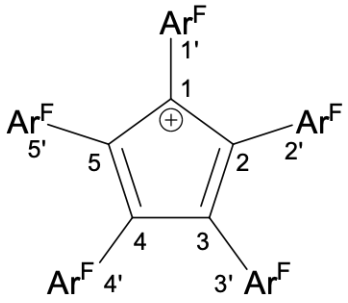

1

Figure S42. Assignment of atom labels.

Table S4. Bond distances [Å] in the singlet und triplet state of **1** and **1 SbF_6** calculated by means of B3LYP-D3BJ/TZP(ZORA).

bond	**1**		**1 SbF_6**	
	singlet	triplet	singlet	triplet
C1-C2	1.458	1.431	1.460	1.431
C2-C3	1.366	1.431	1.365	1.429
C3-C4	1.539	1.434	1.532	1.430
C4-C5	1.371	1.434	1.354	1.432
C5-C1	1.453	1.433	1.474	1.432
C1-C1’	1.434	1.455	1.426	1.454
C2-C2’	1.471	1.455	1.474	1.456
C3-C3’	1.449	1.455	1.451	1.457
C4-C4’	1.446	1.454	1.456	1.455
C5-C5’	1.471	1.454	1.468	1.454

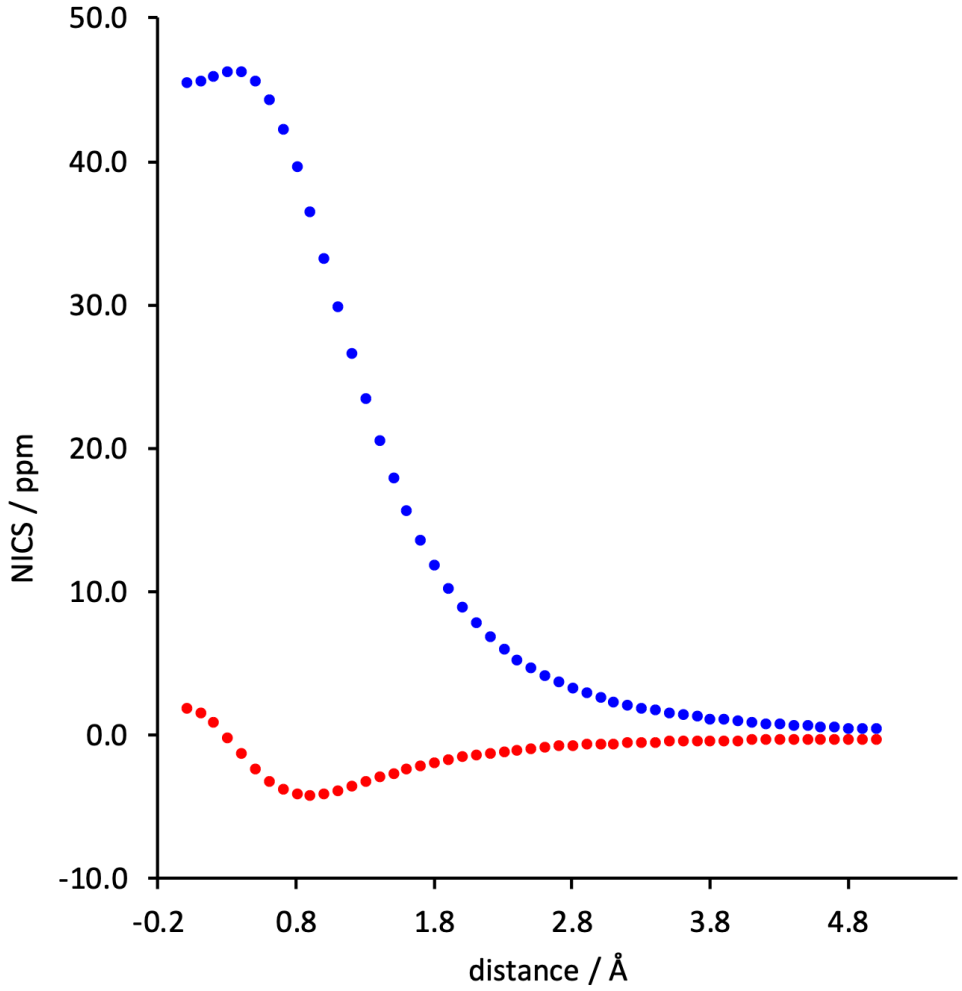

Figure S43. NICS scans of **1** calculated using CAM-B3LYP/def2-TZVP//CAM-B3LYP-D3BJ/6-311++G(d,p). Blue-colored curve refers to singlet state and red-colored curve refers to triplet state.

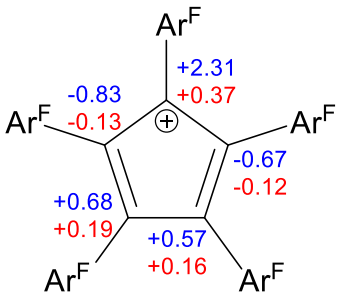

1(singlet)

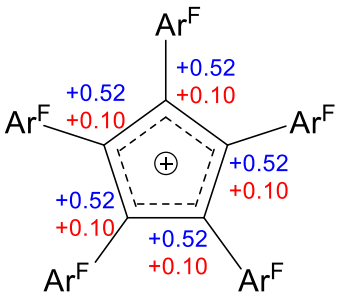

1(triplet)

Figure S44. APT (atomic polar tensor) charges (blue; CAM-B3LYP-D3BJ/6-311++G(d,p)) and NBO (natural bond orbitals) charges (red; CAM-B3LYP/def2-TZVP//CAM-B3LYP-D3BJ/6-311++G(d,p)) of **1** in the singlet (left) und triplet (right).

Calculated HIA and FIA of 1

The structures of Me_3SiH, Me_3SiF, Me_3Si^+, $Cp(C_6F_5)_5^+$ (singlet), $Cp(C_6F_5)_5H$ and $Cp(C_6F_5)_5F$ were optimized using B3LYP-D3(BJ)/def2-TZVPP. To determine the hydride ion affinity (HIA) / fluoride ion affinity (FIA), energy differences were calculated for the reactions:

$Cp(C_6F_5)_5^+$ (singlet) + Me_3SiH → $Cp(C_6F_5)_5H$ + Me_3Si^+

-3830.9595312 + (-409.9693680) → -3831.8835472 + (-409.0821314)

-4240.9288992 Hartree → -4240.9656786 Hartree

(1 Hartree = 2625 kJ/mol) The reaction is 96.5 kJ/mol exothermic.

The hydride affinity of $Cp(C_6F_5)_5^+$ (singlet) is 96.5 kJ/mol higher than that of Me_3Si^+.

$Cp(C_6F_5)_5^+$ (singlet) + Me_3SiF → $Cp(C_6F_5)_5F$ + Me_3Si^+

-3830.9595312 + (-509.3337305) → -3931.1420727 + (-409.0821314)

-4340.2932617 Hartree → -4340.2242041 Hartree

The reaction is 181.3 kJ/mol endothermic.

The fluoride affinity of $Cp(C_6F_5)_5^+$ (singlet) is 181.3 kJ/mol higher than that of Me_3Si^+.

The Me_3SiX (X = H, F)/Me_3Si^+ pair has been established in the literature as a reliable anchor point to calculate hydride and fluoride ion affinities of other Lewis acids. The fluoride affinity of the Me_3Si^+ cation has been calculated to be 952.5 kJ/mol (CCSD(T)/CBS).[32] The hydride affinity of Me_3Si^+ calculated with the same method is 924 kJ/mol.[32]

Since the hydride abstraction from Me_3SiH is exothermic by kJ/mol, the hydride ion affinity of $Cp(C_6F_5)_5^+$ (singlet) is 1020.5 kJ/mol. Since the fluoride abstraction from Me_3SiF is endothermic by 181.3 kJ/mol, the fluoride ion affinity of $Cp(C_6F_5)_5^+$ (singlet) is 771.2 kJ/mol .

Examples for side reactions

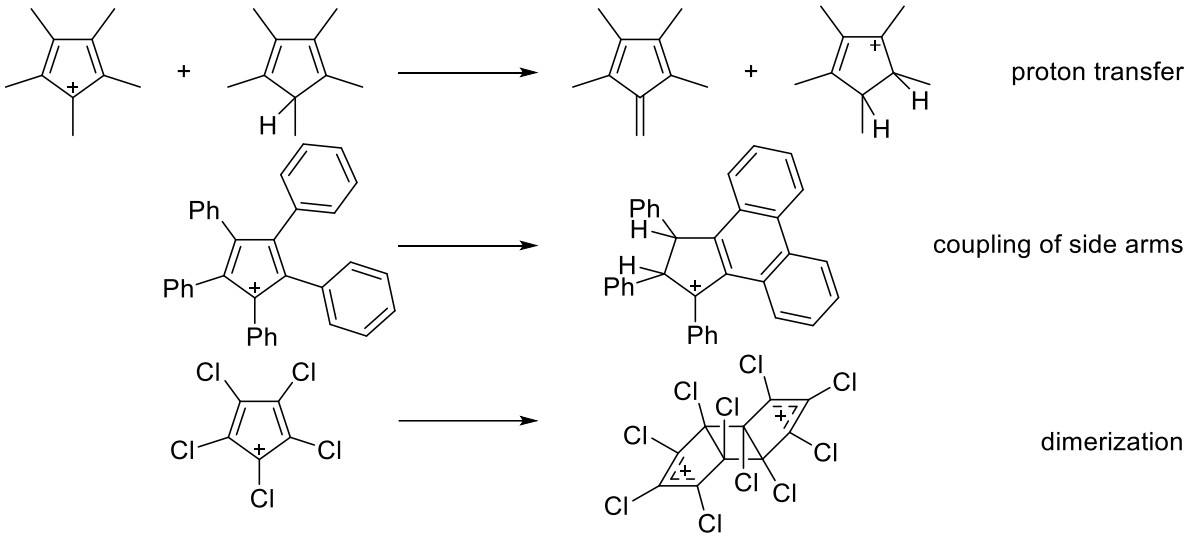

Scheme S42: Examples of side reactions that hindered the isolation of Cp cations.[25-31]

References

1. Boeré, R. T. *et al.* Oxidation of closo-$B_{12}Cl_{12}$- to the radical anion $B_{12}Cl_{12}$*- and to neutral $B_{12}Cl_{12}$. *Angew. Chem. Int. Ed. Engl.* **50**, 549–552 (2011).
2. *Origin(Pro), Version 2016*, OriginLab Corporation, Northhampton, Massachusetts, USA, (2016).
3. Stoll, S. & Schweiger, A. EasySpin, a comprehensive software package for spectral simulation and analysis in EPR. *J. Magnet. Res.* **178**, 42–55 (2006).
4. Webb, A. F. & Gilman, H. Reactions of some perhaloarenes with metals and metal halides. *J. Organomet. Chem.* **20**, 281–283 (1969).
5. Inés, B., Holle, S., Bock, D. & Alcarazo, M. Polyfluorinated Cyclopentadienones as Lewis Acids. *Synlett* **25**, 1539–1541 (2014).
6. Birchall, J. M., Bowden, F. L., Haszeldine, R. N. & Lever, A. B. P. Polyfluoroarenes. Part IX. Decafluorotolan: synthesis, properties, and use as an organometallic ligand. *J. Chem. Soc., A* 747 (1967).
7. Burns, C. T., Shapiro, P. J., Budzelaar, P. H. M., Willett, R. & Vij, A. Bis(permethylcyclopentadienyl)aluminum Compounds: Precursors to $[Cp^*_2Al]^+$ but Not to Cp^*_3Al. *Organometallics* **19**, 3361–3367; 10.1021/om000173x (2000).
8. Sheldrick, G. M. Phase annealing in SHELX-90: direct methods for larger structures. *Acta Cryst.* **46**, 467–473 (1990).
9. Sheldrick, G. M. SHELXL-2017, Program for the Refinement of Crystal Structures University of Göttingen, Göttingen (Germany) (2017). See also: Sheldrick, G. M. Crystal structure refinement with SHELXL, *Acta Cryst.,* **C71**, 3-8 (2015).
10. Hübschle, C. B., Sheldrick, G. M. & Dittrich, B. ShelXle: a Qt graphical user interface for SHELXL. *J. Appl. Cryst.* **44**, 1281–1284 (2011).
11. Frisch, M. J. *et al.* Gaussian 16, Revision A.03, Wallingford CT, (2016).
12. te Velde, G. *et al.* Chemistry with ADF. *J. Comput. Chem.* **22**, 931–967 (2001).
13. Baerends, E. J. *et al.* ADF 2020.1, SCM, Theoretical Chemistry, Vrije Universiteit, Amsterdam, The Netherlands, http://www.scm.com, **2020**.
14. Becke, A. D. Density-functional exchange-energy approximation with correct asymptotic behavior. *Phys. Rev. A* **38**, 3098–3100 (1988).
15. Lee, C., Yang, W. & Parr, R. G. Development of the Colle-Salvetti correlation-energy formula into a functional of the electron density. *Phys. Rev. B* **37,** 785–789 (1988).
16. Miehlich, B., Savin, A., Stoll, H. & Preuss, H. Results obtained with the correlation energy density functionals of becke and Lee, Yang and Parr. *Chem. Phys. Lett.* **157**, 200–206 (1989).
17. Yanai, T., Tew, D. P. & Handy, N. C. A new hybrid exchange–correlation functional using the Coulomb-attenuating method (CAM-B3LYP). *Chem. Phys. Lett.* **393**, 51–57 (2004).
18. Grimme, S., Ehrlich, S. & Goerigk, L. Effect of the damping function in dispersion corrected density functional theory. *J. Comp. Chem.* **32**, 1456–1465 (2011).

19. van Lenthe, E., Ehlers, A. & Baerends, E.-J. Geometry optimizations in the zero order regular approximation for relativistic effects. *J. Chem. Phys.* **110**, 8943–8953 (1999).
20. Wolinski, K., Hinton, J. F. & Pulay, P. Efficient implementation of the gauge-independent atomic orbital method for NMR chemical shift calculations. *J. Am. Chem. Soc.* **112**, 8251–8260 (1990).
21. Julg, A. & Franois, P. Recherches sur la géométrie de quelques hydrocarbures non-alternants: son influence sur les énergies de transition, une nouvelle définition de l'aromaticité. *Theoret. Chim. Acta* **8**, 249–259 (1967).
22. Krygowski, T. M. & Cyrański, M. Separation of the energetic and geometric contributions to the aromaticity of π-electron carbocyclics. *Tetrahedron* **52**, 1713–1722 (1996).
23. Grimme, S. Semiempirical hybrid density functional with perturbative second-order correlation. *J. Chem. Phys.* **124**, 34108 (2006).
24. van Lenthe, E. & Baerends, E. J. Optimized Slater-type basis sets for the elements 1-118. *J. Comput. Chem.* **24**, 1142–1156 (2003).
25. Otto, M. *et al.* The Stable Pentamethylcyclopentadienyl Cation Remains Unknown. *Angew. Chem. Int. Ed. Engl.* **41**, 2275 (2002).
26. Lambert, J. B., Lin, L. & Rassolov, V. The Stable Pentamethylcyclopentadienyl Cation. *Angew. Chem. Int. Ed. Engl.* **41,** 1429–1431 (2002).
27. Breslow, R. & Chang, H. W. The Rearrangement of the Pentaphenylcyclopentadienyl Cation. *J. Am. Chem. Soc.* **83**, 3727-3728 (1961).
28. Rupf, S. M., Pröhm, P. & Malischewski, M. The 2+2 cycloaddition product of perhalogenated cyclopentadienyl cations: structural characterization of salts of the C10Cl102+ and C10Br102+ dications. *Chem. Commun.* **56**, 9834-9837 (2020).
29. Jones, J. N., Cowley, A. H. & Macdonald, C. L. B. The crystal structure of the 'pentamethylcyclopentadienyl cation' is that of the pentamethylcyclopentenyl cation. *Chem. Commun.,* 1520–1521 (2002).
30. Müller, T. Comment on the X-Ray Structure of Pentamethylcyclopentadienyl Cation. *Angew. Chem. Int. Ed. Engl.* **41**, 2276-2278 (2002).
31. Lambert, J. B. Statement. *Angew. Chem. Int. Ed. Engl.* **41**, 2278 (2002).
32. Erdmann, P. Leitner, J. Schwarz & J. Greb, L. Ch*emPhysChem* **21**, 987-994 (2020).